Performance Evaluation of an Automobile Radiator using CuO/Glycerol based Nanocoolant

A dissertation submitted

in partial fulfillment of the requirements

for the award of degree of

Master of Engineering

in

Thermal Engineering

by

Pulkit Jain

Registration No.: 802083009

Under Supervision of:

Dr. Rohit Kumar Singla

(Asst. Professor, MED, TIET)

Dr. Kundan Lal

(Asst. Professor, MED, TIET)

THAPAR INSTITUTE
OF ENGINEERING & TECHNOLOGY
(Deemed to be University)

DEPARTMENT OF MECHANICAL ENGINEERING

THAPAR INSTITUTE OF ENGINEERING AND TECHNOLOGY, PATIALA

July 2022

Dedication

Dedicated to my beloved parents and sister

Certificate

I hereby declare that the thesis titled **"Performance Evaluation of an Automobile Radiator using CuO/Glycerol-based Nanocoolant"** is a genuine record of my work carried out as per the requirements for the award of the degree of **Master of Engineering** in **Thermal Engineering** at **TIET, Patiala** under the supervision of **Dr. Rohit Kumar Singla** (Asst. Professor, MED, TIET) and **Dr. Kundan Lal** (Asst. Professor, MED, TIET) during August 2020 to July 2022. No part of the matter embodied in this report has been submitted to any other university or institute for the award of any degree.

Dated: 25/7/2022

Pulkit Jain

Pulkit Jain
(Registration No. 802083009
TIET, Patiala)

It is certified that the above statement made by the student is correct to the best of my knowledge and belief.

28/7/22

Dr. Rohit Kumar Singla
(Asst. Professor, MED, TIET)

Dr. Kundan Lal
(Asst. Professor, MED, TIET)

Abstract

The ever-increasing trend of energy consumption along with the miniaturization of equipment has led to the discovery of a new class of heat transfer fluids called nanofluids, having extraordinary thermo-physical properties. These nanofluids are colloidal suspensions of nanoparticles in the conventional base fluid such as water, EG, glycerol, etc. In this study, experimental investigation on the heat transfer performance of automobile radiator using DI water, EG based coolant, and glycerol solution along with the CuO/glycerol nanocoolant has been carried out. The overall heat transfer coefficient has been calculated by using the conventional LMTD method. The copper oxide (CuO) nanoparticles are added to the base fluid in three different concentrations of *0.5%, 1.0%, and 1.5% by vol*. along with *0.5 wt. %* of SDS (sodium dodecyl sulfate) as a surfactant. SDS has been used to achieve homogeneous suspension of nanoparticles in the base fluid with longer stability. The coolant side Reynolds number is varied from *25 to 325* while that of the air side is kept constant at 190. The inlet liquid temperature is kept constant at *60℃* and care has been taken to keep the ambient conditions constant at *20℃ DBT* and *45% RH*. Overall, experiments have been conducted on six coolant flow rates (*1, 2, 4, 6, 8, 12 lpm*) and four nanocoolants of different concentrations (*0.0%, 0.5%, 1.0% and 1.5% by vol.*). The effects of these parameters have been studied on temperature drop, heat transfer rate, Nusselt number, convective heat transfer coefficient, and overall heat transfer coefficient for both the coolant and the air side heat transfer. Results show that enhancement of up to *32.5%* can be achieved in overall heat transfer coefficient (tube side) using CuO/glycerol nanofluid of *1.5% by vol*. conc. However, enhancements of up to 15.3% and 22.2% respectively were observed when the lower concentrations of *0.5%* and *1.0% by vol*. were used. Moreover, the effect of nanoparticle concentration has also been studied on the pumping power, where the increase is found to be more at lower coolant flow rates and reduced towards higher coolant flow rates.

Keywords: glycerol, copper oxide (CuO), nanofluid, overall heat transfer coefficient, radiator, performance

Acknowledgment

First of all, I would like to thank the almighty God, who gave me the power to successfully complete the research project in time. Next, I would like to thank my supervisors **Dr. Rohit Kumar Singla** and **Dr. Kundan Lal** for their worthy guidance, continuous encouragement, and timely response as and when required by me. They provided me with technical support, facilities, and skills that helped me to do the research efficiently. They always had a time slot for my doubts and cleared them with so much patience. They were ever ready to work with me, even on weekends. I also thank **Dr. Vikrant Khullar** for his sincere suggestions and advice, given to perform the experiments in a better way. I would like to express my sincere thanks to **Dr. Tarun Kumar Bera**, Head, Mechanical department, TIET for his continuous support and encouragement which helped me keep my morale high.

I also thank **Mr. Charanjeet Singh, Mr. Harcharan,** and other staff of the Heat Transfer lab for providing me with their support and their cooperation.

I would like to thank the staff of the Mechanical department too, that helped me with technical support.

In the last, I would like to thank my family, all my friends, and colleagues, who kept me motivated all the time and for the support, they provided, without which completing this study seems impossible.

Table of Contents

List of Figures

List of Tables

Symbols and Abbreviations

Symbols:

- $\dot{Q}$: heat transfer rate
- $\dot{m}$: mass flow rate
- C_P : specific heat capacity
- ΔT : temperature change
- T_1 : coolant inlet temperature
- T_2 : coolant exit temperature
- T_3 : air inlet temperature
- T_6 : air exit temperature
- $\dot{\forall}$: volume flow rate
- ρ : density
- φ : nanoparticle concentration
- m : mass
- μ : dynamic viscosity
- k : thermal conductivity
- ΔT_{lm} : log mean temperature difference
- Re : Reynolds number
- Pr : Prandtl number
- D_h : Hydraulic Diameter
- α : thermal diffusivity
- ν : kinematic viscosity
- T_m : mean bulk temperature
- Nu : Nusselt number
- h : Convective heat transfer coefficient
- L : characteristic length
- U : overall heat transfer coefficient
- A : area of interface of heat transfer
- δ : tube wall thickness

Subscripts:

- *nf* : nanofluid
- *np* : nanoparticle
- *bf* : base fluid
- *a* : air
- *c* : coolant
- *exp* : experimental
- *calc* : calculated
- *rad* : radiator
- *glyc* : glycerol
- *i* : inner
- *o* : outer

Abbreviations:

- *EG* : ethylene glycol
- *GON* : graphene oxide nanosheets
- *SDS* : sodium dodecyl sulphate
- *CNT* : carbon nanotubes
- *DW* : deionised water
- *SEM* : spectrum electron microscopy
- *DLS* : dynamic light scattering
- *RH* : relative humidity
- *CHTC* : convective heat transfer coefficient

CHAPTER 1: INTRODUCTION

1.1 Introduction

The rising demand for compact and lightweight equipment and automobiles with better thermal efficiencies has created a need for effective thermal management technologies. Effective thermal management may include enhanced heat removal to prevent overheating and its subsequent failure while lowering the cost and size requirements of a heat exchanger. Heat exchangers are devices that transfer heat from one fluid to another. Heat exchangers find their use in many applications like air conditioners, refrigerators, automobiles, solar thermal power plants, textile industry, nuclear power plants, petroleum industry, etc. Heat exchangers can also be classified based on the relative direction of fluid flow i.e. parallel flow, counter flow or cross flow. Automobiles use heat exchangers that are arranged in cross-flow and most of them use fins on the air side to enhance the heat transfer rate through it. Such heat exchangers are called radiators. An automobile radiator is subjected to a heat load of almost one-third of the total heat produced, to keep the temperature of the engine at an optimal level to achieve the best efficiency possible. The radiators are large and bulky and add dead load on the engine and thus affecting the overall performance of the automobile. A large radiator not only adds a lot of unnecessary weight to the vehicle but also increases the drag force which further amounts to a decrease in the vehicle's overall efficiency.

For reducing the size of the radiator without compromising its heat removal rate, various aspects have been considered like modifying the design of the radiator for a better overall heat transfer coefficient or increasing the heat removal rate of the cooling fluid, etc. The research on cooling fluid is getting pace and is the need of the hour. The major drawback of currently used coolants such as ethylene-glycol is its low thermal conductivity, which hinders the effective heat removal from the engine. The low thermal conductivity accounts for lower heat transfer rates and thus adversely affect the engine's performance. Though the nanofluids show enhanced thermal performance but there are some limitations to its commercial use such as:

- Poor long term stability (sedimentation / agglomeration)
- Controlled microstructure
- Economic production of nanoparticles
- Increased pumping power

1.2 Engine Cooling Systems

In Internal Combustion Engines, combustion of fuel and air takes place inside the engine cylinder and hot gases are generated at very high temperatures of 1500-2000 °C. This temperature is high enough to melt the cylinder body and the engine head. Therefore heat removal from the cylinder is crucial for its proper working and achieving the best efficiency. The system employed to cool the engine from very high temperatures to the optimum working temperature is called an Engine Cooling System. An Engine Cooling System should remove heat at a fast rate when the engine begins to overheat [1] . The cooling should be at slower pace at start of the engine, so that the different working parts reach their optimum working temperatures, however, after reaching the critical temperature, the heat removal rate should be sufficient to keep the engine at a specified temperature to achieve maximum efficiency.

In an IC Engine, the total heat of combustion is distributed as follows:
(a) About 30-35% of the total heat produced is used for generating the brake power (useful work).
(b) Around 30% of the total heat is carried away by exhaust gases.
(c) Cooling system is designed to remove the remaining heat (approx. 30-35% of total heat).

The two major operating conditions for an efficient engine cooling system are:
1. It should be capable of dissipating not more than 30-35% of the heat generated in the combustion chamber. Too much removal of heat lowers the thermal efficiency of the engine.
2. It should dissipate the excessive heat at a faster rate, when the engine is hot. But, when the engine is cold, the cooling should be slow enough so that the different working parts of the engine reach their optimum working temperatures in a short period.

There are mainly two types of cooling systems: Air cooled system and Water cooled system.

Air-cooled system: Air-cooled systems are generally used in small engines like motorbikes, scooters, and aero-plane engines. In this system, fins are extruded on the cylinder walls, cylinder head, and other parts of the combustion chamber. The heat generated in the combustion chamber is conducted to the fins and the air flowing over it dissipates the excessive heat.

Water cooled systems: In Water cooled systems, cooling water jackets are provided around the combustion chamber wall. When water is circulated through the jackets, it absorbs the excessive heat. The hot water is then cooled by forced convection occurring due to the motion of the vehicle and the fan. This water is sent back to the cylinder head with the help of a pump and the process continues. A water cooling system mainly consists of:

- Radiator and Fan
- Water pump and Water Jackets
- Thermostat valve
- Antifreeze mixtures (Coolant).

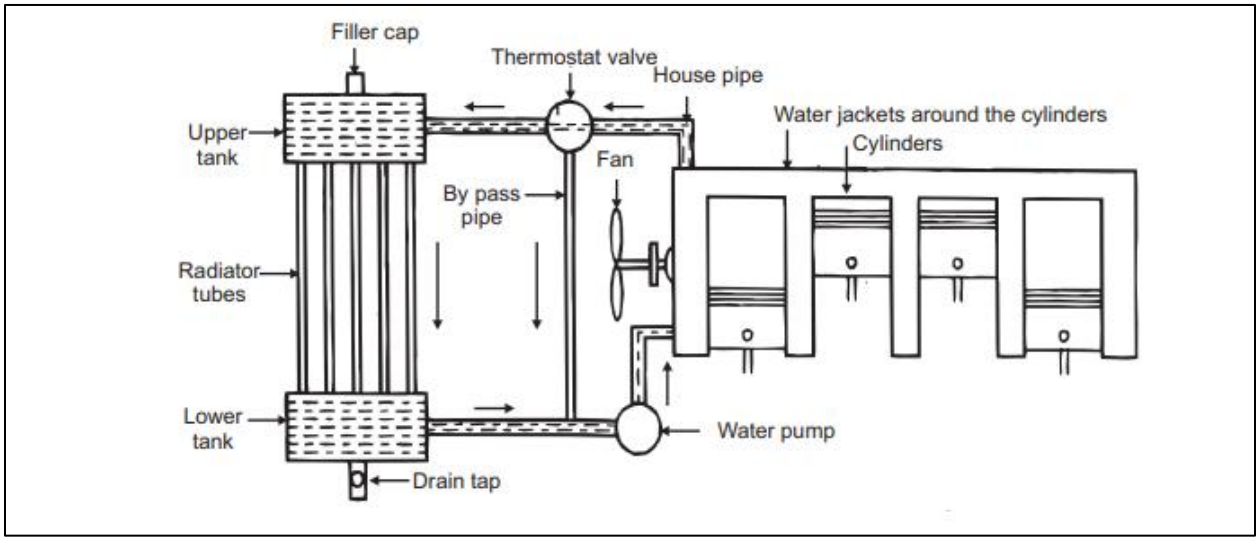

Figure 1: Schematic of water-cooled engine system [2]

1.3 Introduction to Automobile Radiators

The most important components in a water-cooled system are the radiator and coolant. The coolant absorbs the heat from the engine through the water jacket and transfers it to the radiator which then dissipates it to the surrounding air, thus cooling the coolant for further heat removal from the engine. It consists of an upper tank (at top) and a lower tank (at bottom), and a core in the middle. The upper tank receives the water from the engine jackets via hose pipe. When the water flows down through the radiator core, it is cooled partially by the fan which blows air, and partially by the air flow developed by the forward motion of the vehicle. The cooled water then flows to the lower tank connected to the jacket inlet through a water pump using hose pipes.

A radiator core is made up of the following components:

- Inlet tank: It is a small tank through which hot coolant is distributed to thin tubes.
- Pressure Cap: A safety cap to prevent boiling of coolant and allow it to move to a reservoir tank
- Tubes: Very thin tubes attached to the inlet and outlet tank of the radiator. It can be circular or non-circular in cross-section.
- Fins: Fins are attached to the tube to enhance the heat transfer rate.
- Outlet Tank: Collects cooled coolant from tubes and sends it back to the engine block via a water pump.

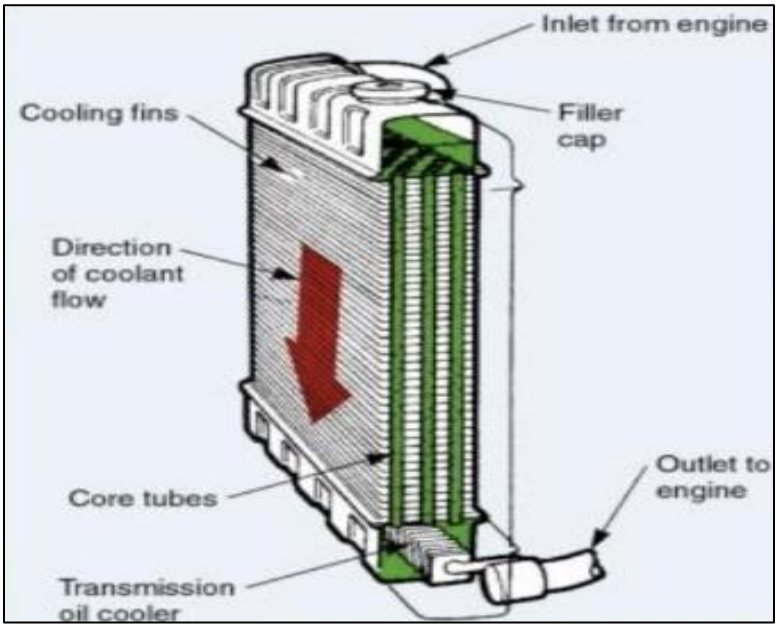

Figure 2: Parts and working of radiator assembly [3]

1.4 Introduction to Radiator Coolants

Water is the best available coolant for thermal purposes due to its unmatched thermal properties, but in regions, with colder climates like that in western countries, it tends to freeze because of low temperature, and the ice thus formed, producing cracks in the cylinder block and radiator tubes. So, to prevent freezing of water at low temperatures, antifreeze mixtures or solutions are added to the cooling water.

Water + Antifreeze = Coolant

An ideal antifreeze solution should have the following properties:

a) It should be water soluble.
b) It should be cheap and easily available.
c) It should have a high boiling point and low freezing point.
d) It should not have any harmful effect on the cooling system.
e) It should not deposit any foreign matter in the cooling system.
f) It should be non-toxic, and non-hazardous to humans.
g) It should not corrode the system.
h) It should be environment friendly.

Though, no single antifreeze possesses all such properties, the following substances have been used as antifreeze solutions in automobile radiators:

(a) methyl alcohol
(b) ethyl alcohol
(c) isopropyl alcohol
(d) ethylene glycol
(e) propylene glycol
(f) glycerol

1.4 History & Advancement of Automobile Coolants

The use of coolants in automobiles can be witnessed from the very beginning of water-cooled engines. In water-cooled engines the water act as the primary cooling agent as it was the fluid with the most optimum thermal and economic properties desirable for a coolant. But due to its higher freezing point of 0 °C, it could not be used in countries with cold climates. Researchers used an aqueous solution of methanol to depress the freezing point but it resulted in boiling point depression also. In the early 20^{th} century, scientists began using glycerin-based coolants that successfully depressed the freezing point and also raised the boiling point of the coolant. But due to its high cost at that time, researchers again searched for a cheaper alternative to the glycerin-based coolant. In 1926, scientists developed a petroleum-based coolant called ethylene glycol, which had all the properties of glycerol and still had a lower price. The glycerol market showed a steep downward trend and almost all of the market was occupied by ethylene glycol-based

coolants. The major drawback of using the EG-based coolant is its toxicity and environmental issues. Further research in this field has promoted the use of Propylene glycol (a less toxic coolant reagent) but approx 90 % market is still occupied by conventional EG-based Coolants. In a bid for a greener, cleaner and safer environment, ASTM recently, in 2014, approved the standards for use of glycerol-based coolants in automobiles [4]. The research on glycerol-based coolants is now getting pace and looks to be a promising base fluid for the preparation of nanofluids due to its superior thermal characteristics to that of the glycol family.

Why prefer glycerol-based coolants over ethylene glycol ones?

- **Bid towards Clean and Green Energy**

  Glycerol is far more environmental-friendly as compared to its counterpart Ethylene glycol. Glycerol can be obtained from biomass by the process of hydrogenation of oils, while EG can only be obtained from petroleum sources.

- **Non-Toxic**

  Glycerol is non-toxic, however, ethylene glycol (EG) is a highly toxic chemical [5]. Studies have revealed that only 1 tbsp of EG can kill a dog and 1 tsp of it can kill a cat. However, glycerol (glycerin) is even used in medicines..

- **Corrosion Resistant**

  While EG-based automobile coolants require corrosion inhibitors to prevent corrosion of radiator core, Glycerol itself prevents metal parts from corrosion.

- **Competitive Price**

  Glycerol was widely used as an automobile coolant about 100 years ago but got replaced with the introduction of cheap ethylene glycol-based coolants. Due to the promotion of using greener energy sources like biodiesel and advancement in technologies, a huge stock pile-up of glycerin has been generated and brought its prices close to that of ethylene glycol. Studies reveal that the production of 100L of biodiesel yields 10L of glycerin. Retail Market Price for Lab Grade Reagents (99% purity): glycerol is Rs 400/L and ethylene glycol is Rs 600/L

- **Higher thermal conductivity**

  Thermal conductivity of glycerol is higher than that of ethylene glycol.

  Thermal conductivity of ethylene glycol – 0.254 W/mK

  Thermal conductivity of glycerol – 0.285 W/mK

- **May form a stable suspension**

  Due to its high dynamic viscosity and density, it may form a stable suspension of nanoparticles when chosen as a base fluid.
- **More opportunities to explore**

  Since ASTM approved the Glycerol standards recently, there is a huge scope of research that awaits to be explored for using Glycerol as a coolant base.

1.6 Nanocoolants

In recent decades, nanocoolants have come to lime light mainly due to their superior heat transfer properties as compared to conventional coolants like water and ethylene glycol. Nanocoolant (or nanofluid) is a fluid containing nanometer-sized particles, called nanoparticles of different materials such as metals, metal oxides, and non-metals. Nanocoolants are next generation fluids that can be used as heat transfer fluids in heat exchangers in place of the conventional fluids. The potential applications of nanocoolant heat transfer include automobile radiators, refrigeration, solar collectors, electronic equipment cooling, machining, etc. One of the major objectives of heat transfer enhancement using nano coolant is to handle high heat fluxes, and to minimize the cost and size of the radiator which in turn will result in the conservation of energy and material.

Nanocoolants can be prepared using two techniques: One-step method and Two-step method

- **One-Step Method**: In this process, nanocoolants are prepared directly into the base fluid using chemical methods, thus assuring high quality and better long stability. This method requires highly advanced techniques and expertise and is usually too expensive and cumbersome for academic research purposes.
- **Two-Step Method**: This is the most common and extensively used method for the preparation of nano coolant. In this method, firstly nano powder is made by different methods and then dispersed in base fluid with the aid of a magnetic stirrer, ultra-sonication, etc. The nanocoolants thus prepared are of somewhat low quality and thus tend to settle down after some time. To overcome this, surfactants may be added to improve the dispersion quality by reducing the surface tension effects.

In this study, to prepare the nanofluid, the two-step method has been used due to its simplicity and economics of use.

[This page is intentionally left blank]

CHAPTER 2: LITERATURE REVIEW

In context to the study undertaken, many relevant research papers were studied. A detailed review of the papers has been presented in this section.

2.1 Literature Review

Nanofluids are colloidal solution of nanometer sized particles in a base fluid. The term nanofluid was used for first time by *Choi et. al.* [6] in mid 90's. Their research in the field of materials reveals that the addition of a minute quantity of nano-sized particles of metals and metal oxides can greatly enhance the thermal conductivity of a fluid. The nanofluids with enhanced thermo-physical properties are the future of most of the applications involving thermal management may it be electronics equipment cooling [7] , process heating [7] , automobile engine cooling [8,9] , refrigeration [10] , electric motor cooling [11] , solar collectors [12–15] , heat pipes [16–18], etc. Various studies [19–24] have shown the dependence of thermal conductivity of nanofluid on its concentration, temperature, size, and even shape of the nanoparticle used apart from the material of the nanoparticle. *Rajan et. al.* [12] studied the temperature dependency of thermal conductivity and viscosity of CuO/EG nanofluid and reported an increase of about 14.1% in thermal conductivity of 1.0% *by vol*. CuO/EG nanofluid at 50°C. He reports an increase in thermal conductivity of nanofluids with nanoparticle concentration and ultrasonication time up to a certain critical time after which there is no significant increase in the thermal conductivity of nanofluids. For the CuO/EG nanofluid, he observes the critical ultrasonication time to be 12 hours. However, the dynamic viscosity of nanofluid tends to decrease with increased nanoparticle concentration. They report a reduction of 13.1% in viscosity values of 1 % *by vol*. conc. of CuO/EG nanofluid, contrary to the general belief of an increase in viscosity on increasing the nanoparticle concentration. They claim the disruption of the hydrogen bonding network on the addition of nanoparticles to be the possible factor contributing to decreasing viscosity. An enhancement of 11.8% in the heat transfer rate of 1% *by vol*. conc. nanofluid has been reported for a temperature difference of fluid to the ambient of 20°C. *Azarfar et. al.* [19] studied the effects of particle concentration and pH to provide the optimal conditions for the highest thermal conductivity of CuO/ Water nanofluid. He reported an enhancement of 47% in thermal conductivity at 1.0% by wt. conc. of CuO/Water nanofluid and at a pH value of 4.0. He

also studied the effect of different surfactants (SDS and Span60) on the long-term stability of CuO/water nanofluid and observed long-term stability of 30 days using SDS surfactant but with Span60 surfactant, nanofluid separated into two phases too earlier. Thus SDS surfactant may be used with nanofluids having CuO nanoparticles. *Ahmadi et. al*. [23] conducted an extensive review of the available literature and found that the nanoparticle shape plays an important role in determining the thermal conductivity of nanofluid. They studied the effect of different shapes of nanoparticles such as: blade-shaped, brick-shaped, spherical-shaped, cylindrical-shaped, and platelet-shaped nanoparticles; effect of temperature, concentration, and size on the thermal conductivity of nanofluids. While metallic oxide nanofluids showed better thermal conductivity for spherical particles, nonmetallic nanofluids present higher thermal conductivity for cylindrical-shaped nano particles. *Sundar et. al.* [25] reported an increase in the thermal conductivity of nanofluids with an increase in the concentration of nanoparticles. He carried out research on CuO and Al_2O_3-based nanofluid at different concentration levels and found a maximum of 47.05% and 61.7% increase in thermal conductivity of CuO/DW and Al_2O_3/DW nanofluids respectively (both at 0.8% *by vol*. conc.). He also demonstrated the temperature dependence of thermal conductivity on the temperature of nanofluid and found that the thermal conductivity shows an increasing trend irrespective of the material and concentration of nanoparticles in the nanofluid.

Peyghambarzadeh et. al. [26] investigated the effect of pH variation on the stability of CuO/Water and Fe_2O_3/Water nanofluids and found a significant effect of pH on the long-term stability of nanofluids. He also carried out experiments to determine the effect of nanofluid concentration on the overall heat transfer coefficient by varying the concentration from 0.15%, 0.45%, and 0.65% *by vol*. and reported a maximum enhancement of 9.0% on using 0.65 % *by vol*. Fe_2O_3/Water nanofluid. *Ganesan et. al*. [27] performed experiments to determine the thermal and electrical conductivities of (Graphene Oxide Nanosheets) GON/Glycerol nanofluid of four different nanoparticle concentrations (0.02%, 0.06%, 0.08%, and 0.10% by wt.) and observed long term stability of more than five months. At 25 °C, he reports an enhancement of 4.5% in thermal conductivity of 0.02 wt. % GON/glycerol nanofluid and at 45 °C he reports an enhancement of 11.7 % in thermal conductivity of 0.1% by wt. GON/Glycerol nanofluid. *Meyer et al.* [28] studied the effect of ultrasonication density on dispersion consistency of Al_2O_3/Glycerol nanofluid according to the average particle size and also reported a model to

determine the same. He reports optimum ultrasonication time to be 6 hours at an ultrasonication energy density of 3 x 10^7 kJ/m^3 and 3 hours at an ultrasonication energy density of 1.5 x 10^7 kJ/m^3 for nanofluids having an average particle size of 20-30nm and 80-100nm respectively. *Shah et. al*. [29] reported an increase in zeta potential value on using PVA coated CuO/EG nanofluid as compared to uncoated CuO/EG nanofluid. They observed zeta potential values to be 42mV and 37mV for uncoated CuO/EG nanofluid of conc. 0.1 wt.% and 0.5 wt. % respectively, however for PVA coated CuO/DW nanofluid, the zeta potential values increase to 52 mV and 47mv respectively. He also reported a trend of decreasing stability on increasing the nanoparticle concentration which he considers to be a result of clustering of nanoparticles. He also mentions an increase in viscosity of nanofluids on increasing nanoparticle concentration and a decrease in viscosity values with time.

Asirvatham et. al. [30] determined the feasibility of using Al_2O_3/glycerin nanofluid for automotive cooling applications for 0.05%, 0.1%, and 0.15% *by vol*. concentrations and reported an enhancement of 62% in heat transfer coefficient at constant heat flux conditions of 6916 W/m^2. They also reported a negligible increase in the pumping power with increase in the nanoparticle concentration and also reported an increase in heat transfer rate enhancement from 28% to 42% on increasing the Reynolds number from 500 to 2000. They also report an increase in the effectiveness of the radiator by 12% at a Reynolds number of 1250. Thus, they suggest the use of glycerol based nanocoolants in automobile radiators as a promising field of research. *Sundari et. al.* [4] examined the performance of Al_2O_3/glycerin nanofluid in car radiators with different experimental conditions and three nanoparticle volume concentrations of 0.1%, 0.2%, and 0.3%. He reported an increase of 54.56% in the heat transfer rate for 0.3% *by vol*. concentration of Al_2O_3/glycerin nanocoolant at constant heat flux conditions and termed it as a promising coolant for automotive applications. *Warrier et. al.* [31] studied the effect of the particle size on the thermal conductivity of nanofluids containing metallic nanoparticles (Ag) and also developed a model to predict the same. He conducted research on silver nanoparticles of sizes 20nm, 30nm-50nm, and 80nm in two different concentrations of 1% and 2% *by vol*. and reported a decrease in thermal conductivity of nanofluid with a decrease in particle size after reaching a critical particle size for lower concentrations while at higher concentrations the size effect is reduced due to agglomeration of particles.

Many researchers have also suggested the use of carbon-based nanoparticles like Carbon Nano Tubes (CNTs) and graphene and fullerenes (C-60) due to their outstanding thermo-physical properties. *Jiang et. al*. [22] tested for CNT/Water nanofluid with loadings from 0.22% to 1% *by vol*. and at temperatures varying from 30 °C to 90 °C. He presented a model to predict the effective thermal conductivity of carbon nanotube-based nanofluid and reported an increase of about 14% in thermal conductivity of nanofluid at room temperature. The low enhancement in thermal conductivity is believed to be due to agglomeration of the CNTs which reduces the effective surface area for heat transfer. Also, the thermal conductivity of nanofluid showed an increasing trend with the temperature.

Apart from using a single nanoparticle for enhancing the thermal conductivity of nanofluids, researchers have started using two or more nanoparticles to get the most beneficial heat transfer fluid. Such nanofluids with two or more nanoparticles are called hybrid nanofluids. Such nanofluids are developed to tackle the problem of stability in nanofluids. *Hayat et. al.* [32] and *Suresh et. al.* [33] are among the many who studied the effect of using two nanoparticle materials on the thermal conductivity of nanofluid. *Sahoo et. al*. [34] used a ternary hybrid nanofluid to study its thermal performance in an automobile radiator. She used CuO, CNT, and graphene nanoparticles to prepare the nanofluid and carried out an extensive study on thermal performance and exergy analysis of heat transfer in an automobile radiator. The ternary hybrid nanofluid showed superior stability and an enhancement of 19.35% in heat transfer rate along with an increase in second law efficiency by 7.2% at a coolant flow rate of 10LPM. Apart from CuO, Al_2O_3, and CNT, researchers have tried a number of nanomaterials like TiO_2 [11], ZnO [13], Ag [32], Fe_2O_3 [35], SiO_2 [36], etc, and have created a large number of options to choose from. Keeping this in mind, *Rathod et. al.* [35] developed a method to select nanoparticles from various options available such that it can give maximum thermal performance at minimum cost. This study is based on the multiple attribute decision-making (MADM) method in which relative weights are assigned to each attribute in the first place and then arranged in order of preference. Weights relative to attributes are assigned using the analytical hierarchy method (AHP) and the order of preference is based on the technique for order preference by similarity to the ideal solution (TOPSIS) method. On the basis of their research, based on the algorithm described above, they suggest CuO and Al_2O_3 as the first and the second preference respectively, for use in preparation of nanofluids.

2.2 Research Gap

Though much improvement has been made from the earliest coolants once used in automobile radiators, the ever-increasing tendency of reducing the size of radiators in automobiles requires a plethora of research to be done in the field of nanocoolants heat transfer enhancement.

- Much research on nanocoolants has been conducted using water or ethylene glycol. However the effects of ethylene glycol on the environment are much more serious due to its toxic nature, so there is a need to develop some new coolants (*Green-Coolants)* [13].
- Recently, the ASTM has approved standards for the use of glycerol as automobile coolants, thus opening up huge scope for research in the field of nanocoolants having base fluid as glycerol.
- Though researchers have started to shift their focus from glycol-based coolants to glycerol-based coolants, still it is an early phase in this direction. Therefore further studies are required to investigate the performance of radiators using glycerol-based coolants.
- Glycerol-based nanocoolants can be a potential option in such applications, however, the issues of nanocoolant performance and their stability remains of prime concern which limits their commercial viability.

Thus, in the present study, performance of glycerol based nanocoolants and their stability have been investigated.

2.3 Objectives

Following are the research objectives

- ✓ To evaluate the thermal performance of DI water, EG based coolant, and glycerol solution in an automobile radiator
- ✓ To study the effect of coolant flow rate, air flow rate, and ambient temperature on the rate of heat transfer
- ✓ To evaluate the thermal performance of CuO/glycerol nanofluid in a radiator type heat exchanger setup
- ✓ To study the effect of nanoparticle concentration on pumping power

Vision: *To* develop an eco-friendly, non-toxic, cost-effective automobile coolant with improved thermal properties.

[This page is intentionally left blank]

CHAPTER 3: EXPERIMENTAL SETUP

3.1 Experimental Setup

To evaluate the thermal performance of coolants in automobile radiators, a specifically fabricated setup named **Radiator type heat exchanger setup** was available. This is a customized setup that allows users to vary air flow rate, coolant flow rate, coolant inlet temperature, and coolant itself. It comes with complimentary software which allows users to log data to the PC. The setup provides values of temperatures, pressures, and flow rates at various locations along the coolant and air flow. It also provides the pumping power of the water pump required to maintain a constant coolant flow rate. Figure 3 shows the radiator-type heat exchanger setup used in the experimental proceedings. The block diagram of the radiator-type heat exchanger setup is shown in Figure 4.

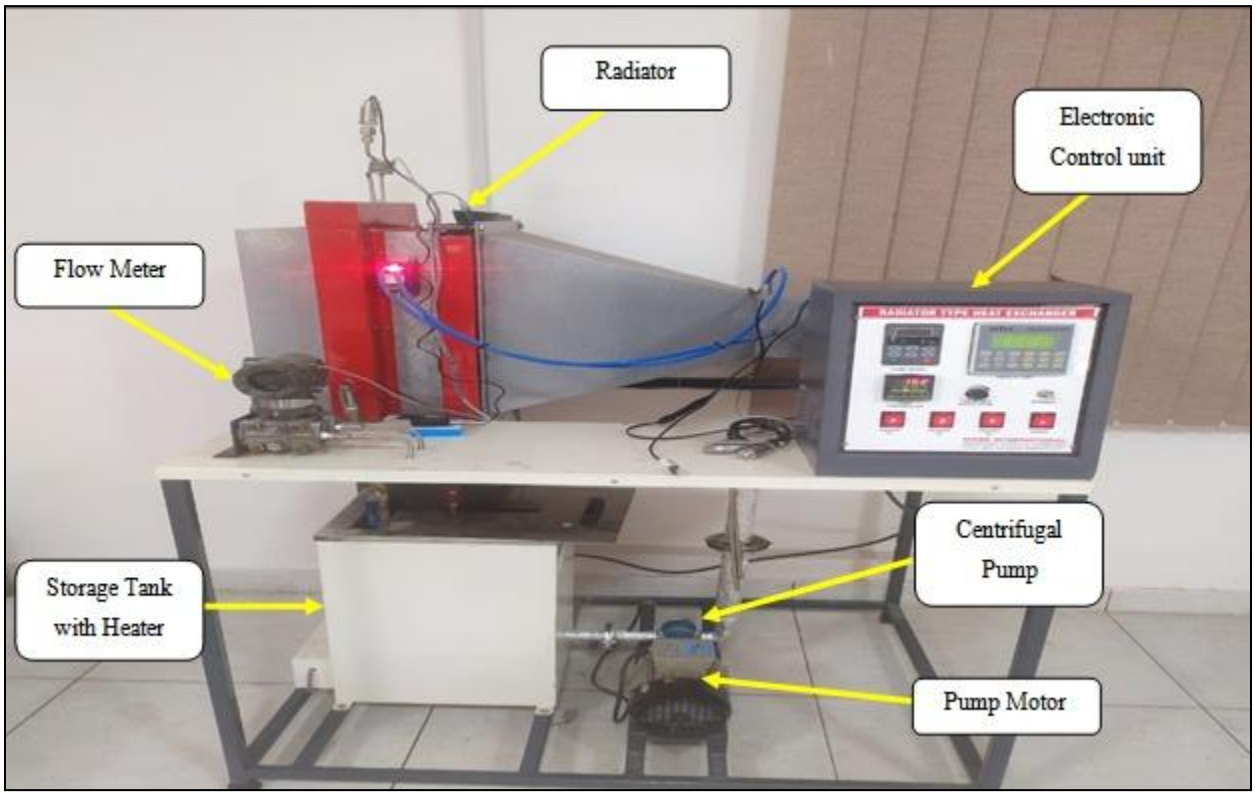

Figure 3: Radiator type heat exchanger setup

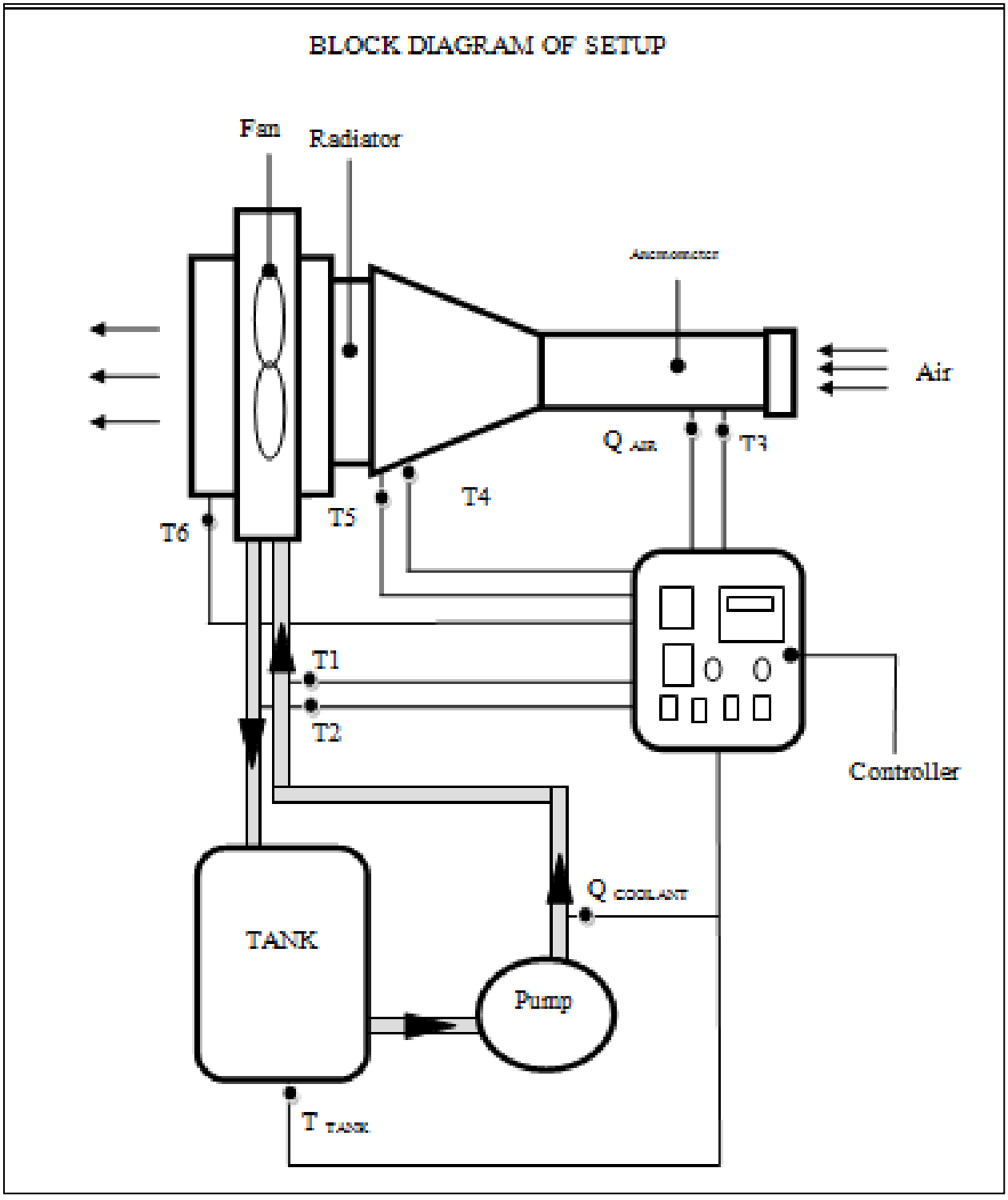

Figure 4: Block diagram of radiator type heat exchanger setup

The Radiator Type Heat Exchanger Setup consists of the following parts;

- **Radiator:** The setup uses a commercial TATA ACE radiator (as shown in Figure 5(a)) for heat exchange purposes which includes an inlet tank at the top, vertical thin tubes with rectangular cross section, and an outlet tank at the bottom. Its specifications are given in Table 1.
- **Fan:** A variable speed fan (as shown in Figure 5(a)) is placed near the radiator to obtain desired volume flow rate of air and create the effect of forced convection. The fan is placed at the air exit side of the radiator.

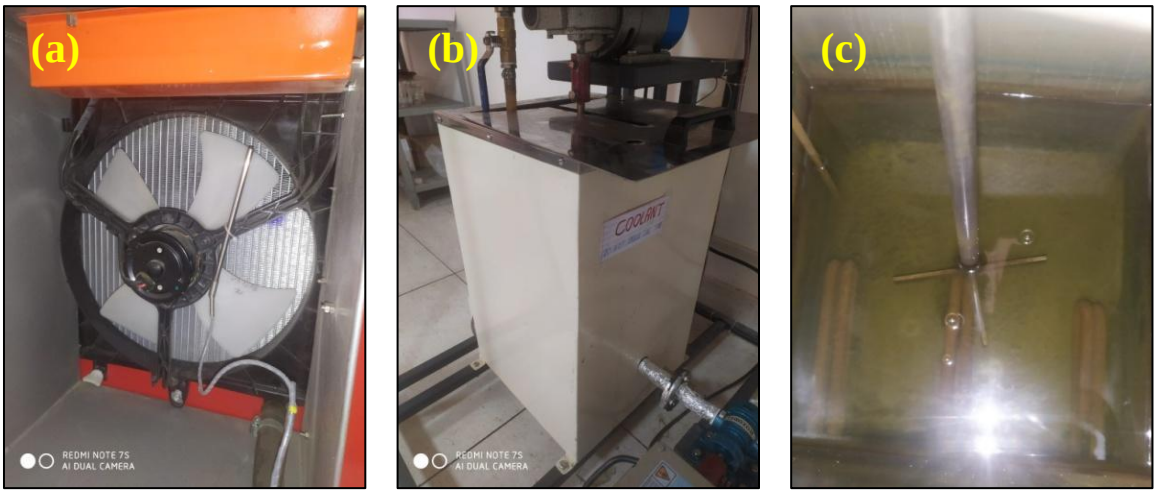

Figure 5: (a) Radiator and Fan assembly, (b) Storage tank, (c) inside view of the tank showing heating elements and stirrer

- **Tank:** A 20L Stainless Steel tank (Figure 5(b)) is used to store the coolant. It is fitted with heating elements and a stirrer.
- **Heating Elements:** Three electric heaters (shown in Figure 5(c)) of 2000W each, along with a PID controller, are used to act as a source of heat flux to the coolant and set a constant temperature of the coolant in the tank.
- **Stirrer:** A constant speed stirrer (shown in Figure 5(c)) has been provided to mix the coolant and nanoparticles uniformly in the tank.

Table 1: Specifications of various components of the radiator

Dimension	Notation	Value
Radiator Length	L_{rad}	440 mm
Radiator Breadth	B_{rad}	310 mm
Radiator Height	H_{rad}	60 mm
Tube Length	L_{tube}	400 mm
Tube Width	W_{tube}	22 mm
Tube Thickness	t_{tube}	2.5 mm
Tube wall thickness	dt_{tube}	0.1 mm
Number of tubes	N_{tube}	34
Fin length	L_{fin}	9 mm
Fin thickness	t_{fin}	0.5 mm
Fin width	W_{fin}	22 mm
Number of fins	N_{fin}	8976
Tube thermal conductivity	k_{tube}	238 W/mK
Fin thermal conductivity	k_{fin}	238 W/mK

- **Pump and motor assembly:** A centrifugal pump (Figure 6(a)) is used to make the coolant flow through the circuit with the help of an induction motor (0.5HP,1400rpm)
- **Flow Meter:** A differential pressure type flow meter (as shown in Figure 6(b)) is used to measure the flow rate of coolant through the radiator.

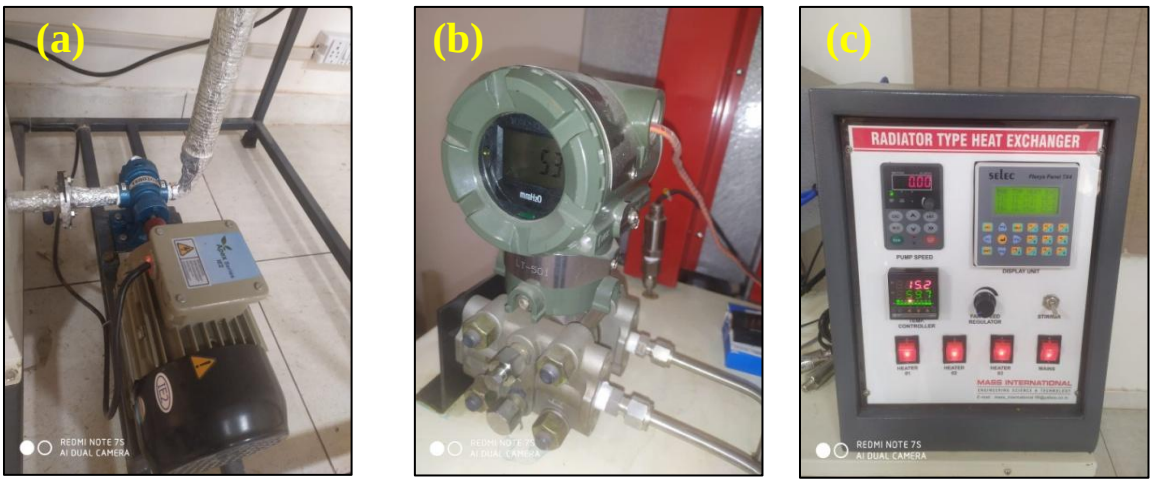

Figure 6: (a) Pump and motor assembly, (b) flow meter, (c) Electronic controller

- **Electronic Controller:** An electric controller (shown in Figure 6(c)) has been provided to adjust/set/control the variable parameters like flow rates of air and coolant, coolant inlet temperatures, etc.
- **Pressure Sensor:** four coil type pressure sensors can be employed at desired locations, but are not employed yet.
- **Anemometer:** A hot wire anemometer is used to determine the volume flow rate of air flowing through the inlet duct.
- **Thermocouples:** A number of k-type thermocouples have been placed at various locations (as shown in Figure 7) such as coolant tank, coolant inlet to the radiator, coolant outlet from the radiator, air inlet to the radiator, air outlet to the radiator, fins of radiator and ambient air temperature.

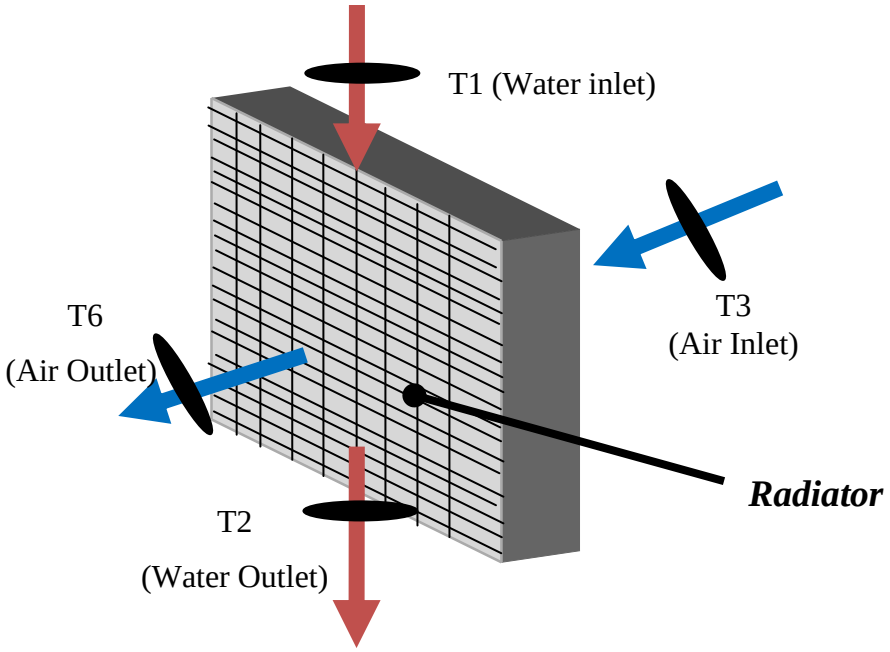

Figure 7: Location of various thermocouples across the radiator

- **Software:** The Radiator type heat exchanger comes with dedicated software that logs the data to the PC/system for further processing.

3.2 Auxiliary Equipments

- **Magnetic Stirrer with hot plate:** to mix nanoparticles in the base fluid.(Figure 8(a))
- **TDS meter:** to measure TDS of water to check for its purity.(Figure 8(b))

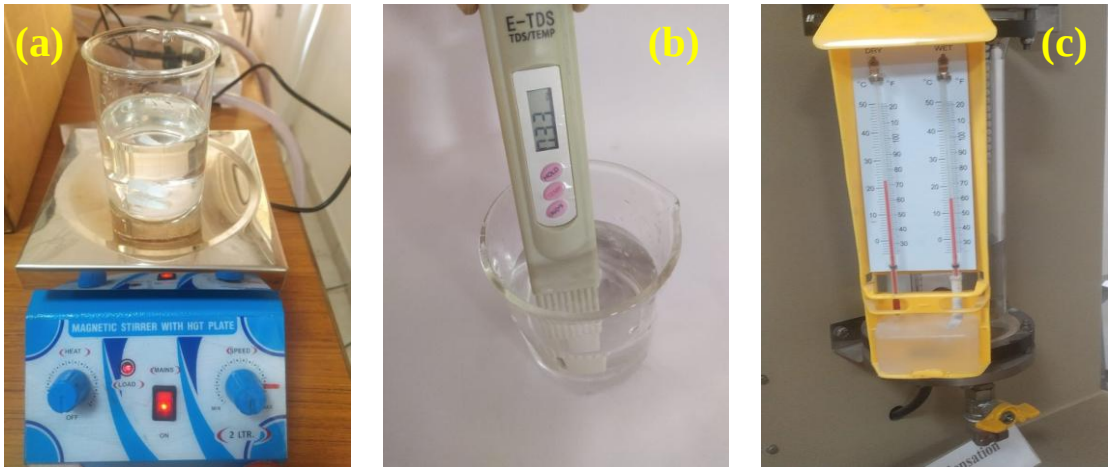

Figure 8: (a) Magnetic stirrer, (b) TDS meter, (c) Hygrometer

- **Wet and Dry Bulb Hygrometer:** to measure the relative humidity of the air. (Figure 8(c))
- **Decagon KD2 Pro:** to measure the thermal conductivity of nanofluids. (Figure 9(a))
- **Electronic weighing balance:** to measure the desired mass of nanoparticle. (Figure 9(b))
- **Bath type Ultra-Sonicator:** to disperse nanoparticles uniformly in the base fluid. (Figure 9(c))

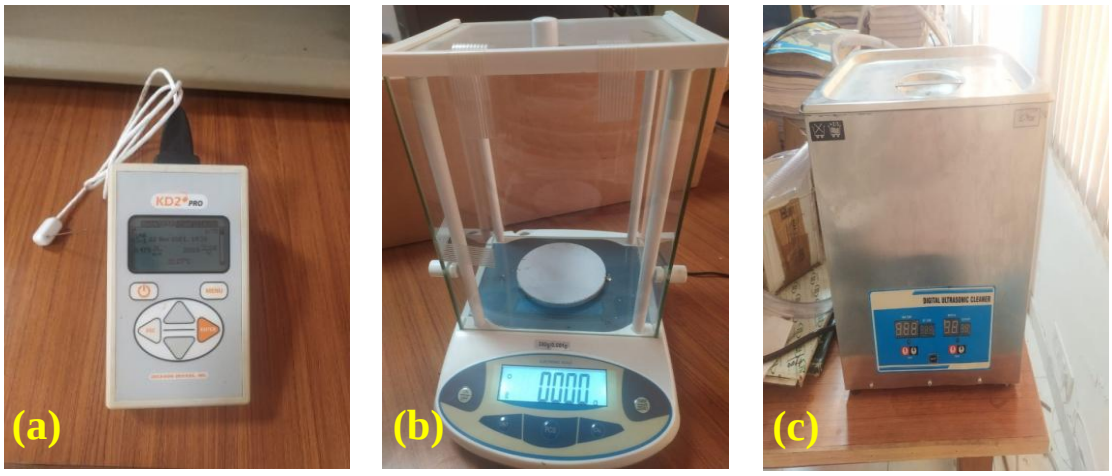

Figure 9: (a) KD2 Pro, (b) Electronic weighing machine, (c) Bath-type Ultrasonicator

3.3 Equipment Uncertainty

The uncertainty of equipment is the general fluctuation of values during the experimental observations or the least count of the equipment (i.e. precision) if the values appear to be relatively stable.

Equipment uncertainty for various quantities measured using the equipment is given in Table 2.

Table 2: Equipment / measurement uncertainty

Equipment	Measured quantity	Symbol	Uncertainty
DP flow meter	Coolant flow rate	$\dot{\forall}_c$	± 0.1 lpm
Hot wire anemometer	Air flow rate	$\dot{\forall}_a$	± 50 lpm
k-type thermocouples	Various temperatures	T_1, T_2, T_3, T_6, T_A, T_{tank},	± 0.1 °C
Voltmeter	Voltage	V	± 1Volt
Ammeter	Current	I	± 0.1 Amp
TDS meter	TDS	TDS	± 0.1 ppm
KD2 Pro	Thermal conductivity	k	± 0.005 W/mK
Electronic weighing balance	Mass of nanoparticles, SDS	m_{np}	± 0.001 grams
Dry and wet bulb hygrometer	DBT, WBT	DBT, WBT	±0.1 °C

[This page is intentionally left blank]

CHAPTER 4: METHODOLOGY

The successful completion of any work depends on the methodology followed to perform it. Thus, it is important to develop the methodology carefully in any research work. The methodology followed during the research work is divided into two sections. In the first part, simple experiments were performed using DI water to study the effect of coolant flow rate, air flow rate, and ambient temperature on the temperature drop, and rate of heat transfer. Similar experiments were also performed with an EG based coolant and a glycerol solution of strength 40% *by vol*ume (at room temperature). The next section deals with the preparation, characterization, and experimental investigation of CuO/glycerol solution-based nanofluid. Once the nanofluid is prepared and characterized for its thermo-physical properties, the experimental procedure as mentioned in section 4.1.2 is followed to evaluate the thermal performance of the nanofluid. The same procedure is repeated using nanofluids of different concentrations.

4.1 Parametric thermal performance evaluation based on DI water, EG based coolant and glycerol solution

This section contains the methodology followed, the variable parameters of the setup, the experimental procedure of radiator type heat exchanger and KD2 Pro, Data reduction from raw data available as observations of experiments, and the mathematical modeling of temperature values to useful quantities like temperature drop and rate of heat transfer.

4.1.1 Methodology

To have a good understanding of the automobile radiator cooling phenomenon and hands-on experience with it, a number of experiments were performed by varying liquid/coolant flow rate, air flow rate, and ambient temperature on the heat transfer rate of the radiator. Apart from changing the variable parameters, experiments were also conducted by changing the coolant to conduct a comparative study on the rate of heat transfer and pumping power. Using Radiator Type Heat Exchanger Setup the following parameters were varied, to study their effect on the rate of heat transfer:

1. **Coolant Flow Rate**: Coolant flow rate was varied using a variable speed centrifugal pump to study the effect of six different coolant flow rates: *1,2,4,6,8,12 lpm*
2. **Coolant Inlet Temperature**: using a PID controller, coolant inlet temperature or storage tank temperature was maintained at 60 °C.
3. **Air Flow Rate**: The air flow rate was varied using a variable speed electric fan, to study the effect of three different air flow rates: *7636, 8707, 10250 lpm*
4. **Coolant**: after performing experiments on *DI Water,* experiments were performed using *EG based coolant, and Glycerol solution* to study their thermal performance.
5. **Ambient Air Temperature**: effect of ambient temperature was also studied when the temperature dropped from *28℃ to 18℃* due to seasonal change.

4.1.2 Experimental Procedure

The following experimental procedure was followed to perform the experiments on the radiator-type heat exchanger and KD2 Pro:

(a) Radiator-type heat exchanger

Step 1: Calibration of coolant flow meter
(The coolant flow meter needs to be calibrated before each experiment to ensure that the readings are accurate and within the desirable range of uncertainty. Calibration of flow meter is achieved when the meter shows zero pressure difference across it (when the pump is in off state) i.e., zero value of coolant flow rate when the pump is off).

Step 2: Coolant flow rate, coolant temperature, and air flow rate are set to the desired value using the digital control panel.

Step 3: Values of temperatures, flow rates, and pressures are logged to the PC using the dedicated software after 1 min interval.
(This is done till the last 20 values stabilize i.e. variation in temperature is less than ±0.1 deg C. This usually takes around 50-60 minutes).

Step 4: The heater is switched off to allow the coolant to cool down to room temperature. (Usually takes around 15-20 minutes).

Step 5: Steps 3 and Step 4 are repeated twice to obtain reliable data and to ensure repeatability of experimental results.

Note: Similarly, various sets of experiments are performed using different combinations of variable parameters like coolant flow rate, air flow rate, coolant temperature, coolant, ambient conditions, etc.

Total experiments performed (in Section 4.1): 60 sets of experiments (performed thrice each)

(b) KD2 Pro

Step 1: Calibration of KD2 Pro
(The KD2 Pro is calibrated with the specimen of glycerol provided along with it to ensure its accuracy. The values usually show errors of less than 0.005 W/mK while the permissible error tolerance is that of 0.01W/mK, as prescribed by the manufacturer).

Step 2: Measurement of thermal conductivity of the sample
(This is done three times, after an interval of 30 minutes each, to ensure the reliability and accuracy of results thus obtained.)

4.1.3 Data Reduction

The raw data obtained from radiator-type heat exchanger software is processed in MS Excel to reduce it to the directly usable parameters.

Step 1: The last 20 (stable) values of the raw data, of each set of readings, obtained from the software are averaged and noted on a separate worksheet as shown in Figure 10.

Step 2: The same method is repeated for all the three readings of same operating conditions. Then they are further averaged out to get the most reliable figures along with the associated error in it. (as shown in Figure 10)

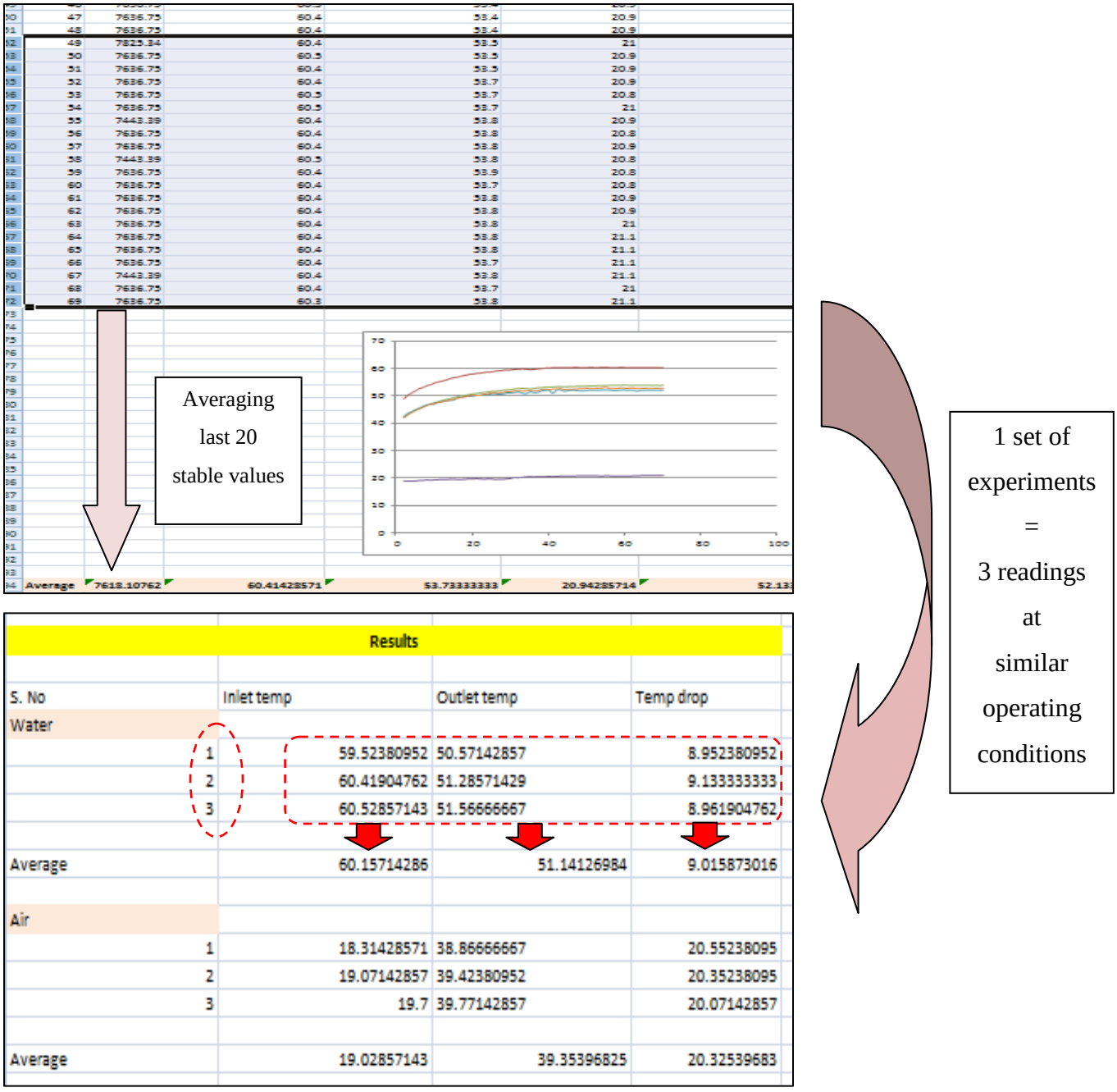

Figure 10: Calculations for data reduction of raw data (representative only)

Step 3: The values of temperatures thus obtained are noted on another worksheet to compute and analyze the results (shown in the representative form in Figure 11), using mathematical modeling described in section 4.1.4.

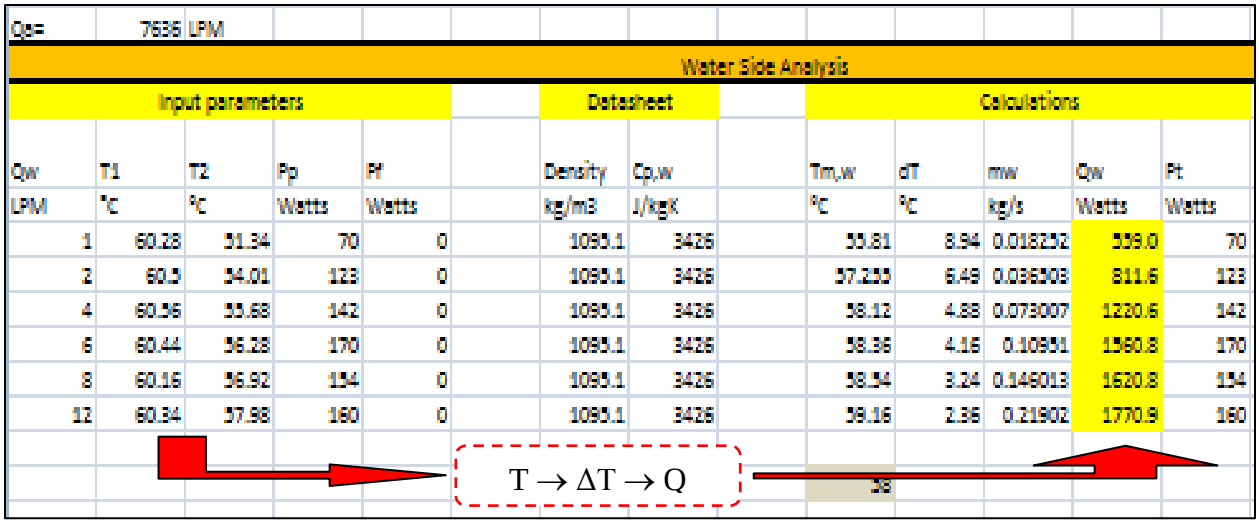

Qs= 7636 LPM

Water Side Analysis

Input parameters					Datasheet		Calculations				
Qw	T1	T2	Pp	Pf	Density	Cp,w	Tm,w	dT	mw	Qw	Pt
LPM	°C	°C	Watts	Watts	kg/m3	J/kgK	°C	°C	kg/s	Watts	Watts
1	60.28	51.34	70	0	1095.1	3426	55.81	8.94	0.018252	559.0	70
2	60.5	54.01	123	0	1095.1	3426	57.255	6.49	0.036503	811.6	123
4	60.56	55.68	142	0	1095.1	3426	58.12	4.88	0.073007	1220.6	142
6	60.44	56.28	170	0	1095.1	3426	58.36	4.16	0.10951	1560.8	170
8	60.16	56.92	154	0	1095.1	3426	58.54	3.24	0.146013	1620.8	154
12	60.34	57.98	160	0	1095.1	3426	59.16	2.36	0.21902	1770.9	160

Figure 11: processing of raw data to useful results (representative only)

4.1.5 Mathematical Modeling

On getting the raw data processed after data reduction in Section 4.1.3, averaged values of the following parameters (input parameters) are obtained:

- T_1: Coolant inlet temperature (°C)
- T_2: Coolant exit temperature (°C)
- T_3: Air inlet temperature (°C)
- T_6: Air outlet temperature (°C)
- ∀c : Coolant flow rate (lpm)
- ∀a : Air flow rate (lpm)
- DBT: Dry Bulb Temperature (ambient) (°C)
- WBT: Wet Bulb Temperature (ambient) (°C)

The most desired quantity to be determined from the experiments is the heat transfer rate of air and coolant, calculated using Eq.(1):

$$\dot{Q} = \dot{m} \times C_P \times \Delta T \quad (1)$$

where, $\dot{m}$ is mass flow rate calculated using Eq. (2)

$$\dot{m} = \rho \times \dot{\forall} \quad (2)$$

ΔT is the temperature drop, given by Eq.(3)

$$\Delta T = T_1 - T_2 \tag{3}$$

Table 3 shows the values of density, specific heat capacity of Air, DI water, ethylene glycol, glycerol and their aqueous solutions determined at bulk mean temperature calculated using Eq.(4):

$$T_m = \frac{T_{in} + T_{out}}{2} \tag{4}$$

To calculate the values of density and specific heat capacity for ethylene glycol based coolant and glycerol solution, Eq.(5) and Eq.((6) have been used.

$$\rho_{mix} = \frac{\rho_A \times V_A + \rho_B \times V_B}{V_A + V_B} \tag{5}$$

$$C_{p,mix} = \frac{\dot{m}_A C_{p,A} + \dot{m}_B C_{p,B}}{\dot{m}_A + \dot{m}_B} \tag{6}$$

Table 3: Properties of Air, DI Water, EG, Glycerol, and their aqueous solutions

Coolant	Density	Specific heat capacity	Bulk Mean Temperature
Air	1.165 kg/m^3	1006 J	35 °C
DI Water	985 kg/m^3	4180 J	56 °C
Ethylene glycol (pure)	1110 kg/m^3	2433 J	50 °C
Glycerol (pure)	1260 kg/m^3	2350 J	50 °C
Ethylene glycol (mix-50%)	1095 kg/m^3	3426	56 °C
Glycerol (mix - 40%)	1085 kg/m^3	3409	56 °C

Values of DBT and WBT are used to determine the relative humidity of ambient air using a relative humidity table.

Voltage and Current Values are taken from the digital display of the console to calculate the power consumption of pump using the Eq.(7)

$$Pumping\ Power = Voltage \times Current \tag{7}$$

4.2 Thermal Performance Evaluation of CuO/Glycerol Nanocoolant

After successful testing of glycerol solution as a coolant in the radiator-type heat exchanger, it was decided to test glycerol-based nanocoolant for thermal performance evaluation using the same setup. The use of CuO nanoparticles was decided by using the MDMA approach mentioned by [35].

4.2.1 Methodology

This section comprises the methodology followed to prepare, characterize and study the thermal performance of CuO/glycerol nanocoolant of different concentrations. Apart from the characterization of nanofluid, nanoparticles were also characterized before preparing nanofluid. To obtain the results in quantitative form, parameters such as temperature drop across the radiator, rate of heat transfer, and Overall heat transfer coefficient have been calculated and utilized for comparison of nanofluids of different concentrations. In total 4 concentrations (0%, 0.5%, 1.0%, and 1.5% *by vol*.) of nanofluid have been prepared by using a two-step method, and tested for 6 different coolant flow rates in the Radiator type heat exchanger setup.

Before nanofluid preparation, the nanoparticles were characterized for their crystalinity (using XRD), particle size (using SEM), and chemical composition (using EDS or EDAX). Thermophysical properties of nanofluid have been determined by using Eq. (9), (10), (11), and (16). Section 4.2.2 outlines the materials and methods used to prepare the nanofluid, and its characterization.

After nanofluid characterization, it is used in the radiator-type heat exchanger setup where it is tested for six different coolant flow rates (1, 2, 4, 6, 8, and 12 lpm) by following the experimental procedure as mentioned in section 4.1.2. The data obtained from the radiator-type heat exchanger is then reduced to usable parameters like temperature drop and rate of heat transfer as explained in section 4.1.3. Section 4.2.3 gives information on variable parameters and operating conditions during the experiments. Apart from determining the temperature drop and heat transfer rate; the Nusselt number, CHTC, and overall heat transfer coefficients of both air and coolant sides were also determined (explained in section 4.2.4).

4.2.2 Materials and Methods

This section describes the materials used in pursuance of the study, and the methods undertaken to prepare and characterize the nanoparticles, and nanofluids.

(a) Materials

Copper Oxide (CuO) Nanoparticles of purity at least 99% and of size 30nm to 50nm were purchased from AdNano Technologies, India. Glycerol of 99% purity was purchased from Bharat Chemicals and Instruments, India. DI water of TDS less than 31ppm was used wherever required. Sodium dodecyl sulfate bought from Lobachemie, India was used as surfactant. All materials used in the present work were of analytical grade. A magnetic stirrer and bath-type ultrasonicator were employed to homogeneously mix nanoparticles in the base fluid. To test the thermal conductivity of nanofluids, Decagon KD2Pro was used.

(b) Nanoparticle Characterization

CuO (copper (II) oxide) nanoparticles, of 99% purity, were purchased from AdNano Technologies, India. The bulk density of CuO nanoparticles is 0.66 g/cc. Before preparing nanofluid, nanoparticles were characterized for their shape, size, and elemental composition using XRD spectroscopy and SEM and EDS techniques. A cold field emission scanning electron microscope (Carl Zeiss Sigma 500) and an Energy Dispersive X-ray Spectrometer (Bruker, QUNTAX 200) were employed to determine the morphological characteristics of nanoparticles. An X-ray Diffractometer (Xpert Pro) was used to determine the phase of nanoparticles present.

(c) Nanofluid Preparation

Nanofluids can be prepared by using either the one-step method or the two-step method. Though the stability of nanofluids prepared using the one-step method is extraordinarily higher than that obtained by using the two-step method, most researchers use the two-step method for the preparation of nanofluids due to its simplicity and economics of preparation. In the two-step method, the first step includes synthesis or procurement of nanoparticles which are then dispersed in the base fluid in the second step. Nanoparticles tend to agglomerate over time due to strong van-der Waals interactions and thus physical and/or chemical treatment is always desired to keep them dispersed uniformly in the base fluid. Ultrasonication, surfactants, high shear

mixing, and stirring are usually employed to achieve the stability of nanofluids for a long period of time.

Hence, the CuO/glycerol nanofluid was prepared using SDS surfactant with a two-step method. Base fluid was prepared by mixing pure glycerol with DI water in a 40:60 ratio. Thereafter, CuO nanoparticles were dispersed in glycerol solution (base fluid) using a magnetic stirrer and bath-type ultrasonicator.

To prepare nanofluids of different volume concentrations, a known quantity of nanoparticles of CuO is added to the base fluid. Base fluid was taken as a mixture of 40% *by vol*. Glycerol (Glycerin) and 60% *by vol*. DI Water. The amount of nanoparticles required was calculated using the formula given by Eq.(8) :

$$\emptyset = \frac{\frac{m_{np}}{\rho_{np}}}{\frac{m_{np}}{\rho_{np}} + \frac{m_{bf}}{\rho_{bf}}} \tag{8}$$

Where, m_{np} stands for the mass of nanoparticle, m_{bf} for the mass of base fluid, ρ_{np} for bulk density of nanoparticles and ρ_{bf} for density of the base fluid.

The required quantity of CuO nanoparticles and SDS surfactant were added to the base fluid and stirred for 30 minutes using a magnetic stirrer. The solution thus obtained was ultrasonicated for 120 minutes using a bath-type ultra-sonicator to obtain a homogeneously mixed nanofluid solution.

Thus, samples of 0.5%, 1.0%, and 1.5% *by vol*. were prepared using this method.

(d) Nanofluid Characterization

The density and specific heat of the nanofluids have been calculated using the correlations (9) and (10), respectively:

$$\rho_{nf} = \varphi\rho_{np} + (1-\varphi)\rho_{bf} \tag{9}$$

$$C_{p,nf} = \varphi\left(\frac{\rho_{np}}{\rho_{nf}}\right)C_{p,np} + (1-\varphi)\left(\frac{\rho_{bf}}{\rho_{nf}}\right)C_{p,bf} \tag{10}$$

where, subscripts nf, np, and bf refer to nanofluid, nanoparticle, and base fluid respectively, and φ represents volume fraction of nanoparticles in nanofluid and others have their usual meaning.

To determine the dynamic viscosity and effective thermal conductivity of nanofluids, various models have been proposed by researchers.

Wang's [37] model: $$\mu_{nf} = \mu_{bf} * (1 + 7.3\varphi + 123\varphi^2) \quad (11)$$

Einstein's [38] model: $$\mu_{nf} = \mu_{bf} * (1 + 2.5\ \varphi) \quad (12)$$

Pak and Cho's [38] model: $$\mu_{nf} = \mu_{bf} * (1 + 39.11\ \varphi\ + 533.9\varphi^2\ ) \quad (13)$$

Batchelor's [38] model $$\mu_{nf} = \mu_{bf} * (1 + 2.5\ \varphi\ + 6.5\varphi^2\ ) \quad (14)$$

Brinkman's model [39]: $$\mu_{nf} = \mu_{bf} * \left(\frac{1}{(1-\varphi)^{2.5}}\right) \quad (15)$$

In this study, the model proposed by Wang et. al. [37] has been used to determine the dynamic viscosity of nanofluid.

Likewise, there are a number of models present to determine the thermal conductivity of nanofluids.

Maxwell's model [37] : $$\frac{K_{nf}}{K_{bf}} = 1 + \left(\frac{3 * \left(\frac{K_{np}}{K_{bf}} - 1\right) * \varphi}{\left(\frac{K_{np}}{K_{bf}} + 2\right) - \left(\frac{K_{np}}{K_{bf}} - 1\right)\varphi}\right) \quad (16)$$

Hamilton and Crosser's model [40]: $$\frac{K_{nf}}{K_{bf}} = \left[\frac{K_{np} + (n-1)K_{bf} - \varphi(n-1)(K_{bf} - K_{np})}{K_{np} + (n-1)K_{bf} + \varphi(K_{bf} - K_{np})}\right] \quad (17)$$

Where, n is shape factor: n = 3 for spherical nanoparticles

Bruggeman's model [41] : $$\varphi\left[\frac{K_{np} - K_{eff}}{K_{np} + 2K_{eff}}\right] + (1 - \varphi)\left[\frac{K_{bf} - K_{eff}}{K_{bf} + 2K_{eff}}\right] = 0 \quad (18)$$

The model presented by Maxwell et. al. [37] has been used in this study to determine the thermal conductivity of nanofluid.

4.2.3 Variable Parameters and Operating Conditions

Unlike the experiments done in the previous section, not too many parameters have been changed to study their effect on the heat transfer performance of the coolant. To investigate the enhancement in the heat transfer rate of coolant, nanofluids of different concentrations have been used across different coolant flow rates. Other variable parameters such as air-flow rate, coolant inlet temperature, etc have been kept constant at 8707 lpm and 60 °C respectively. The ambient conditions such as temperature and relative humidity have been tried to be the same during all

the experiments but minor fluctuations could not be controlled. The following table provides information about various parameters, their values, and uncertainty/error:

Table 4: Variable parameters and operating conditions during experiments

Parameter / Variable	**Notation**	**Value(s)**	**Unit**	**Uncertainty**
Coolant volume flow rate	$\forall_{liq}$	1,2,4,6,8,12	lpm	± 0.1 lpm
Coolant Inlet Temperature	T1	60	°C	± 1 °C
Nanoparticle concentration	φ	0, 0.5, 1.0, 1.5	% *by vol*. conc.	± 0.01 %
Air volume flow rate	$\forall_{air}$	8707	lpm	± 50 lpm
Air Inlet Temperature	T3	20	°C	± 1 °C
Relative Humidity of ambient air	RH	45	%	± 3%

4.2.4 Mathematical modeling

The temperature values have been modeled into overall heat transfer coefficients using two different approaches, to differentiate the experimental (using the LMTD method) and theoretical (using Nusselt number correlations) parts and validate the experimental results.

(a) Using the LMTD method (Experimental Results)

The heat transfer rate of the coolant side and air were calculated using Eq. (19) and (20), respectively.

$$\dot{Q}_c = \dot{m}_c \times C_{p,c} \times \Delta T_c \tag{19}$$

$$\dot{Q}_a = \dot{m}_a \times C_{p,a} \times \Delta T_a \tag{20}$$

where, $\dot{m}$ is the mass flow rate, C_p represents the specific heat and ΔT is the temperature drop/gain by the fluid. Subscripts c and a represent coolant and air respectively.

The mass flow rate is calculated using Eq. (2).

To further mitigate the randomness of results, the average heat transfer rate is calculated by using Eq. (21)

$$\dot{Q}_{ave} = (\dot{Q}_c + \dot{Q}_a)/2 \quad (21)$$

Overall heat transfer coefficient for both coolant (inner) and air (outer) sides have been calculated by using the relations given by Eq. (22) and (23), respectively.

$$U_{i,exp} = \frac{\dot{Q}_c}{A_i\, \Delta T_{lm}} \quad (22)$$

$$U_{o,exp} = \frac{\dot{Q}_a}{A_o\, \Delta T_{lm}} \quad (23)$$

where subscripts *i* and *o* represent values on the inner and outer sides respectively. *A* represents the area of the heat exchange surface and ΔT_{lm} is the Log Mean Temperature Difference (LMTD) across the radiator, calculated by Eq. (24)

$$\Delta T_{lm} = \frac{\Delta T_1 - \Delta T_2}{\ln\left(\frac{\Delta T_1}{\Delta T_2}\right)} \quad (24)$$

where, ΔT_1 and ΔT_2 represent the temperature difference between the two heat transfer fluids at the inlet and exit of a cross-flow heat exchanger, given by Eq. (25) and (26), respectively.

$$\Delta T_1 = T_{hot,in} - T_{cold,in} = T_1 - T_3 \quad (25)$$

$$\Delta T_2 = T_{hot,out} - T_{cold,out} = T_2 - T_6 \quad (26)$$

(b)Using Nusselt number correlations (Theoretical Results)

Nusselt Number is a function of Reynolds number and Prandtl Number Eq.(27) . Many correlations exist for different flow conditions as Nusselt number depends on a number of factors such as forced convection/ free convection, constant temperature heat transfer/constant flux heat transfer and geometry of the heat transferring area, etc.

$$Nu = f(Re, \mathrm{Pr}) \quad (27)$$

Sieder-Tate correlation [42] for laminar flow regime is provided in the Eq.

$$Nu = 1.86\left(\frac{RePr}{L/D_h}\right)^{\frac{1}{3}}\left(\frac{\mu}{\mu_s}\right)^{0.14} \quad (28)$$

Shah and London [43] provides another correlation for laminar flow region given by Eq.

$$Nu = 4.364 + 0.0722\left(\frac{RePrD_h}{L}\right) \quad (29)$$

Maiga et. al. [44] suggests a correlation for fully developed laminar flow region, given in Eq.

$$Nu = 0.28\, Re^{0.35}\, Pr^{0.3} \tag{30}$$

Dehghandokht et. al. [45] provides a correlation for flow through a compact heat exchanger, given in Eq.

$$Nu = 0.951\, Re^{0.173} Pr^{1/3} \tag{31}$$

After much consideration, the correlation given by Maiga et. al. [44] was selected for air-side Nusselt number calculation, and that provided by Dehghandokht et. al. [45] was selected for coolant-side Nusselt number calculation.

for air side, $$Nu = 0.28\, Re^{0.35}\, Pr^{0.36}$$

for tube side, $$Nu = 0.951\, Re^{0.173} Pr^{1/3}$$

Reynolds Number and Prandtl Number are calculated using the relation given by Eq. (32) and (33), respectively:

$$Re = \frac{\rho \times \mathrm{v} \times D_h}{\mu} \tag{32}$$

$$\mathrm{Pr} = \frac{\nu}{\alpha} = \frac{C_p \times \mu}{k} \tag{33}$$

where, D_h represents hydraulic diameter, and v represents the velocity of the fluid (air and coolant) calculated using Eq. (34), (35), and (36),(other symbols having their usual meaning)

$$D_h = \frac{4A}{P} \tag{34}$$

$$v_{air} = \dot{\forall}_{air} / A_{rad,net} \tag{35}$$

$$v_{coolant} = \dot{\forall}_{coolant} / A_{tube,net} \tag{36}$$

$\dot{\forall}$ represents the volume flow rate of fluid and $A_{rad,net}$, $A_{tube,net}$ represents the net area of heat transfer of air and tube side respectively, calculated using Eq. (37) and (38).

$$A_{rad,net} = A_{rad} - (A_{tube,net} + A_{fin,net}) \tag{37}$$

$$= (L \times H)_{rad} - (N_{tube} \times L_{tube} \times t_{tube} + N_{fin} \times L_{fin} \times t_{fin})$$

$$A_{tube,net} = N_{tube} \times L_{tube} \times B_{tube} \tag{38}$$

Values of Prandtl Number (Pr) of air and coolant at mean bulk temperature are given in Table 5

Table 5: Values of kinematic viscosity and thermal diffusivity of fluids

Fluid	Prandtl Number (Pr)	Mean Bulk Temperature (°C)
Air	0.707	30
DI Water	3.56	50
Glycerol solution	647.74	50

Value(s) of Reynolds numbers for different coolants is also given in Table 6.

Table 6: Value(s) of Reynolds Number for different fluids

Fluid	Reynolds Number
Air	190
DI Water	72, 145, 290, 436, 581, 872
CuO/glycerol solution – 0.0% *by vol.*	27, 54, 108, 162, 216, 324
CuO/glycerol solution – 0.5% *by vol.*	26, 53, 106, 159, 213, 319
CuO/glycerol solution – *1.0% by vol.*	26, 52, 104, 157, 209, 313
CuO/glycerol solution – *1.5% by vol.*	25, 51, 102, 153, 204, 306

Convective Heat Transfer Coefficient (CHTC) is related to Nusselt Number, given by Eq. (39) :

$$h = Nu \times \frac{k}{L} \tag{39}$$

where k is the thermal conductivity of fluid and L is the characteristic length (i.e., D_h)

Once CHTC for both inner and outer surfaces are found, the overall heat transfer coefficient can be calculated from the relation given by Eq. (40):

$$\frac{1}{U_{calc}A} = \frac{1}{h_i A_i} + \frac{\delta}{kA} + \frac{1}{h_o A_o} \tag{40}$$

where, δ represents the thickness of tube wall, subscripts *i* and *o* represent inner and outer side respectively.

Note: *U_{calc} and U_{exp} are then compared for validation of experimental results and data.*

CHAPTER 5: RESULTS AND DISCUSSION

5.1 Parametric thermal performance evaluation based on DI water, EG based coolant and glycerol solution

This section comprises the analysis of results obtained from experiments performed on the radiator-type heat exchanger using DI water, EG based coolant, and glycerol solution. The section explains the effect of coolant flow rate, air flow rate, and ambient air temperature on the temperature drop and heat transfer rate of coolant. The effect of various coolants on heat transfer performance has also been studied by using an EG based coolant and glycerol solution of optimum strength.

5.1.1 Results using DI water

To have a better understanding of the working of a radiator-type heat exchanger, experiments on the setup were conducted by varying the parameters as given in Table 7.

Table 7: Value(s) of variable parameters for experiments with DI water

Variable parameter		Value(s)	Units	Uncertainty
1.	Coolant flow rate	1, 2, 4, 6, 8, 12	lpm	± 0.1 lpm
2.	Air flow rate	7636, 8707, 10250	lpm	± 50 lpm
3.	Ambient air temperature	18, 28	°C	± 1 °C
Total Experiments : 36				

Using the mathematical modeling presented in section 4.1.5, the temperature values were converted to useful quantities such as temperature drop and heat transfer rate. The results of various experiments are illustrated in the following sub-sections:

a) Effect of coolant flow rate on temperature drop
b) Effect of air flow rate on temperature drop
c) Effect of ambient temperature on temperature drop
d) Effect of coolant flow rate on the heat transfer rate
e) Effect of air flow rate on the heat transfer rate
f) Effect of ambient temperature on the heat transfer rate

(a) Effect of coolant flow rate on temperature drop

The effect of coolant flow rate on temperature drop of coolant was studied using DI Water as coolant. The temperature drop showed a decreasing trend with an increase in coolant flow rate. This inverse trend of temperature drop may be attributed to the fact that at higher flow rates, the contact time of coolant (heat source) with air (heat sink) reduces, and thus the temperature drop of coolant decreases on increasing the coolant flow rate. This trend is observed in all conditions, of varying air flow rates and ambient temperature. This trend has been validated by the results of *Asirvatham et. al*. [30], who presents a similar trend of temperature drop with coolant flow rate. Figure 12 shows the trend of temperature drop against coolant flow rate for DI water at a coolant inlet temperature of 60 °C and ambient air temperature of 28 °C. At a coolant flow rate of 1 lpm, a temperature drop of 5.86 °C is achieved, while at a coolant flow rate of 12 lpm, the temperature drop reduces to 1.72 °C.

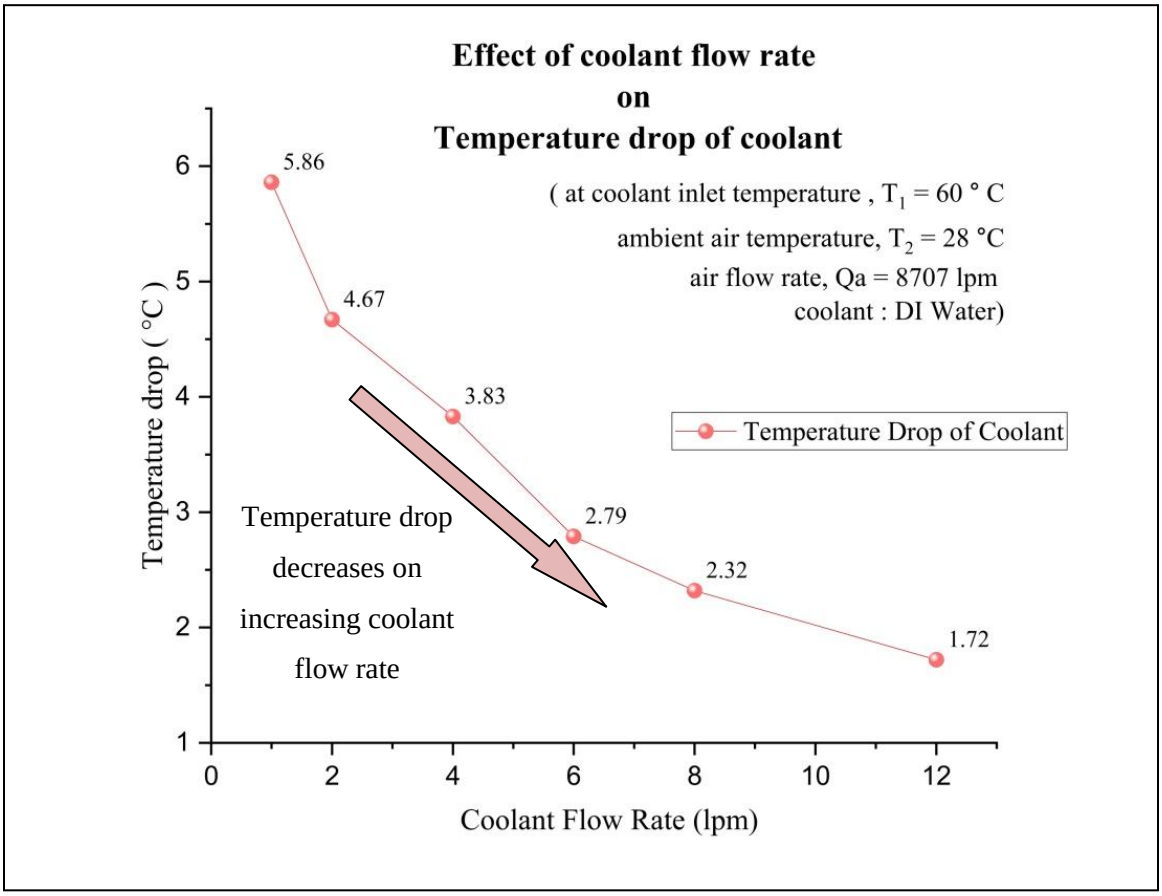

Figure 12: Effect of coolant flow rate on temperature drop of coolant (DI Water)

(b) Effect of air flow rate on temperature drop

The temperature drop of coolant (DI Water) highly depends on the air flow rate. The temperature drop increases on increasing the air flow rate. Figure 13 shows the effect of air flow rate on the temperature drop of coolant. For a coolant flow rate of 1 lpm, the temperature drop increases from 4.73 °C to 6.8 °C, increasing the air flow rate from 7636 lpm to 10250 lpm. A similar trend is observed in all such cases where the air flow rate is changed. A similar trend is also observed in a study by *Sahoo et. al.* [34] which confirms the reliability of the results obtained. The increase in a temperature drop of coolant on increasing the air flow rate can be attributed to a higher heat transfer rate at a higher flow velocity of fluids.

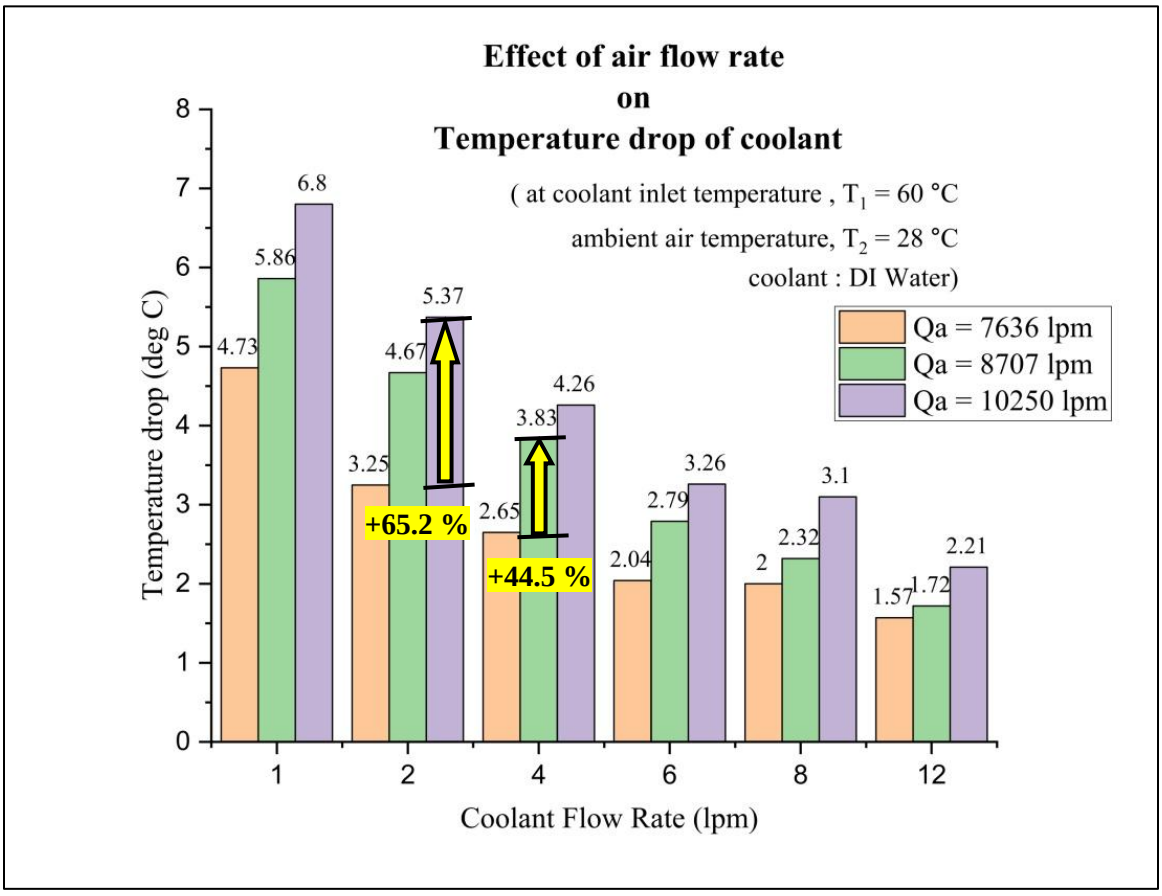

Figure 13: Effect of air flow rate on temperature drop of coolant (DI Water)

(c) Effect of ambient temperature on temperature drop

The effect of ambient temperature on the temperature drop of coolant was studied at two different ambient temperatures of 18°C and 28°C. The ambient temperature plays a major role in determining the heat transfer characteristics of coolant. The temperature drop of coolant increases when the ambient temperature decreases. Figure 14 shows the effect of ambient temperature on the temperature drop of coolant. At a coolant flow rate of 1 lpm, the temperature drop enhances from 5.86 °C to 7.81 °C, when the ambient temperature falls from 28 °C to 18 °C. A similar trend is observed for other coolant flow rates. This effect may be because of a higher heat transfer rate at lower ambient temperatures, as given by Newton's Law of cooling or convective heat transfer, Eq.(41). According to the relation, rate of heat transfer depends directly on the temperature difference between the hot surface and surrounding fluid (air).

$$Q_{conv} = h\ x\ A\ x\ (T_{surface} - T_{ambient}) \tag{41}$$

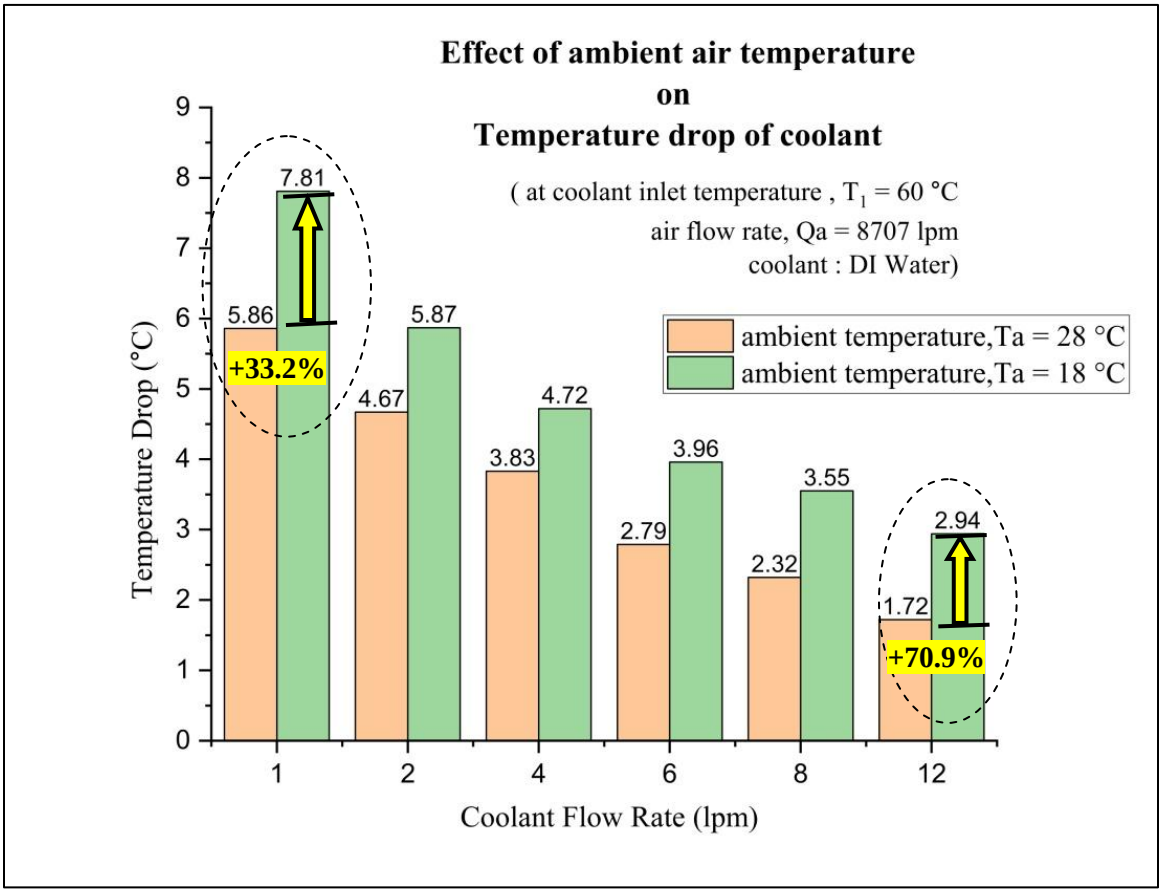

Figure 14: Effect of ambient temperature on temperature drop of coolant (DI water)

(d) Effect of coolant flow rate on the heat transfer rate

The heat transfer rate shows an increasing trend with an increase in coolant flow rate. Although the temperature drop had shown a reverse trend (decreasing), its effect is overcome by a greater increase in the mass flow rate of the coolant. Thus the overall effect of increasing the coolant flow rate is to increase the rate of heat transfer of coolant. Figure 15 shows the effect of coolant flow rate on the rate of heat transfer of coolant. At a coolant flow rate of 1 lpm, the rate of heat transfer is 402 Watts, but on increasing the coolant flow rate to 12 lpm, the rate of heat transfer increases to 1416 Watts, i.e. more than 250% increase in heat transfer rate. A similar trend is observed on all coolant flow rates, and also on varying other parameters like air flow rate and ambient temperature. The trend is similar to the results presented by *Filho et. al.* [46] thus confirming the reliability of the setup and results obtained.

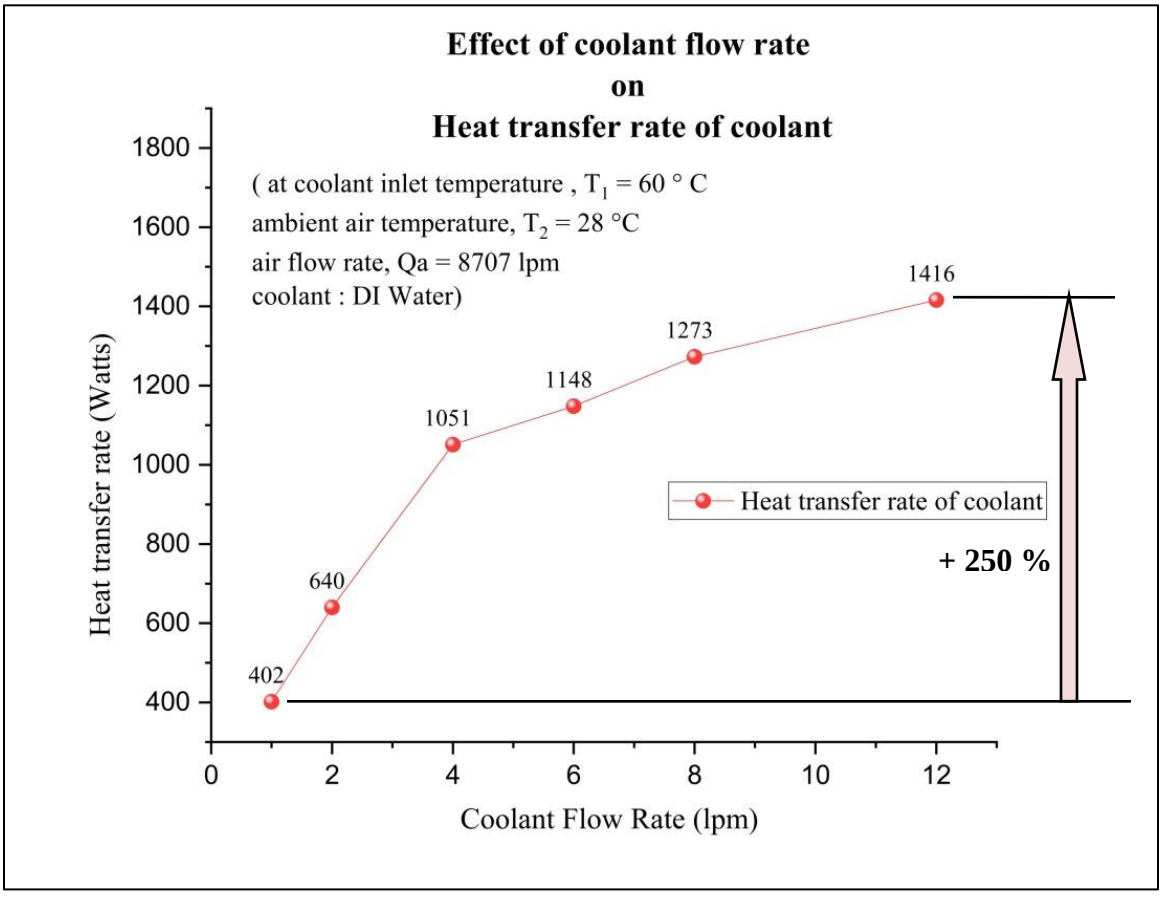

Figure 15: Effect of coolant flow rate on the heat transfer rate of coolant (DI water)

(e) Effect of air flow rate on the heat transfer rate

The heat transfer rate of coolant shows an increasing trend, on increasing the air flow rate. As the air flow rate increases, the air side convective heat transfer coefficient increases, and thus there is an increase in the heat transfer rate of coolant. Figure 16 shows the effect of air flow rate on the rate of heat transfer of coolant. To demonstrate the effect, three air flow rates of 7636 lpm, 8707 lpm, and 10250 lpm have been compared in the plot. Like the temperature drop of coolant, the heat transfer rate of coolant is also highly dependent on the rate of air flow. At a coolant flow rate of 1 lpm, the heat transfer rate increases from 324 Watts to 466 Watts on increasing the air flow rate from 7636 lpm to 10250 lpm, i.e. 43.8% increase in heat transfer rate of coolant. At a coolant flow rate of 12 lpm, the heat transfer rate increases from 1292 Watts to 1819 Watts when the air flow air rate is increased from 7636 lpm to 10250 lpm, i.e. 40.7 % increase in heat transfer rate of coolant. A similar trend is observed for other coolant flow rates also. The trend of enhancement of heat transfer rate can be verified from the results of *Sahoo et. al*. [34], which shows a similar trend of heat transfer rate enhancement.

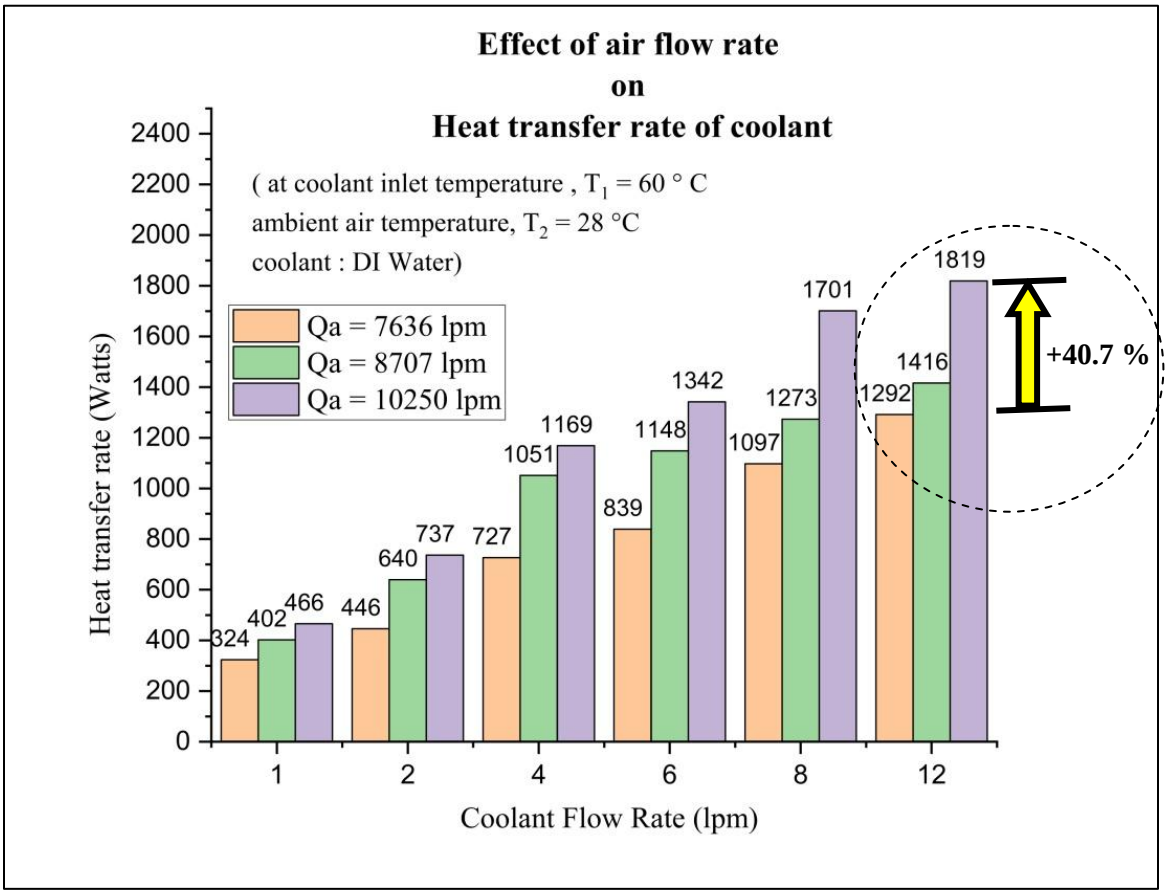

Figure 16: Effect of air flow rate on the heat transfer rate of coolant (DI Water)

(f) Effect of ambient temperature on the heat transfer rate

The ambient temperature plays a significant role in determining the heat transfer rate. According to Newton's law of cooling, the convective heat transfer rate is directly dependent on the temperature of the ambient fluid, i.e. air. The results obtained also confirm this, as the ambient temperature decreases heat transfer rate increases. Figure 17 shows the effect of ambient temperature on the rate of heat transfer of coolant. At a coolant flow rate of 1 lpm, the heat transfer rate increases from 402 Watts to 535.9 Watts when the ambient air temperature is decreased by 10° C (from 28° C to 18° C). At a coolant flow rate of 12 lpm, the heat transfer rate increases from 1416 Watts to 1869 Watts when the ambient air temperature decreases by 10 ° C. Similar results are obtained on other coolant flow rates also.

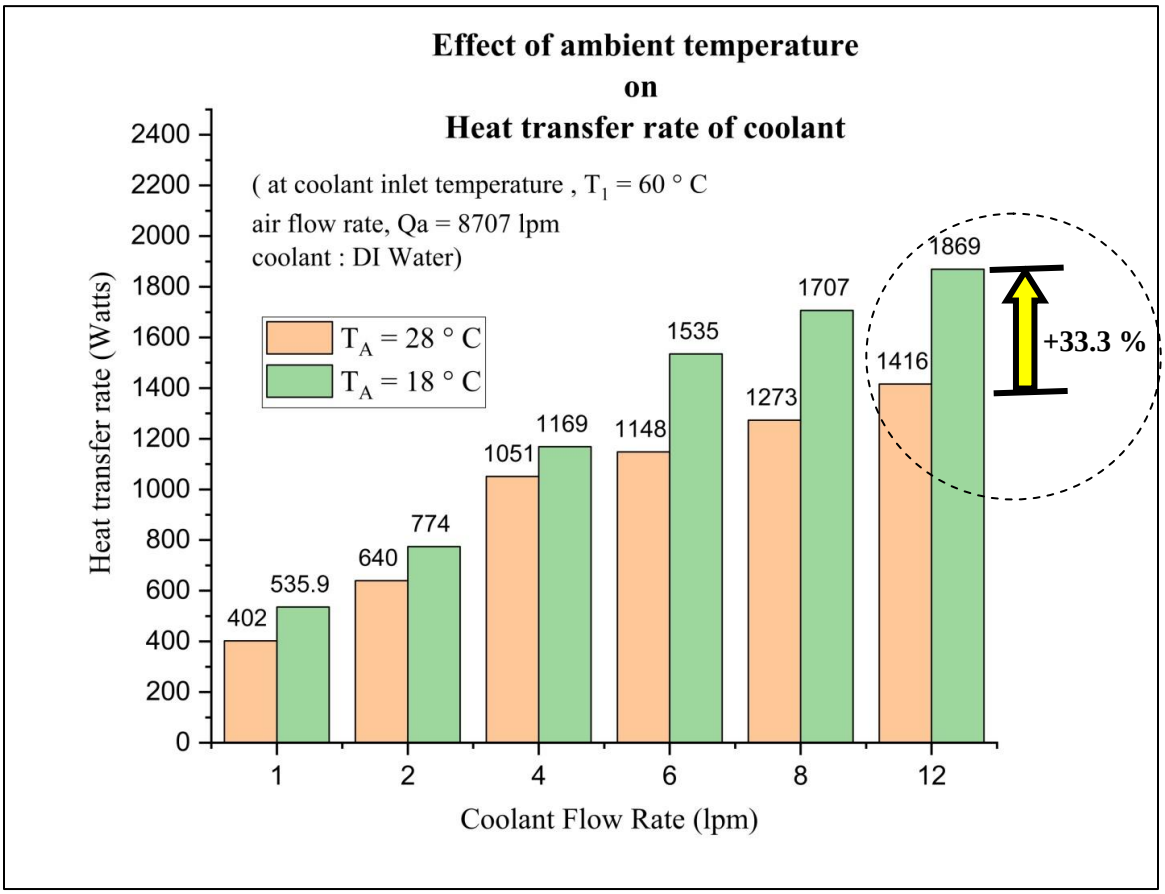

Figure 17: Effect of ambient temperature on the heat transfer rate of coolant (DI water)

5.1.2 Results using EG based coolant

After performing experiments on DI water, experiments on EG based coolant were performed. Before performing experiments, the coolant was diluted to 50% *by vol*. by adding the same amount of DI Water to the coolant. The effect of six coolant flow rates (1, 2, 4, 6, 8and 12 lpm) and two air flow rates (7636, 8707 lpm) was studied on the heat transfer rate of coolant (Table 8). Experiments were performed at an ambient temperature of 28 °C ± 1°C with a relative humidity of 45% ± 3%. A comparison of the results of EG based coolant with that of water has also been presented in this section.

Table 8: Variable parameters for experiments using EG based coolant

Variable parameter		Value (s)	Units	Uncertainty
1.	Coolant flow rate	1, 2, 4, 6, 8, 12	lpm	± 0.1 lpm
2.	Air flow rate	7636, 8707	lpm	± 50 lpm
Total Experiments: 12				

(a) Effect of coolant flow rate on the heat transfer rate

The heat transfer rate of EG based coolant shows a similar trend to that using DI Water. The heat transfer rate increase on increasing the coolant flow rate as shown in Figure 18. At a coolant flow rate of 1 lpm, the heat transfer rate is 325 Watts which increases to 1410 Watts at a coolant flow rate of 12 lpm. There is almost a 300% enhancement in heat transfer rate at a coolant flow rate of 12 lpm when compared with that at a coolant flow of 1 lpm. This trend is similar to the trend observed in the case of DI water, thus confirming the reliability of the results. The same trend is observed for all other coolants as well. But the higher heat transfer rate at a higher coolant flow rate comes with higher input power, i.e. higher pumping power required to pump the coolant at higher speeds. Thus, optimum coolant flow rates should be determined before opting for higher coolant flow rates for sake of a higher heat transfer rate.

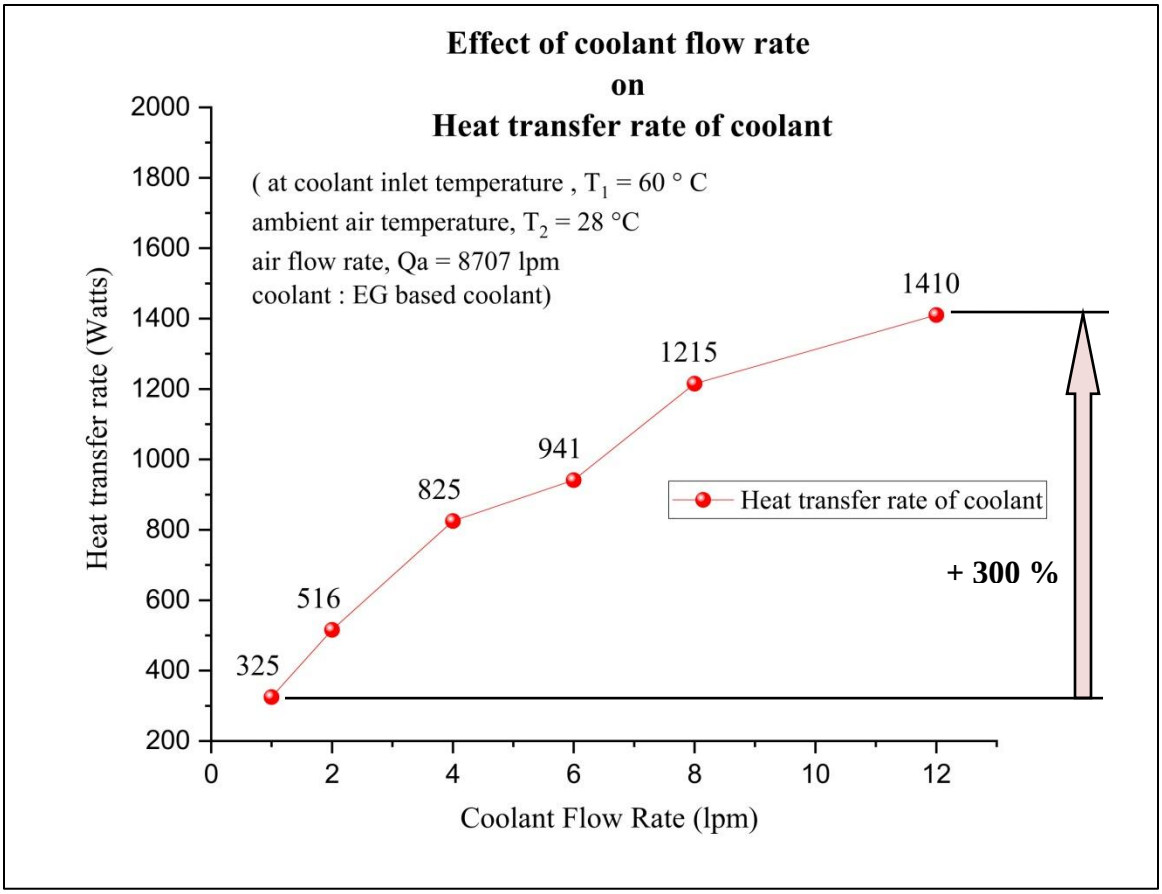

Figure 18: Effect of coolant flow rate on the heat transfer rate of coolant (EG based coolant)

(b) Effect of air flow rate on the heat transfer rate

The heat transfer rate of EG based coolant shows a similar trend to that using DI Water. The heat transfer rate increase on increasing the air flow rate. Figure 19 shows the effect of air flow rate on the rate of heat transfer. At a coolant flow rate of 1 lpm, the heat transfer rate increases from 285 Watts to 325 Watts, when the air flow rate is increased from 7636 lpm to 8707 lpm, i.e. around a 14% increase in the rate of heat transfer. At a coolant flow rate of 12 lpm, the heat transfer rate increases from 1185 Watts to 1410 Watts, i.e. around 18 % enhancement in heat transfer rate. This trend is similar to the trend observed in the case of DI water, thus confirming the reliability of the results. The same trend is observed for all other coolants as well.

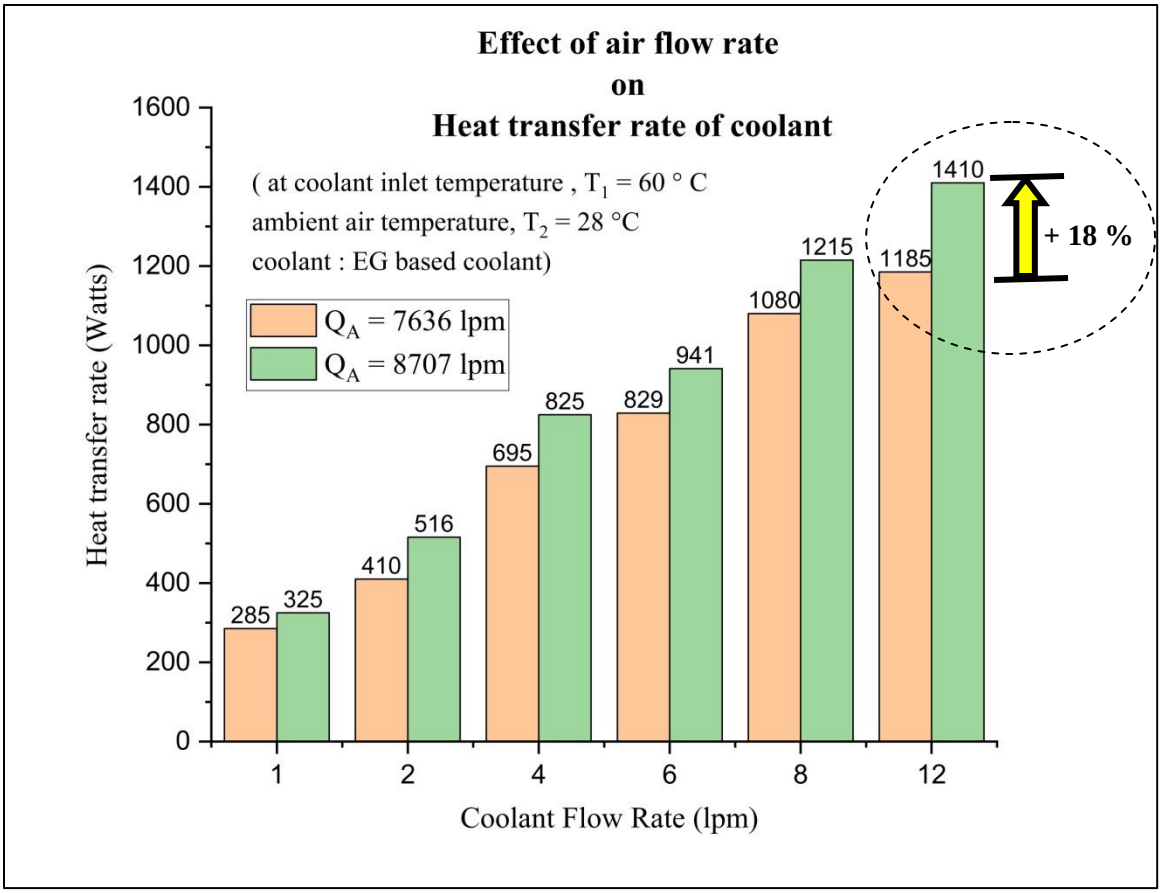

Figure 19: Effect of air flow rate on the rate of heat transfer of coolant (EG based coolant)

(c) Comparison of results with DI Water results

The heat transfer rates of DI water and EG based coolant were compared as shown in Figure 20. At a coolant flow rate of 1 lpm, the heat transfer rate observed using DI Water is 402 Watts but that observed using EG based coolant is just 325 Watts. This means that the EG based coolant could just achieve around 80% of the heat transfer rate obtained using DI water. At a coolant flow rate of 6 lpm, the heat transfer rate achieved using EG based coolant is around 82% of that achieved using DI water.

The reduction in the heat transfer rate of coolant may be attributed to its weaker thermophysical properties in comparison to that of DI water, such as constant pressure specific heat capacity of DI water is around 4180J/kgK while that of EG based coolant (50% ethylene glycol solution) is just 3426 J/kgK. But at higher coolant flow rates, the difference between the heat transfer rates reduces gradually.

At a coolant flow rate of 8 lpm, the heat transfer rates achieved by using DI water and EG based coolant are 1273 and 1215 respectively. This means, that around 95% of the heat transfer rate achieved by DI water is observed using the EG based coolant. At a further higher coolant flow rate of 12 lpm, the difference in heat transfer rates almost vanishes, and 99.5% of the heat transfer rate is achieved using the ethylene glycol-based EG based coolant.

Such a trend may be due to the smaller contact time between hot surface and fluid at higher speeds. Thus, on average for all coolant flow rates, the EG based coolant can achieve 86% of the heat transfer rate obtained using DI water as coolant.

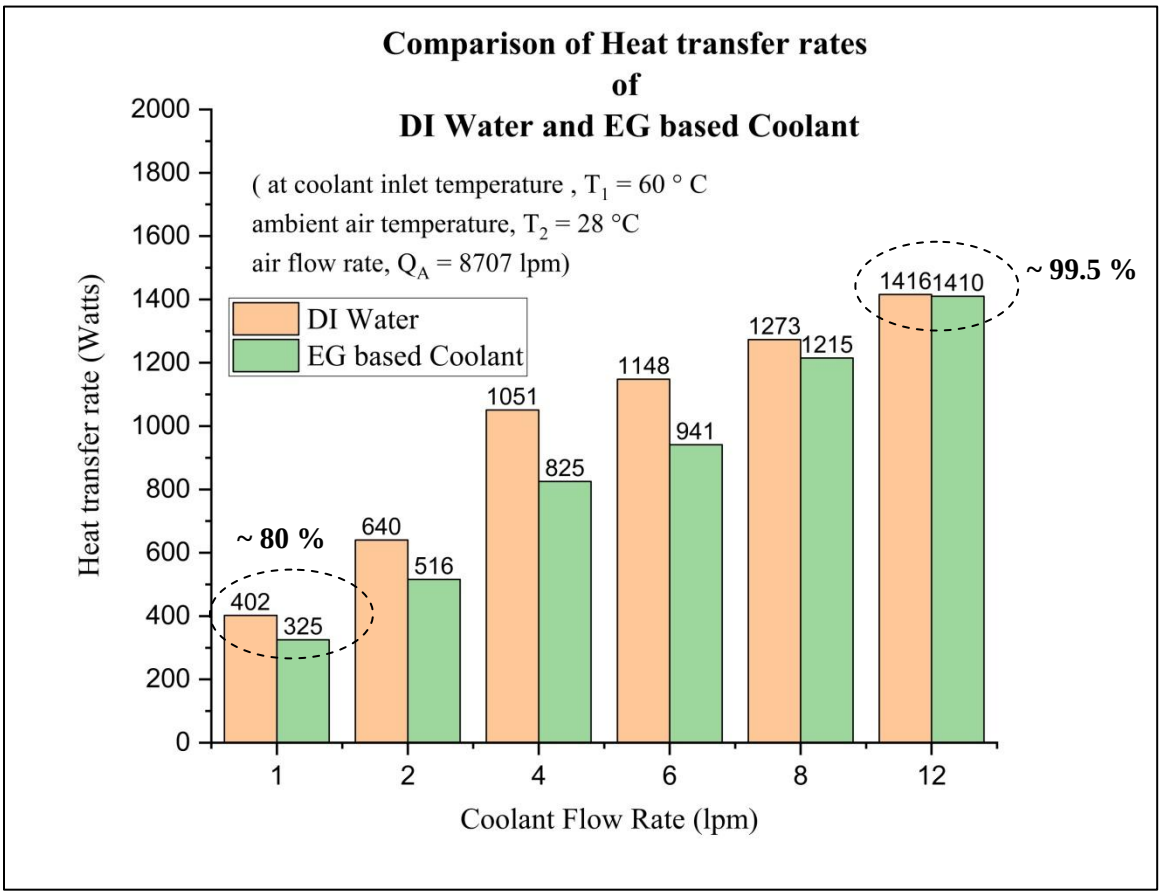

Figure 20: Comparison of heat transfer rates of DI water and EG based coolant

5.1.3 Results using glycerol solution

After performing experiments on EG based coolant and considering the recent advancements in a relatively new category of coolant called 'green-coolants' or eco-friendly coolants, the need for research in this field was observed. So, experiments on the Radiator type heat exchanger were performed using glycerol solution. Since 95 % of the automobile coolant market is captured by ethylene glycol-based coolants, it was difficult to find glycerol-based coolant, and even more difficult to determine the composition of the coolant as it is kept highly confidential by the manufacturers. So, instead of using a EG based coolant, we focused on using an aqueous solution of glycerol.

To find the optimum strength of the solution, various thermophysical properties were considered like its boiling point, freezing point, thermal conductivity, and viscosity. The values of the thermo-physical properties were taken from a handbook on the physical properties of glycerol and its aqueous solutions (shown in Table 9). Observing the values, the strength of 40% of glycerol was chosen for experimental investigation on the radiator-type heat exchanger.

Table 9: Values of boiling points, freezing points and viscosity of aqueous solutions of glycerol of various strengths

Strength of glycerol	Boiling Point (°C) [47]	Freezing Point (°C) [47]	Viscosity (cP) [47]
0%	100	17	0.5494
10%	100.9	-2.2	0.68
20%	101.8	-5.3	0.87
30%	102.9	-8.8	1.16
40% (selected)	***104.5***	***-17.2***	***1.162***
50%	106.7	-21.5	2.37
60%	109.6	-34	3.76
70%	114	-41.5	6.61
80%	121.5	-22.5	13.6
90%	139.8	-2.7	35.5
100%	290	17	142

The thermal conductivity of glycerol solutions of different strengths was measured by using KD2 Pro, the results of which are shown in Figure 21.

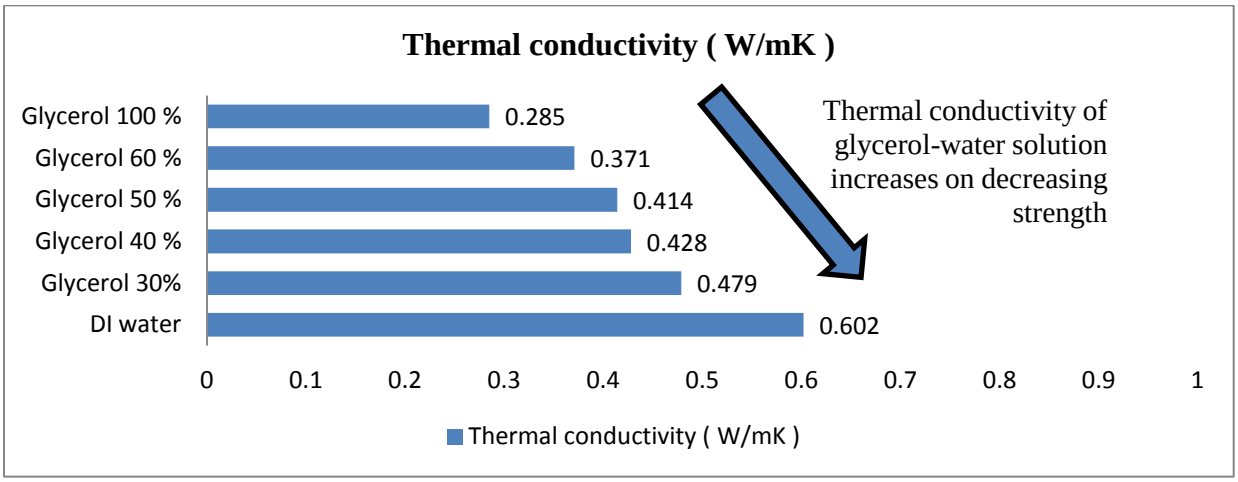

Figure 21: Thermal conductivity of glycerol solutions of various strengths

The effect of six coolant flow rates (1, 2, 4, 6, 8, 12 lpm) and two air flow rates (7636, 8707 lpm) was studied on the heat transfer rate of coolant (Table 10). Experiments were performed at an ambient temperature of 18 °C ± 1 °C with a relative humidity of 45% +/- 3%. A comparison of the results of glycerol solution with that of water has also been presented in this section.

Table 10: Parameters for experiments using glycerol solution

Variable parameter		Value (s)	Units	Uncertainty
1.	Coolant flow rate	1, 2, 4, 6, 8, 12	lpm	± 0.1 lpm
2.	Air flow rate	7636, 8707	lpm	± 50 lpm
Total Experiments: 12				

The results of various experiments are illustrated in the following sub-sections:

(a) Effect of coolant flow rate on the heat transfer rate

The heat transfer rate of glycerol solution shows a similar trend to that observed using DI Water. The heat transfer rate increase on increasing the coolant flow rate (Figure 22). At a coolant flow rate of 1 lpm, the heat transfer rate is 429 Watts which increases to 1664 Watts at a coolant flow rate of 12 lpm. There is almost a 287 % enhancement in heat transfer rate at a coolant flow rate

of 12 lpm when compared with that at a coolant flow of 1 lpm. This trend is similar to the trend observed in the case of DI water thus confirming the reliability of the results.

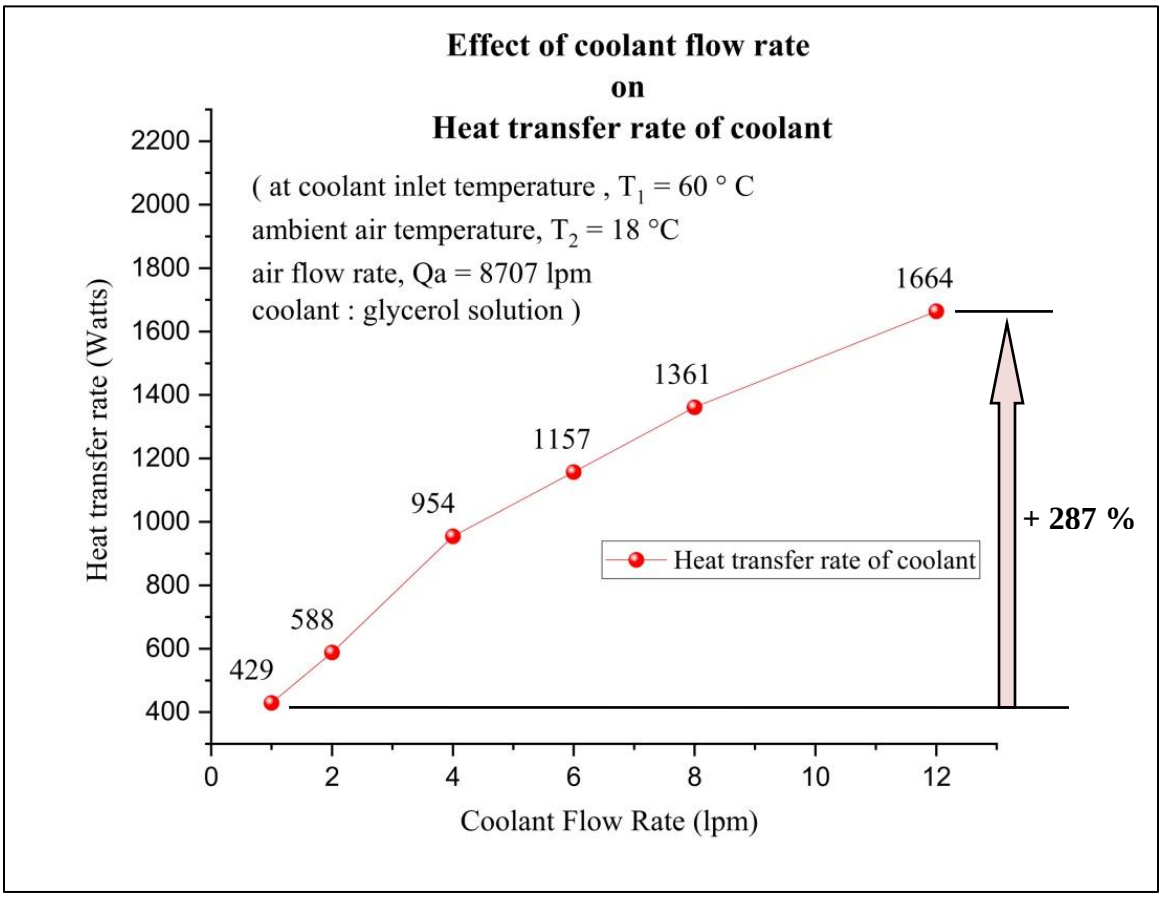

Figure 22: Effect of coolant flow rate on the heat transfer rate of coolant (glycerol solution)

(b) Effect of air flow rate on the heat transfer rate

The heat transfer rate of coolant using glycerol solution shows a similar trend to that using DI Water and EG based coolant. The heat transfer rate increases on increasing the air flow rate. Figure 23 shows the effect of air flow rate on the rate of heat transfer. At a coolant flow rate of 1 lpm, the heat transfer rate increases from 400 Watts to 429 Watts, when the air flow rate is increased from 7636 lpm to 8707 lpm, i.e. around a 7.25 % increase in the rate of heat transfer. At a coolant flow rate of 12 lpm, the heat transfer rate increases from 1464 Watts to 1664 Watts, i.e. around 13.6 % enhancement in heat transfer rate. This trend is similar to the trend observed in the case of DI water and EG based coolant, but the enhancement observed is much lesser than

that observed in the case of DI water and EG based coolant. Thus it can be said that the effect of air flow rate on the heat transfer rate using glycerol solution as coolant is not as significant as it is in other cases.

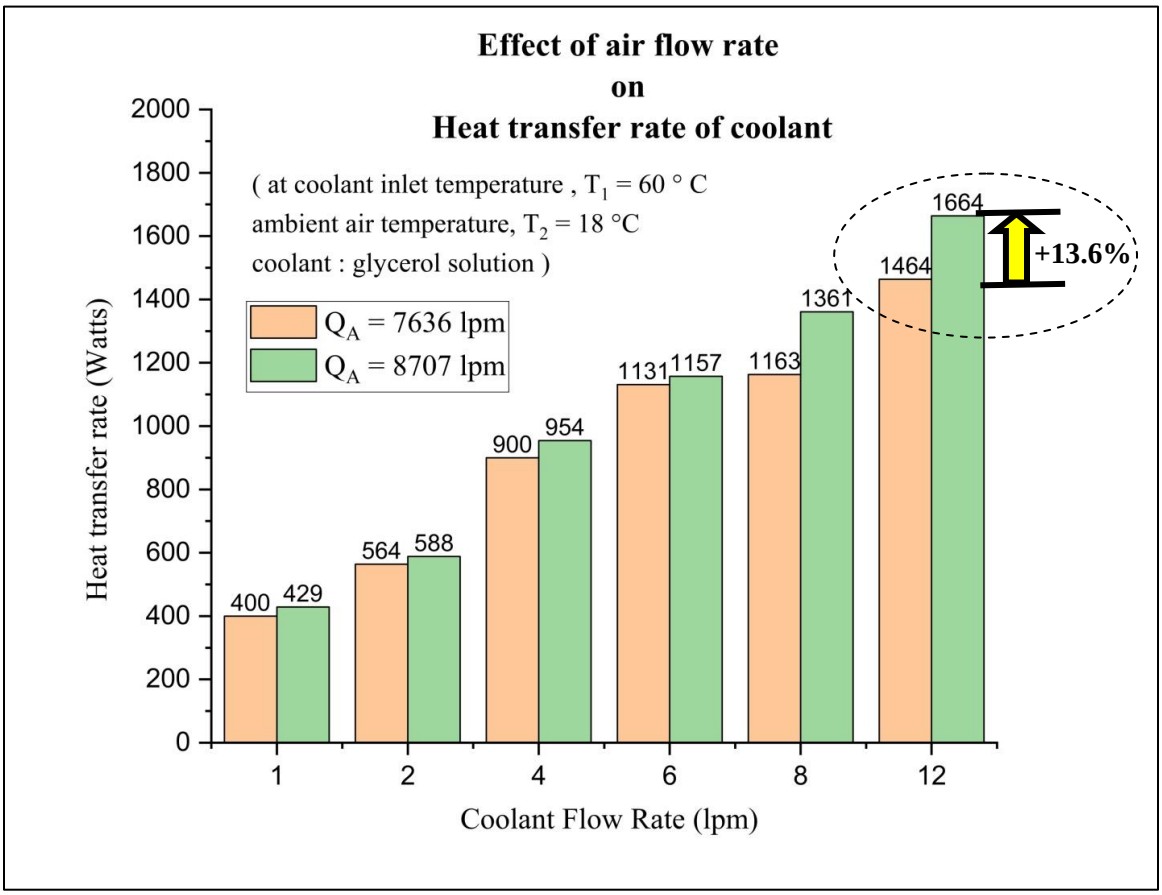

Figure 23: Effect of air flow rate on the heat transfer rate of coolant (glycerol solution)

(c) Comparison of heat transfer rates on using DI water and glycerol solution

The heat transfer rates of DI water and glycerol solution were compared as shown in Figure 20. At a coolant flow rate of 1 lpm, the heat transfer rate observed using DI Water is 535 Watts but that observed using glycerol solution is just 429 Watts. This means that the glycerol solution could just achieve around 80% of the heat transfer rate obtained using DI water. At a coolant flow rate of 4 lpm, the heat transfer rate achieved using glycerol solution is around 81.6 % of that achieved using DI water. The reduction in the heat transfer rate of coolant may be attributed to its weaker thermophysical properties in comparison to that of DI water, such as constant pressure

specific heat capacity of DI water is around 4180J/kgK while that of glycerol solution (40% strength) is just 3409 J/kgK. But at higher coolant flow rates, the difference between the heat transfer rates reduces gradually. At a coolant flow rate of 12 lpm, almost 89 % of the heat transfer rate is achieved using the glycerol solution. Thus, on average for all coolant flow rates, the EG based coolant can achieve 81 % of the heat transfer rate obtained using DI water as coolant.

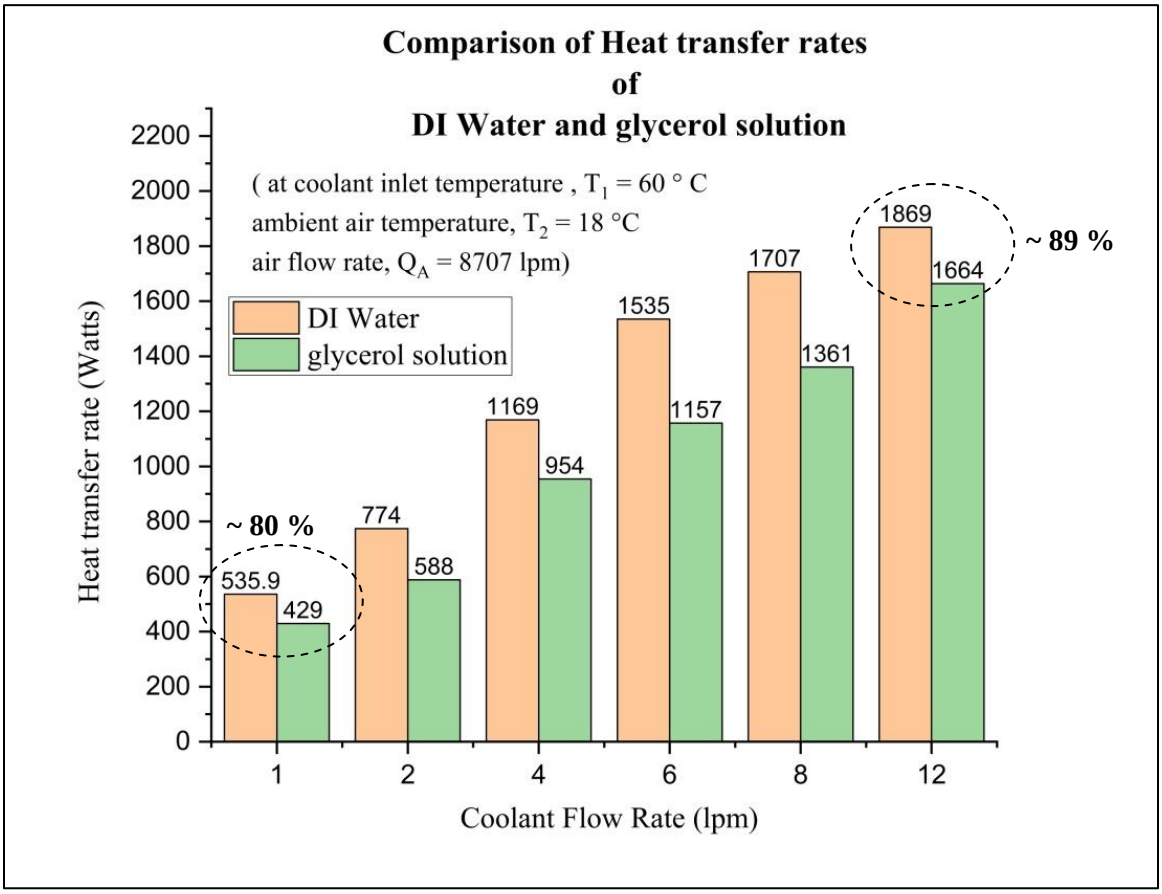

Figure 24: Comparison of heat transfer rates using DI water and glycerol solution

(d) Pumping Power

Pumping power is the power required by a water pump to pump the coolant at a certain flow rate. As the coolant flow rate increases, not only does the heat transfer rate increase, but however the input power (pumping power) also increases. Thus it is an important factor to be considered while evaluating the thermal performance of the radiator.

Pumping power was calculated by using current and voltage values displayed on the console. Figure 25 shows the comparison between pumping power required by DI water and glycerol solution. At lower flow rates, glycerol solution consumes more power than DI Water due to its high viscosity. However, at higher flow rates the difference between power consumption almost vanishes may be due to the lubricating effects of glycerol. At a flow rate of 1 LPM, the pumping power is 18% more for glycerol solution than DI Water, while it is just 4% more at a coolant flow rate of 12 LPM.

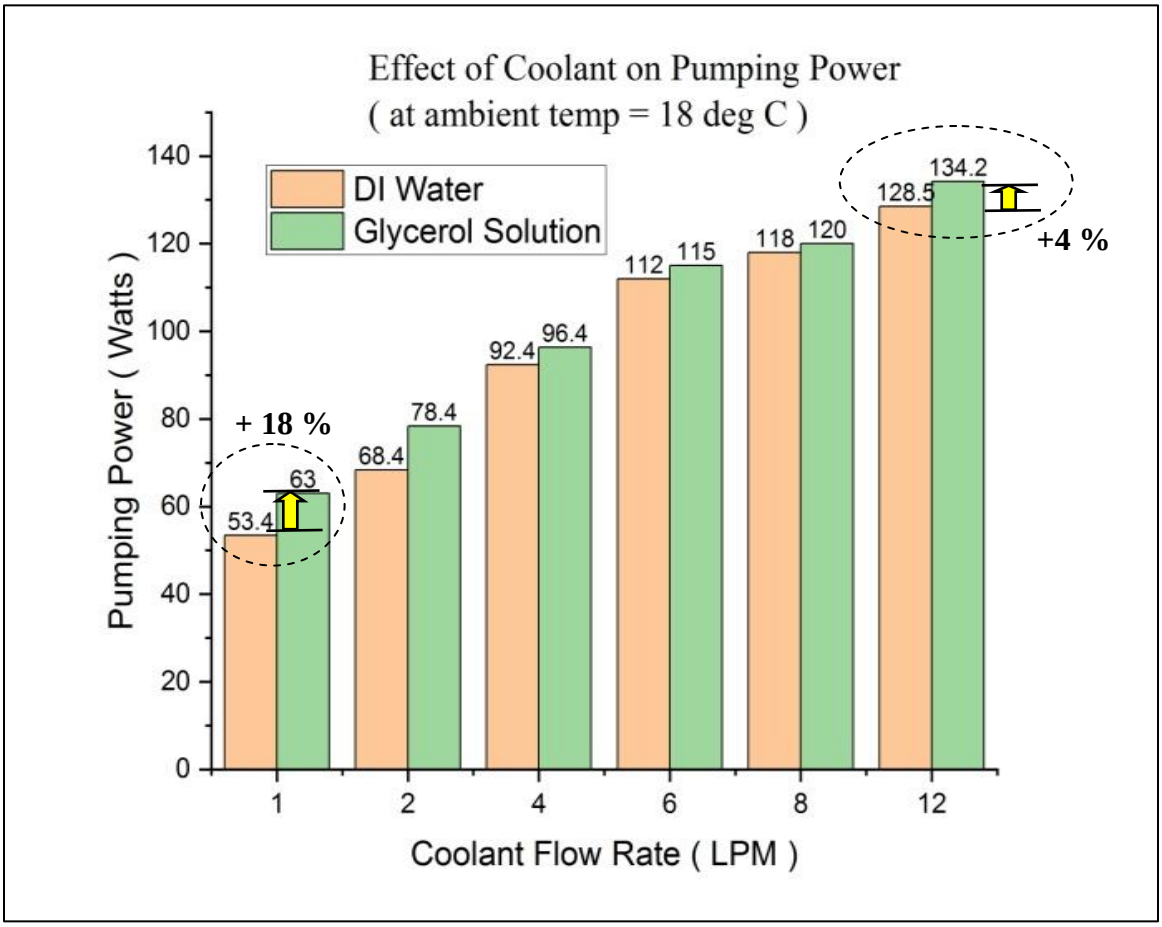

Figure 25: Pumping power comparison of DI water and glycerol solution

5.2 Nanoparticle characterization

The morphology of nanoparticles plays an important role in determining the thermo-physical properties and stability of nanofluids. Nanoparticles of Copper (II) oxide were examined for their particle size (using SEM), chemical composition (using EDAX), and crystalinity (using XRD) of their structure. The results are as follows:

5.2.1 SEM (Scanning Electron Microscope)

Scanning Electron Microscope (SEM) is an electron microscopic technique that generates images of samples by scanning the surface with a focused beam of electrons. Generally, the resolution of SEM is about 1 nm -10 nm, but it can vary depending on the instrument.

The SEM was done to determine the particle size using Carl Zeiss Sigma 500. The result (in Figure 26) shows, that the average particle size of CuO nanoparticles is about 20 nm, which is smaller than that mentioned by the manufacturer (50 nm – 80 nm). Also, the shape of CuO nanoparticles appears to be spherical which is as per literature and manufacturer's data.

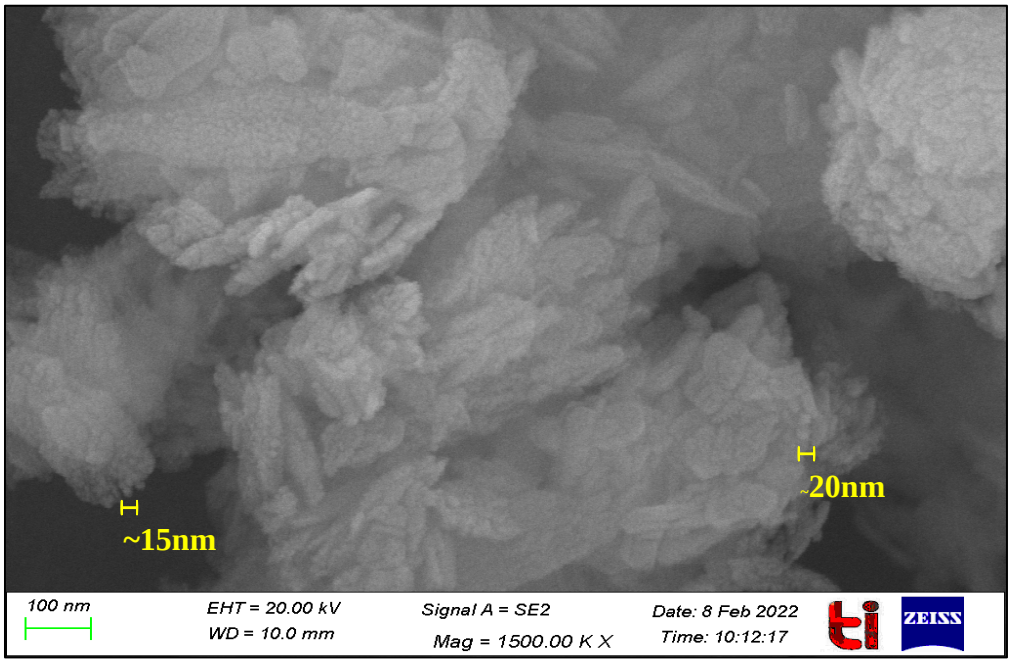

Figure 26: SEM image of CuO nanoparticle sample

5.2.2 EDS (Energy Dispersive X-ray Spectroscopy)

Energy Dispersive x-ray Spectroscopy (EDS) is a technique used to determine the chemical composition of a substance. It is based on the interaction of x-rays with the sample, i.e. each element has a unique atomic structure allowing a unique set of peaks on its electromagnetic emission spectrum. Bruker's QUANTAX 200 setup was employed to perform the EDS.

Table 11 gives details of the components of nanoparticles in their respective concentration (as found). Figure 27 shows a plot of peaks corresponding to the elements present. Apart from major peaks, minor peaks indicate the impurities added during the coating of nanoparticles on the coating tape, thus these peaks do not actually correspond to the nanoparticle material and hence should be neglected.

Table 11: Table showing the elemental composition of CuO nanoparticle sample

Element	At. No.	Netto	Mass Norm. [%]	Atom [%]	abs. error [%] (1 sigma)	rel. error [%] (1 sigma)
O	8	18615	25.20	57.22	0.97	4.69
Cu	29	44410	74.80	42.78	2.05	3.34
		Sum	**100.00**	**100.00**		

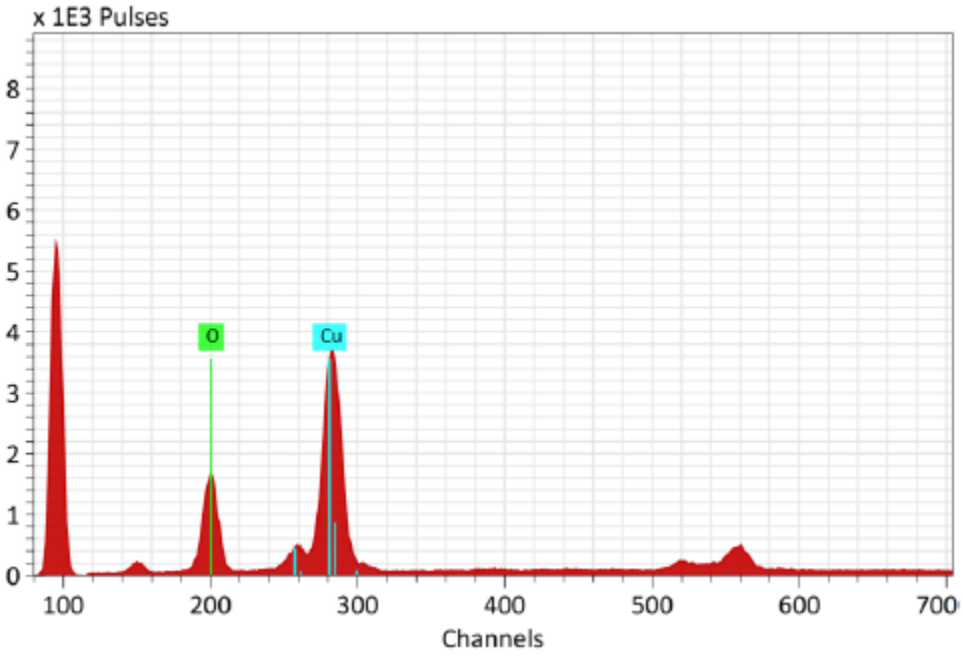

Figure 27: Characteristic peaks of elements found in CuO nanoparticle sample

5.2.3 XRD (X-ray Diffraction)

X-ray Diffraction or X-ray crystallography is a technique used to determine the atomic and molecular structures of a crystal. In XRD, a beam of x-ray is fallen on a crystal sample, which diffracts it in many specific directions, which is collected by a crystallographer, and a 3-D image of atom/ molecule is generated. Thus, using XRD structure as well as the phase of the element present in the sample can be determined.

X'Pert Pro powder XRD setup was employed to determine the crystalline size, structure, and phase of the CuO nanoparticle sample. Figure 28 shows the observed XRD pattern of CuO nanoparticles. The peaks correspond to the phases of elements present in the sample.

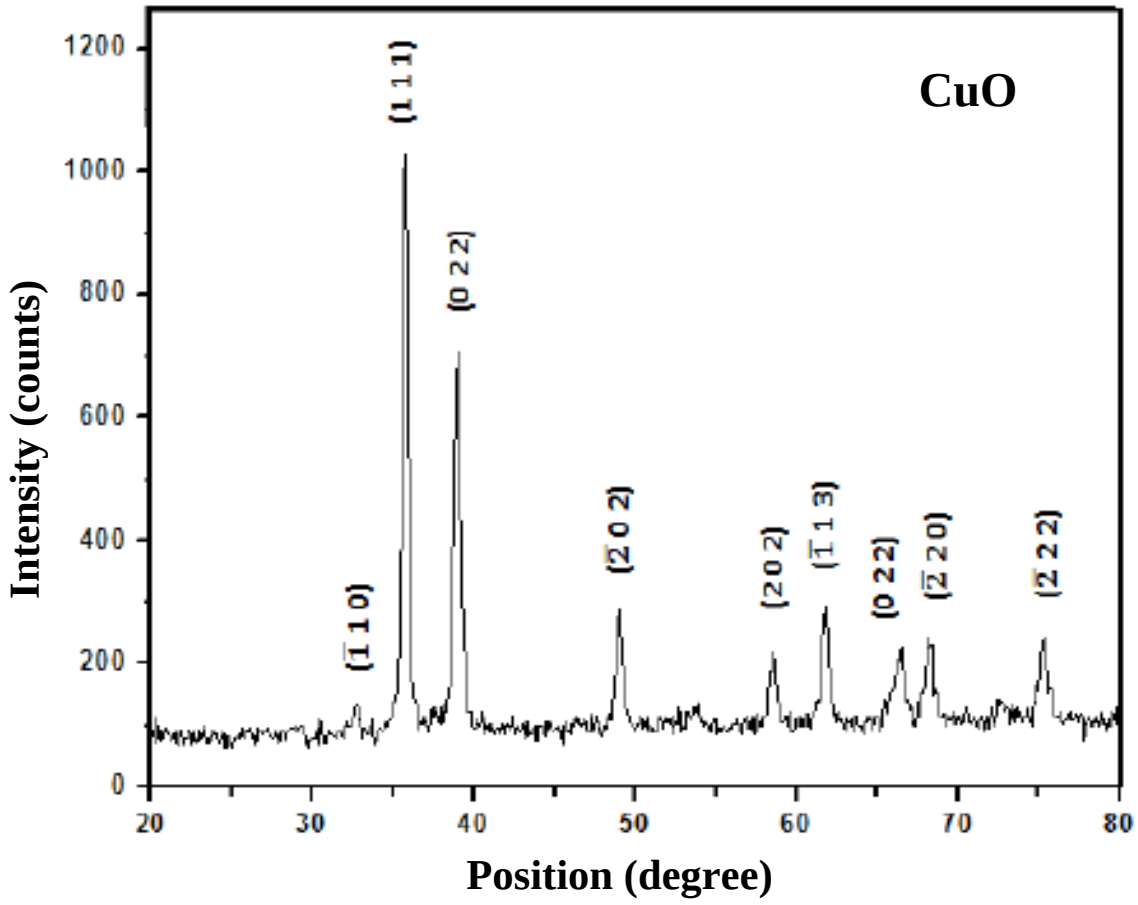

Figure 28: Peaks corresponding to the elements and their phases present in nanoparticle powder

5.3 Nanofluid Characterization

After characterization of CuO nanoparticles, nanofluid was prepared by using two-step method as discussed in section 4.2.2 (b). The thermo physical properties of nanofluid were determined by using methods presented in section 4.2.2 (c)

Different models from available literature have been utilized to determine the various thermophysical properties of nanocoolants of different concentrations. The thermophysical properties such as density, specific heat capacity, dynamic viscosity, and thermal conductivity have been calculated using the theoretical models and plotted against the concentration of CuO nanoparticles in the nanocoolant.

Table 12 shows the thermo-physical properties of nanoparticles and the base fluid.

Table 12: Thermo-physical properties of base fluid and CuO nanoparticles

Fluid/Particle	Density (kg/m^3)	Specific heat (J/kgK)	Dynamic viscosity (Pa.s)	Thermal Conductivity (W/m^2K)
Base Fluid (Glycerol solution-40%)	1085	3409	0.00162	0.428
CuO Nanoparticle	6400	531	*NA*	33

5.3.1 Effective density

The density of fluid plays an important role in determining its heat transfer characteristics. In the present study, the density of nanofluid has been calculated by using the rule of mixture (Eq. 9). The variation of density of nanofluid against the nanoparticle concentration has been plotted in Figure 29. On increasing the concentration of nanoparticles, the density of nanofluid increases. This is due to the higher density of nanoparticles in comparison to that of the base fluid. The increase in density of nanofluids are 2.39%, 4.88%, and 7.28% respectively for 0.5% *by vol*., 1.0% *by vol*., and 1.5% *by vol*. CuO/glycerol nanofluid when compared with the base fluid having 0.0% *by vol*. CuO nanoparticles.

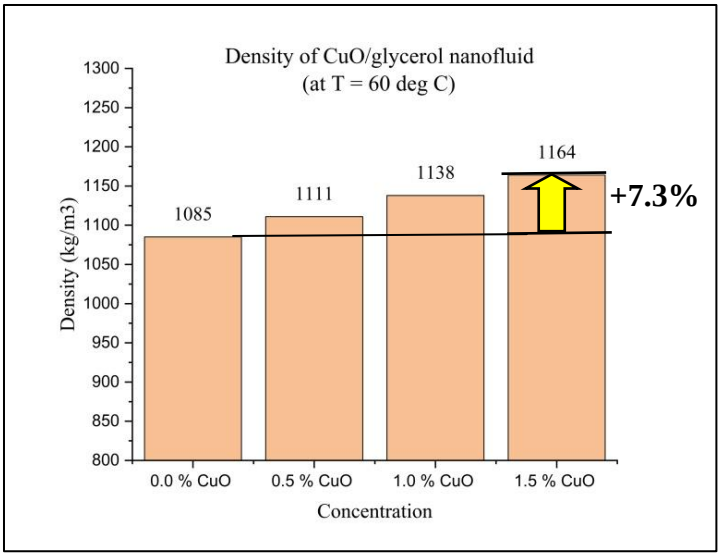

Figure 29: Densities of nanofluid of different concentrations

5.3.2 Effective specific heat capacity

The specific heat capacity of fluid is the maximum amount of heat it can retain at a given temperature. For a nanofluid, it can be obtained by using the relation given in Eq. (10)

The effect of conc. on the specific heat capacity of the nanofluid is demonstrated in Figure 30. Specific heat capacity of the nanofluid decreases on increasing the particle concentration in the nanofluid. This trend is due to the smaller value of specific heat for nanoparticles of CuO when compared with that of the base fluid.

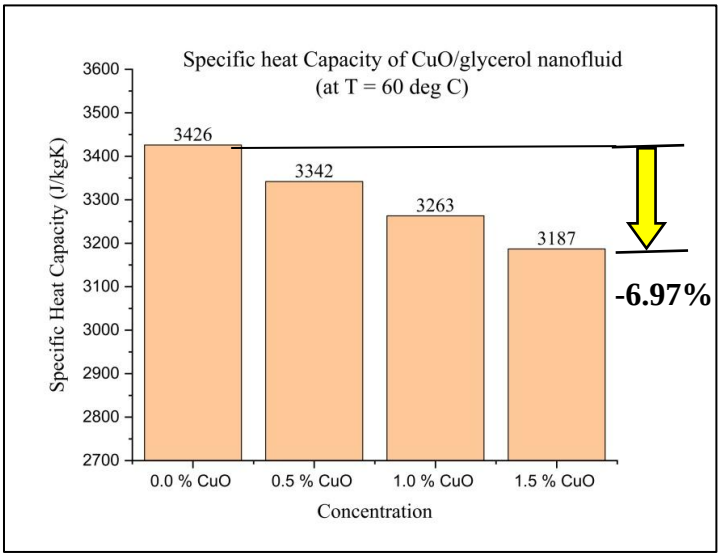

Figure 30: Specific heat capacity of CuO/glycerol nanocoolant

5.3.3 Effective dynamic viscosity

The viscosity of a fluid is the resistance to its movement or flow, offered by the cohesive forces present between its layers. To determine the effective dynamic viscosity of nanofluid, the correlation (Eq. (11)) given by *Wang et. al*. [37] has been used. The effect of concentration on the effective dynamic viscosity of the nanofluid has been illustrated in Figure 31. The dynamic viscosity of nanofluid increases with an increase in nanoparticle concentration in nanofluid. The viscosity increase by: 3.7%, 8.0%, and 13.6% respectively for 0.5% *by vol*., 1.0% *by vol*., and 1.5% *by vol*. CuO/glycerol nanofluid when compared with the base fluid having 0.0% *by vol*. CuO nanoparticles.

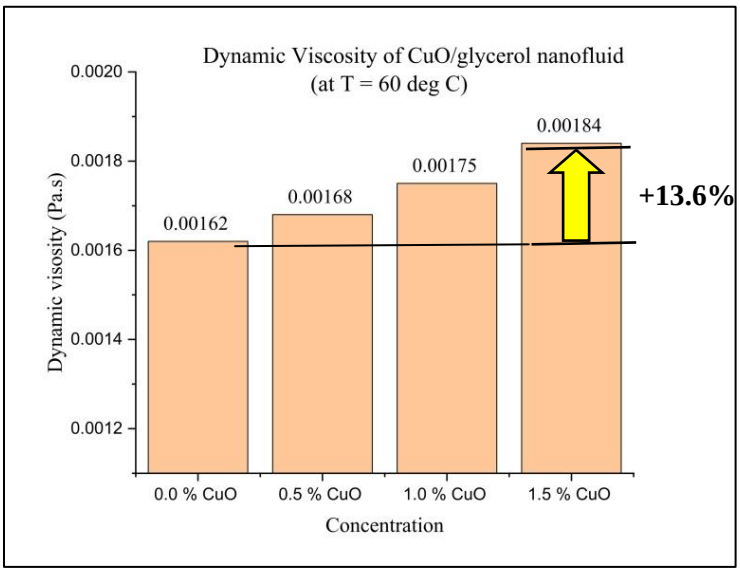

Figure 31: Dynamic viscosity of nanocoolant with nanoparticle concentration

5.3.4 Effective thermal conductivity

The thermal conductivity of a fluid is its ability to conduct heat. The correlations usually depend on the size, shape, and nature of the nanoparticle. In the present study the thermal conductivity of CuO/Glycerol nanocoolant has been determined by using the relation given by Maxwell et. al. [37] in Eq. (16). Thermal conductivity of nanofluid increases with an increase in particle concentration (Figure 32). The increase in thermal conductivity is 1.47%, 2.99%, and 4.48% respectively for 0.5% *by vol*., 1.0% *by vol*., and 1.5% *by vol*. CuO/glycerol nanofluid when compared with the base fluid.

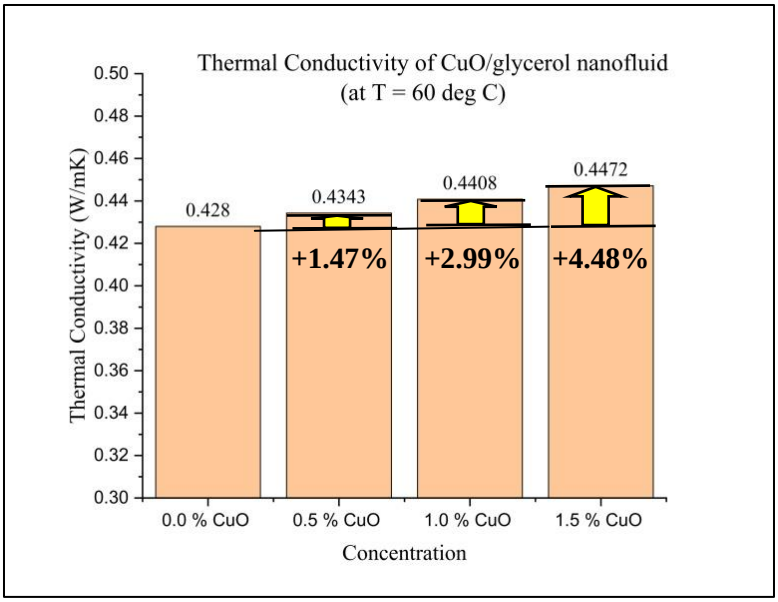

Figure 32: Thermal conductivity of nanofluids of different concentrations

5.4 Thermal performance evaluation of CuO/glycerol nanocoolant

This section comprises the analysis of results obtained from experiments performed on radiator-type heat exchanger using CuO/glycerol nanocoolant. The section illustrates the effect of nanoparticle concentration on the temperature drop, heat transfer rate, CHTC, and Overall heat transfer coefficient of nanocoolant. Apart from coolant side analysis of heat transfer, effects on air side heat transfer parameters have also been studied. The effect of six coolant flow rates and four nanoparticle concentrations was studied on the heat transfer rate of coolant (Table 13). Experiments were performed at an ambient temperature of 18 °C ± 1°C with a relative humidity of 45% ± 3%.

Table 13: Variable parameters for experiments using nanocoolant

Variable parameter		Value (s)	Units	Uncertainty
1.	Coolant flow rate	1, 2, 4, 6, 8, 12	lpm	± 0.1 lpm
2.	Nanoparticle concentration	0.0%, 0.5%, 1.0%, 1.5%	*by vol.*	± 0.01 %
Total Experiments: 24				

5.4.1 Effect on temperature drop of nanocoolant

The effect of particle concentration on the temperature drop of nanocoolant is shown in Figure 33.

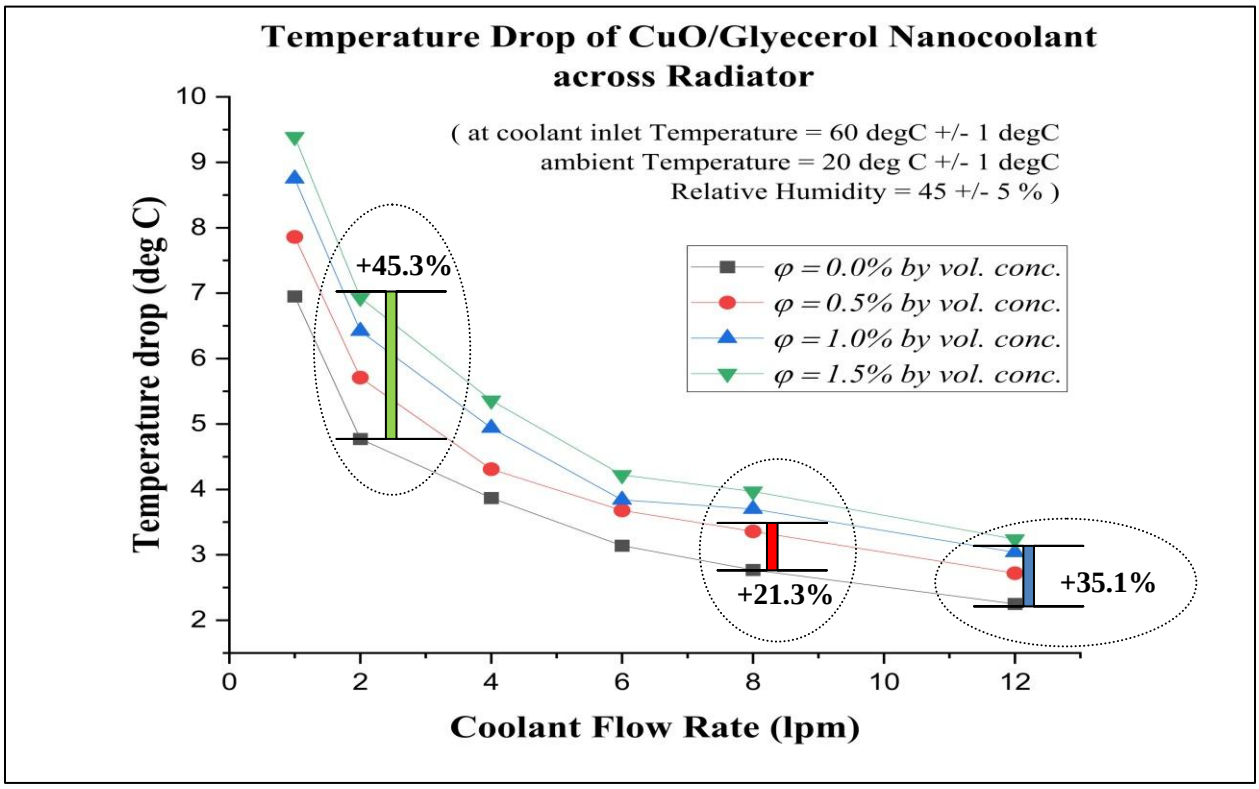

Figure 33: Comparison of temperature drop of coolant (using CuO/glycerol nanocoolant)

As observed in the previous section, on increasing the coolant flow rate, the temperature drop shows an inverse trend (hyperbolic form: y = k/x). The effect of increasing the concentration of CuO nanoparticles is observed to have increased the temperature drop of nanocoolant. Maximum enhancement of 45.3 % is observed in a temperature drop of nanocoolant across the radiator at a coolant flow rate of 2 lpm for CuO nanoparticle concentration φ = 1.5 % *by vol*. However, for other lower concentrations of CuO, φ = 0.5% *by vol*. and 1.0% *by vol*., maximum enhancements of 21.3% and 35.1% are observed at coolant flow rates of 8lpm and 12 lpm, respectively. On average, the enhancement in a temperature drop of nanocoolant (across all coolant flow rates) for particle concentrations of 0.5% *by vol*., 1.0% *by vol*., and 1.5% *by vol*. is 17.3%, 29.9%, and 40.1% respectively.

5.4.2 Effect on temperature gain of air

The effect of particle concentration and coolant flow rate on the temperature drop of nanocoolant has been shown in Figure 33.

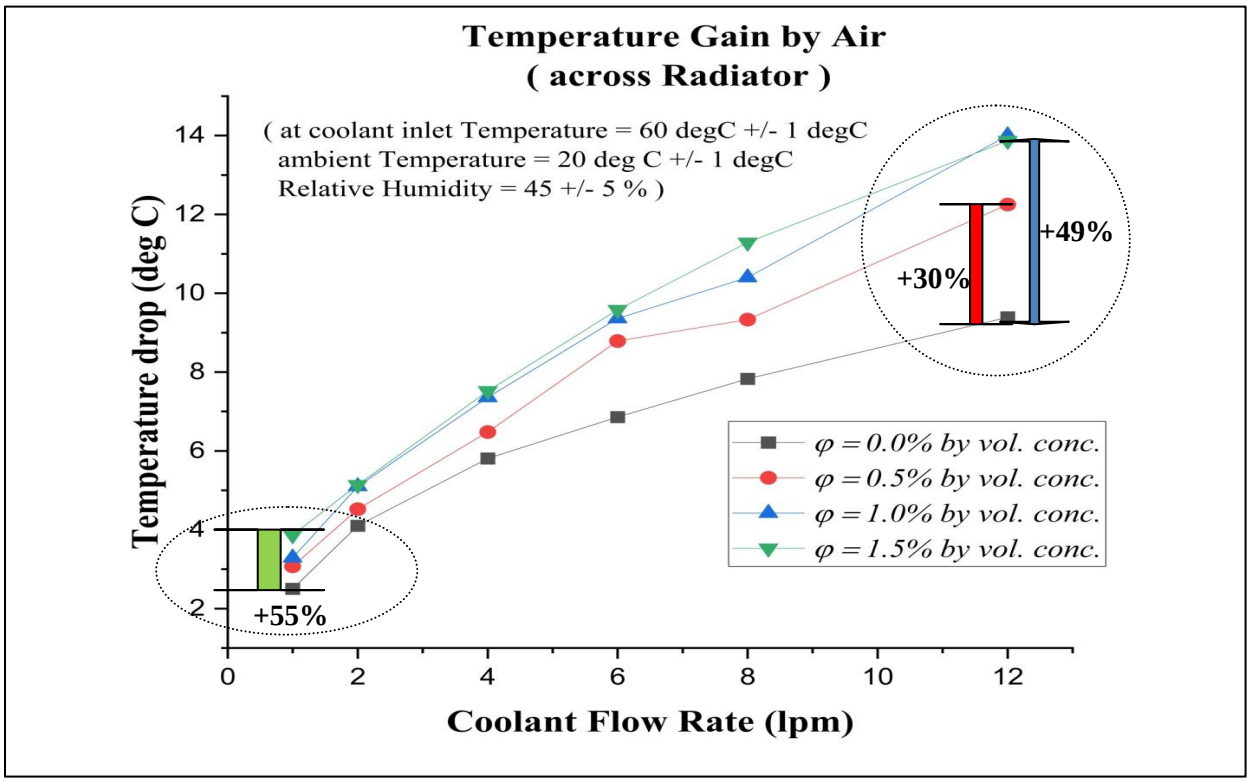

Figure 34: Comparison of temperature gain by air (using CuO/glycerol nanocoolant)

On increasing the coolant flow rate, the trend shown by temperature gain of air is somewhat between linear to parabolic in nature. The effect of increasing the concentration of CuO nanoparticles is observed to have increased the temperature gain by air. For air-side temperature gain, a maximum enhancement of 55% is observed for CuO nanoparticle concentration φ = 1.5 % *by vol*. at a coolant flow rate of 1 lpm. For other lower concentrations of CuO, φ = 0.5% *by vol*. and 1.0% *by vol*., maximum enhancements of 30% and 49% is observed at a coolant flow rate of 12 lpm.

Similarly average enhancement for temperature gain by air (across all coolant flow rates) for nanocoolant of concentrations, φ = 0.5% *by vol*., 1.0% *by vol*., and 1.5% *by vol*. is 20.4%. 33.5% and 40.2% respectively.

5.4.3 Effect on the heat transfer rate

(a) Tube-side

As per the trend observed in the last section, the heat transfer rate of nanocoolant increases on increasing the coolant flow rate. The effect of increasing the concentration of CuO nanoparticles in the nanocoolant is studied in this section. Figure 35 shows the effect of coolant flow rate and particle concentration on the heat transfer rate of coolant.

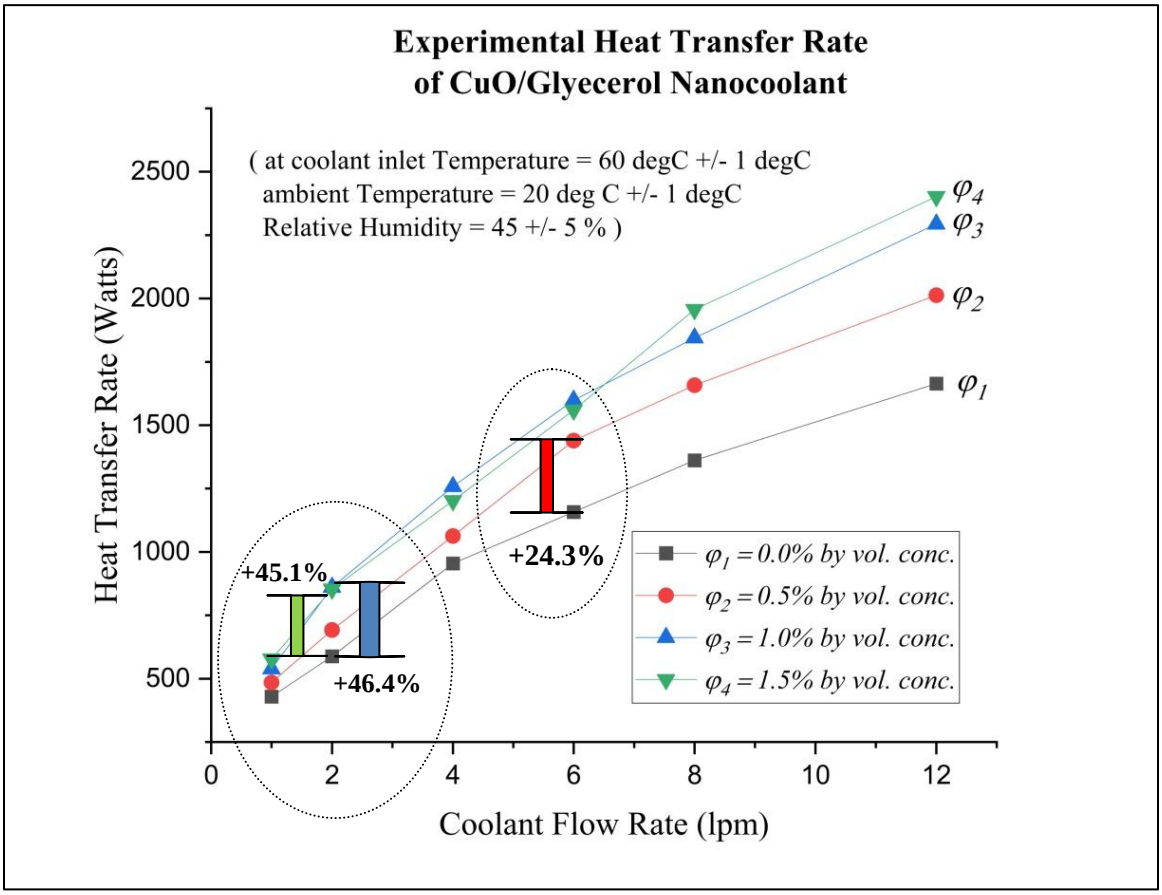

Figure 35: Effect of nanoparticle concentration on the heat transfer rate of nanocoolant

The maximum enhancement of coolant side heat transfer rate is observed to be 46.4% for nanoparticle concentration of 1.0% *by vol*. at a coolant flow rate of 2 lpm, while that for φ = 1.5% *by vol*. is found to be 45.1% at the same conditions. The reason for the decline in heat transfer rate enhancement on increasing the nanoparticle concentration may be attributed to the fact that the specific heat capacity of nanocoolants of higher concentration is lower, so despite enhanced temperature drop at the same condition the relative enhancement in the heat transfer

rate of coolant has slightly decreased. For φ = 0.5% *by vol*., the maximum enhancement in heat transfer rate is 24.3% at a coolant flow rate of 6 lpm. On average, the enhancements in the heat transfer rate of nanocoolant (across all coolant flow rates) for concentrations 0.5% *by vol*., 1.0% *by vol*., and 1.5% *by vol*. are 18.2%, 35.9%, and 38.1% respectively.

(b) Air-side

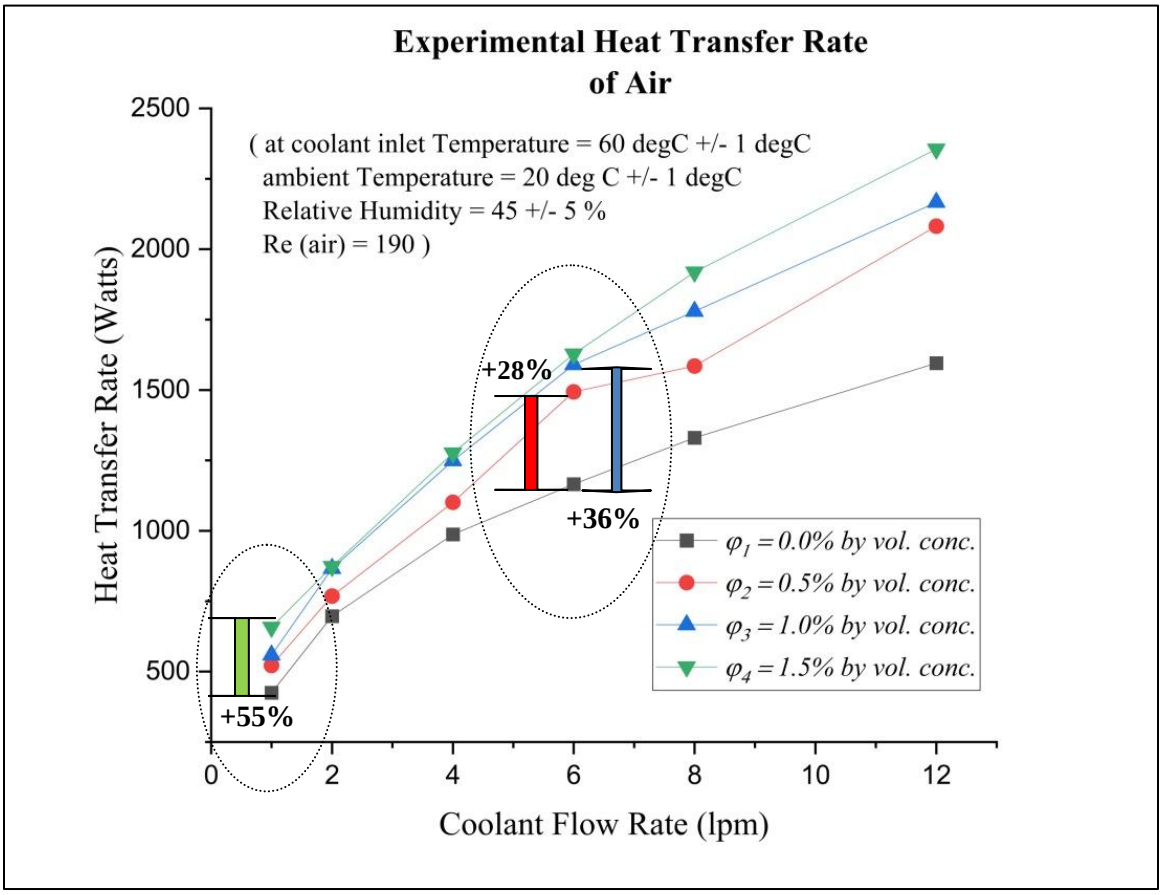

Figure 36: Figure showing the effect of particle concentration on rate of heat transfer of air

The trend observed in the heat transfer rate of air is similar to that observed in the heat transfer rate of coolant. Figure 36 shows enhancement in the heat transfer rate of air for different concentrations of CuO nanoparticles. The maximum enhancement of air-side heat transfer rate is observed to be 54.8% for nanoparticle concentration of 1.5% *by vol*. at a coolant flow rate of 1 lpm. For other lower concentrations of CuO nanoparticles φ = 0.5% *by vol*. and 1.0% *by vol*., it is found to be 28.6% and 36.4% at coolant flow rates of 6lpm. Unlike the deviation of results observed in heat transfer rate enhancement in the case of coolant, the results obtained here are

free from such deviations, and the relative enhancement increases on increasing the particle concentration. On average, the enhancements in the heat transfer rate of air (across all coolant flow rates) for concentrations of 0.5% *by vol*., 1.0% *by vol*., and 1.5% *by vol*. of nanocoolant are 19.7%, 31.4%, and 40.1% respectively.

5.4.4 Equality of heat transfer rates of air and tube side

In order to check the consistency of results, the heat transfer rate on both the air and coolant side should be equal in every experiment, as per the law of conservation of energy. Thus, the heat transfer rates for the air and coolant side have been compared for the experiments performed on the base fluid in Figure 37. The heat transfer rate shows very close relationship between them as observed from figure below. Minor variations might have occurred due to absorption of heat by apparatus or fluctuations in ambient temperature.

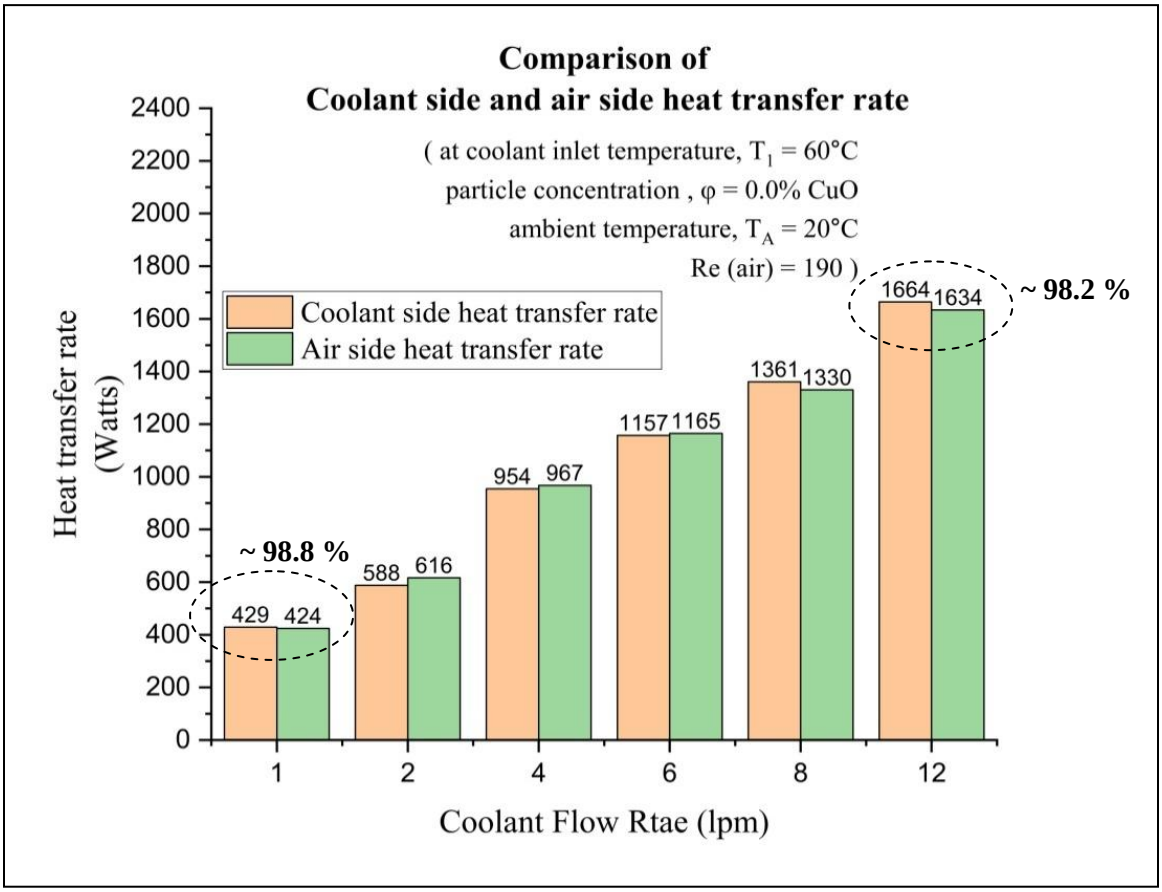

Figure 37: Comparison of heat transfer rates of coolant and air side

5.4.5 Effect on Nusselt Number and CHTC (tube side)

Nusselt number is the ratio of convective heat transfer to the conductive heat transfer within a fluid. In forced convection, the Nusselt number depends on the Reynolds number and Prandtl number of the fluid. The tube side Nusselt number is calculated using the correlation given by Dehghandokht et.al.[26].

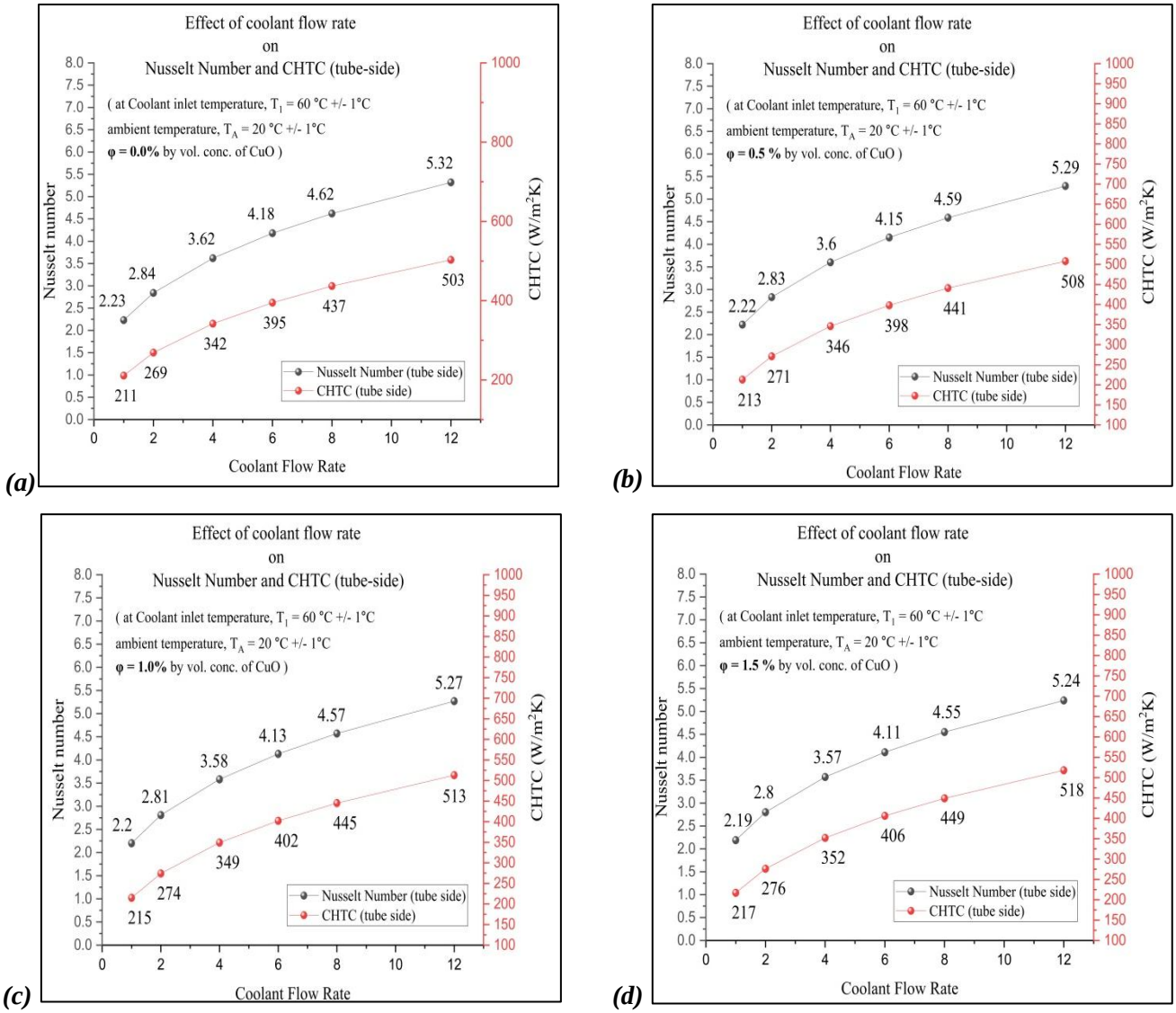

Figure 38: Effect of coolant flow rate on Nusselt number and CHTC of nanocoolant of different concentrations (a) 0.0% CuO, (b) 0.5% CuO, (c) 1.0% CuO, (d) 1.5% CuO

The effect of coolant flow rate on Nusselt number and CHTC of nanocoolants of different concentrations is shown in Figure 38. Nusselt number shows an increasing trend with an

increase in coolant flow rate. For nanocoolant with particle concentration, φ = 0.0% *by vol*., Nusselt number increases from 2.23 to 5.32 on increasing coolant flow rate from 1 lpm to 12 lpm. A similar trend is observed for nanocoolants with different particle concentrations. However, on increasing the nanoparticle concentration, the values Nusselt number show a declining trend, which may be due to the slight decrease in values of the Reynolds number (as shown in section 4.2.4).

Convective heat transfer coefficient or film coefficient is the constant of proportionality between the heat flux and the temperature difference (driving force). CHTC can be determined using Eq.

$$Nu = \frac{hL}{k} \quad (42)$$

From Figure 38, it is observed that the CHTC increases from 211 W/m^{2}K to 503 W/m^{2}K on increasing the coolant flow rate from 1lpm to 12 lpm. A similar trend is observed for other nanocoolants also. Unlike the Nusselt number, CHTC shows an increasing trend with an increase in particle concentration. At a coolant flow rate of 1 lpm, the values of CHTC increase steadily from 211 W/m^{2}K to 213 W/m^{2}K to 215 W/m^{2}K to 217 W/m^{2}K, on increasing the particle concentration gradually from 0.0% CuO *by vol*. to 1.5% CuO *by vol*.

The reason for this increase, is an enhancement in thermal conductivity of the nanocoolant (on increasing the particle concentration), despite the decrease in the value of Nusselt number.

5.4.6 Effect on Overall heat transfer coefficient (experimental)

Overall heat transfer coefficient (both, tube-side and air-side) has been used to evaluate the thermal performance of the CuO/glycerol nanocoolant. Experimental Overall heat transfer coefficient has been calculated from experimental data using reverse engineering methodology (as explained in section 5.1). The overall heat transfer coefficient shows an increasing trend with the concentration of nanoparticles in the nanocoolant, which is shown in the following sub-sections:

(a) Tube-side

Figure 39 shows the effect of particle concentration on the tube-side overall heat transfer coefficient. The overall heat transfer coefficient shows an increasing trend with an increase in nanoparticle concentration. The maximum enhancement of 32.5% occurs at coolant flow rate of

2 lpm for φ = 1.5% *by vol*. For other particle concentrations of φ = 0.5% *by vol*. and 1.0% *by vol*. the enhancements are 15.3% and 22.2% at coolant flow rates of 4lpm and 1lpm, respectively. The average enhancement over all the coolant flow rates is found to be 13.8%, 21.3% and 31.0% for nanoparticle concentration φ = 0.5% *by vol*., 1.0% *by vol*. and 1.5% *by vol*. respectively.

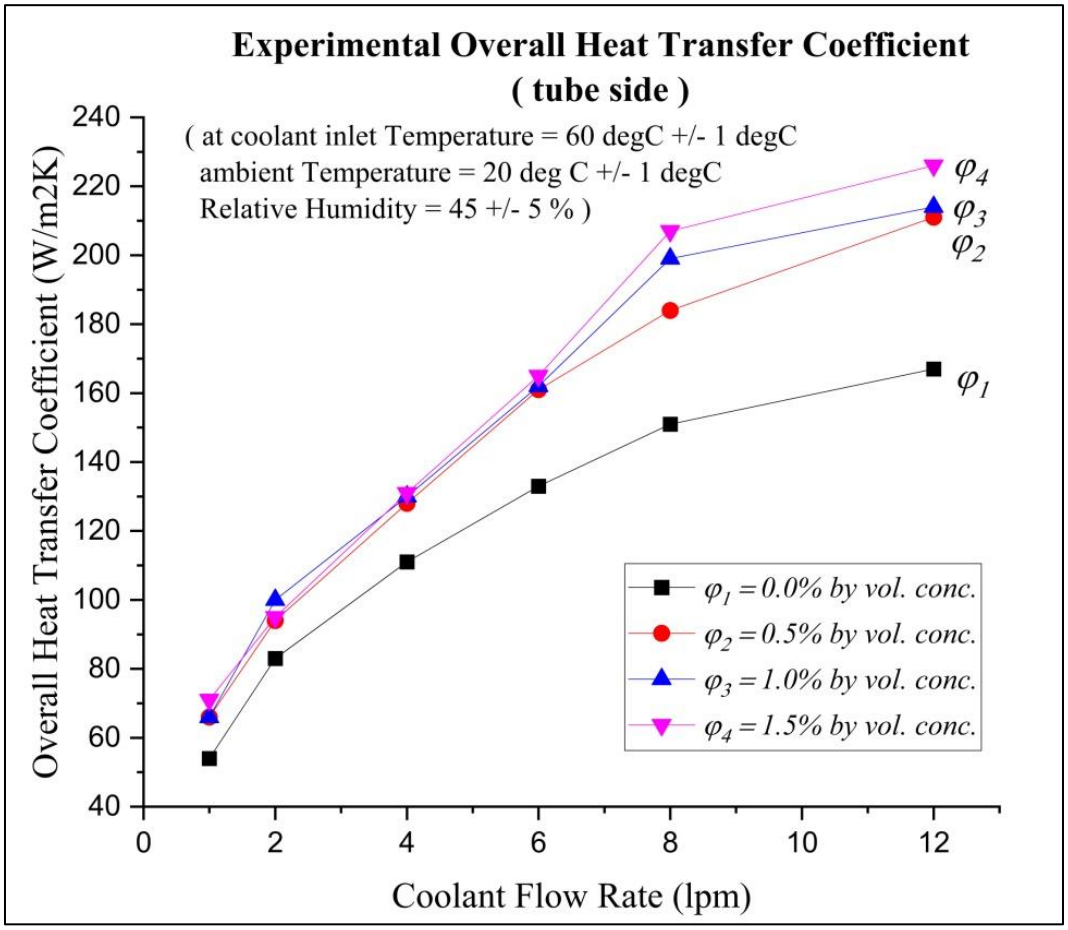

Figure 39: Tube-side Overall heat transfer coefficients (experimental) for different concentrations of nanocoolant

Figure 40 shows the enhancement in tube side overall heat transfer coefficient w.r.t. the base fluid. The enhancement trend follows a similar pattern for all three nanocoolants of particle concentration φ = 0.5% *by vol*., 1.0% *by vol*., and 1.5% *by vol*.

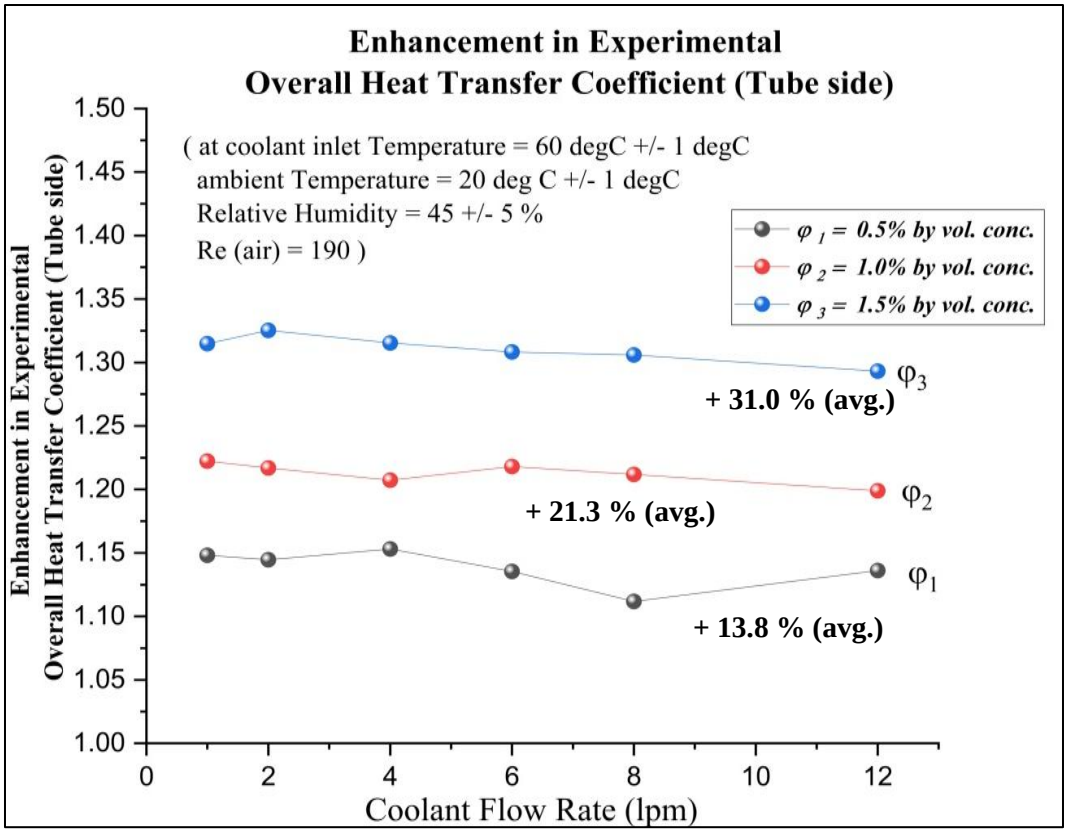

Figure 40: Enhancement in tube-side overall heat transfer coefficient on increasing the particle concentration

(b) Air-side

Figure 41 shows the effect of particle concentration on the air-side overall heat transfer coefficient. The overall heat transfer coefficient shows an increasing trend with an increase in nanoparticle concentration. The maximum enhancement of 37.5% occurs at coolant flow rate of 12 lpm for φ = 1.5% *by vol*. For other particle concentrations of φ = 0.5% *by vol*. and 1.0% *by vol*. the maximum enhancements are 14.3% and 26.8% at coolant flow rates of 1lpm and 8lpm, respectively. The average enhancement over all the coolant flow rates is found to be 12.4%, 22.8% and 33.3% for nanoparticle concentration φ = 0.5% *by vol*., 1.0% *by vol*. and 1.5% *by vol*. respectively. Figure 42 shows the enhancement in tube side overall heat transfer coefficient w.r.t. the base fluid. The enhancement trend follows a similar pattern for all three nanocoolants of particle concentration φ = 0.5% *by vol*., 1.0% *by vol*., and 1.5% *by vol*.

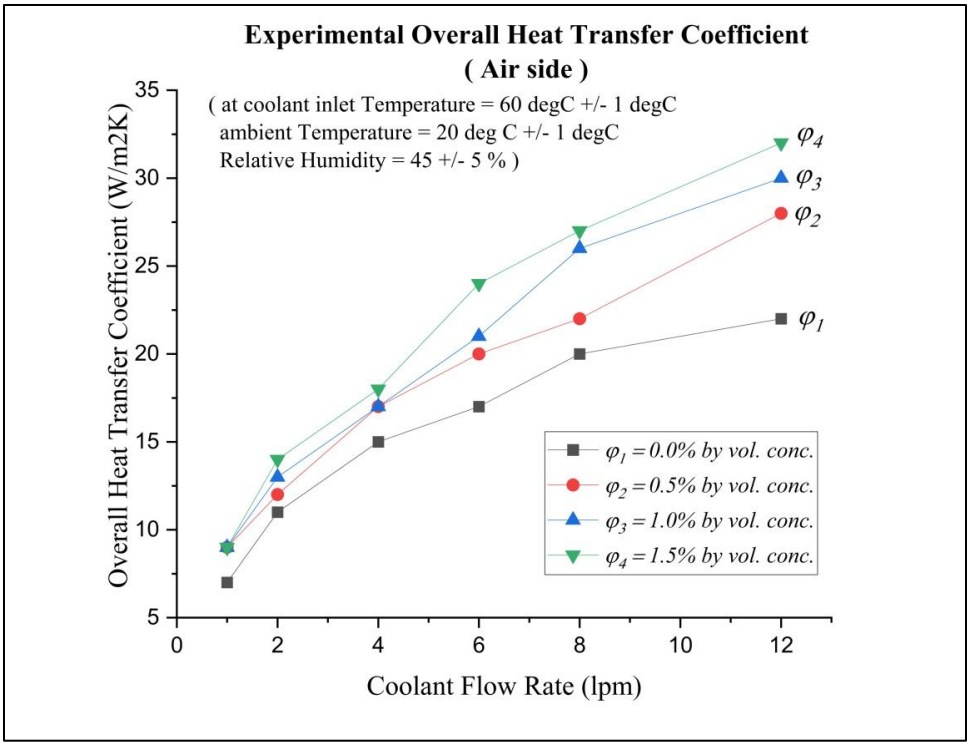

Figure 41: Air-side Overall heat transfer coefficients (experimental) for different concentrations of nanocoolant

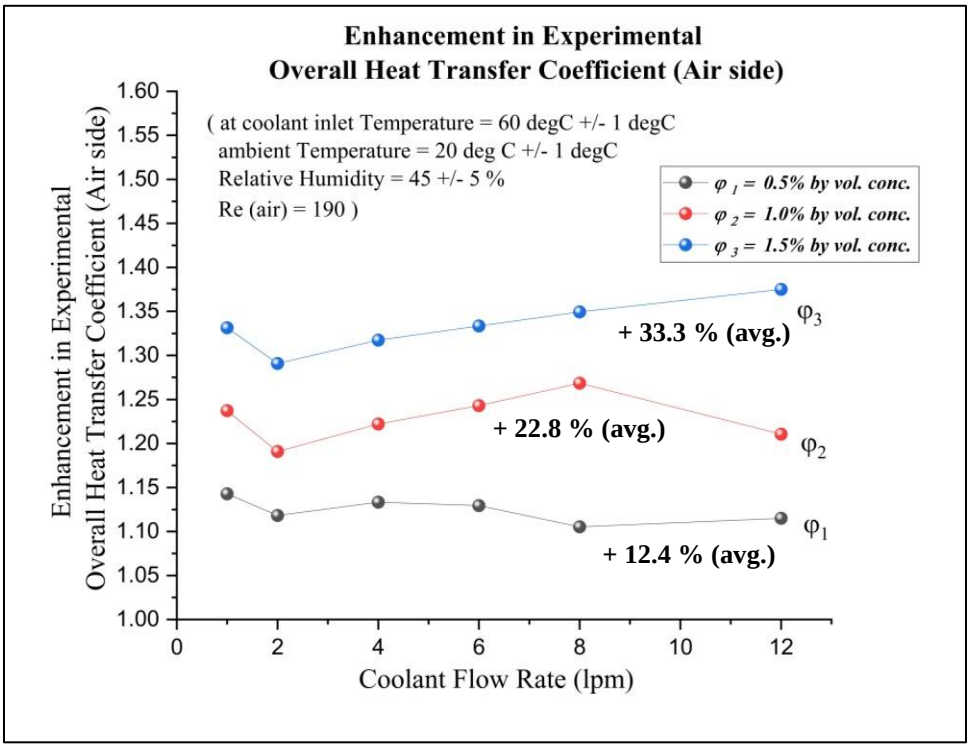

Figure 42: Enhancement in air-side overall heat transfer coefficient on increasing the particle concentration

5.4.7 Comparison of experimental and theoretical results

In this sub-section, Experimental overall heat transfer coefficients have been compared with the calculated overall heat transfer coefficients. As mentioned in section 4.2.2, the theoretical overall heat transfer coefficient has been calculated using correlations given by Maiga et. al. [44] and Dehghandokht et. al. [45] respectively for tube-side and air-side calculations. In general, the overall heat transfer coefficient shows an increasing trend with coolant flow rate and nanoparticle concentration.

Figure 43 shows the comparison of experimental and calculated overall heat transfer coefficients for base fluid (0.0% *by vol*. conc. of CuO). Deviation from theoretical results is observed for both the tube-side and air-side overall heat transfer coefficients. Taking the relative error of all the values of coolant flow rate, the deviation from calculated results is found to be 12.3 % and 16.8 % respectively for both the tube-side and air-side coefficients.

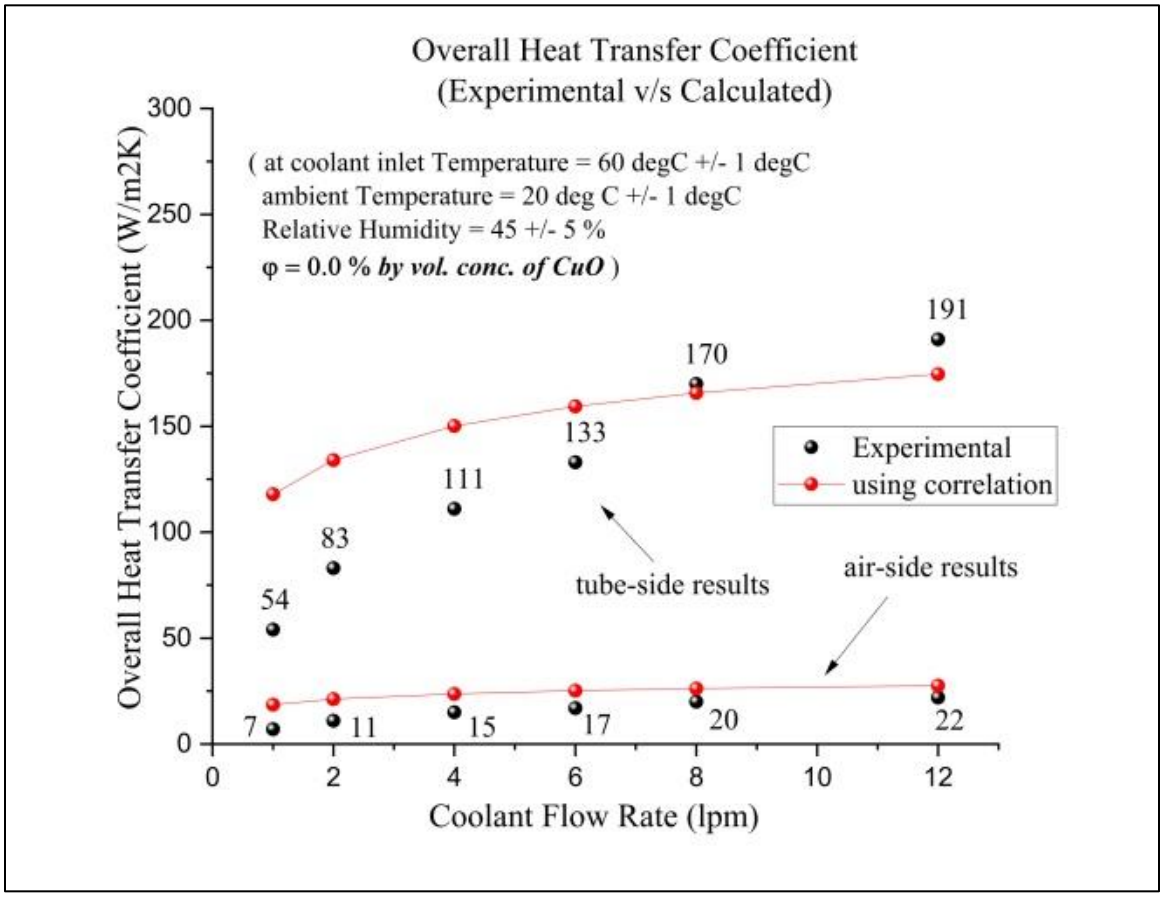

Figure 43: Comparison of experimental and calculated overall heat transfer coefficients for base fluid (0.0% *by vol*. conc. of CuO)

Figure 44 shows the comparison of experimental and calculated overall heat transfer coefficients for nanofluid having 0.5 % *by vol*. conc. of CuO. Deviation from theoretical results is observed for both the tube-side and air-side overall heat transfer coefficients. The experimental results for tube side coefficients overlap with the theoretical results at coolant flow rate of 6 lpm, but deviate at both the sides (i.e. at lower and higher coolant flow rates). For air-side results, the experimental values exactly match with the theoretical ones at coolant flow rate of 12 lpm, but slight deviation is observed towards lower coolant flow rates.

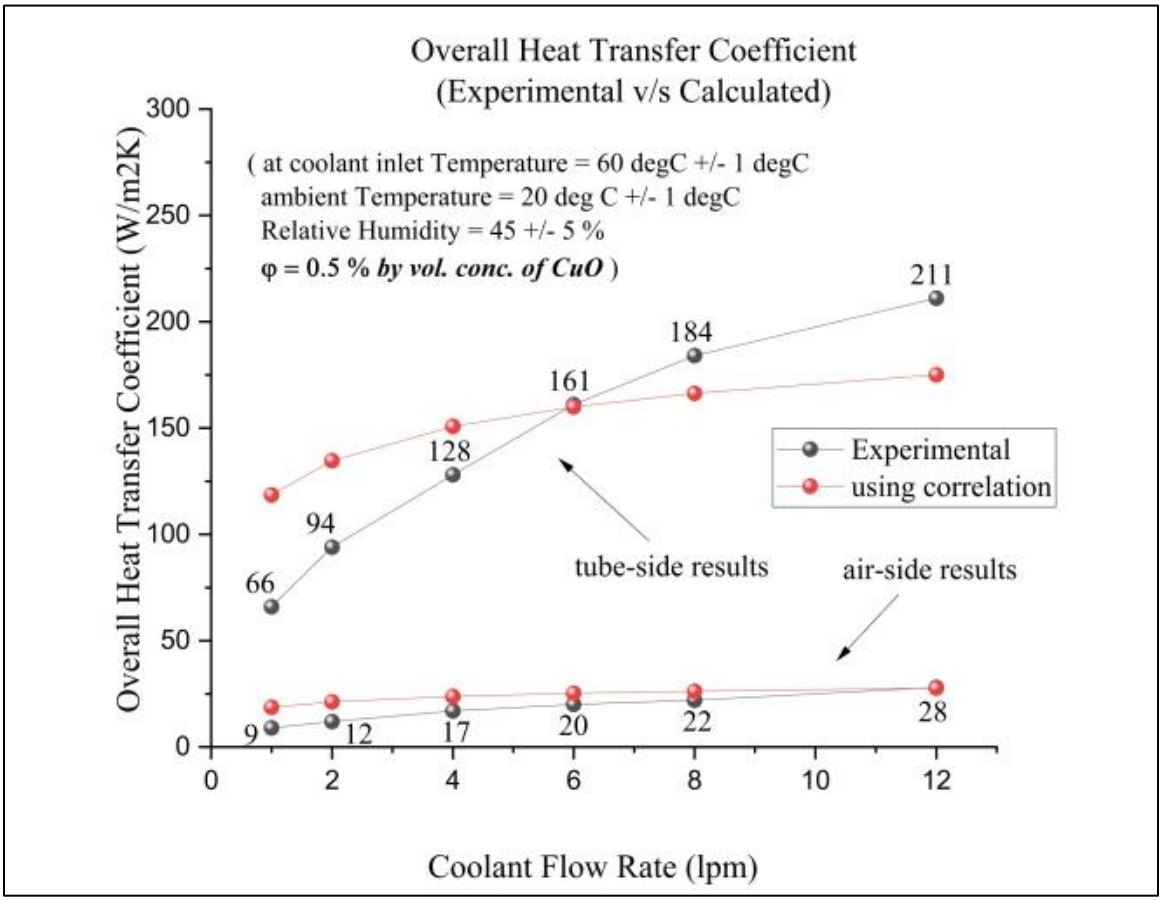

Figure 44: Comparison of experimental and calculated overall heat transfer coefficients for nanofluid (0.5% *by vol*. conc. of CuO)

Taking the relative error of all the values of coolant flow rate, the deviation from calculated results is found to be 10.7 % and 14.2 % respectively for both the tube-side and air-side coefficients.

Figure 45 shows the comparison of experimental and calculated overall heat transfer coefficients for nanofluid having 1.0 % *by vol*. conc. of CuO. Deviation from theoretical results is observed for both the tube-side and air-side overall heat transfer coefficients. The experimental results for tube side coefficients overlap with the theoretical results at coolant flow rate of 6 lpm, but deviate at both the sides (i.e. at lower and higher coolant flow rates). For air-side results, the experimental values exactly match with the theoretical ones at coolant flow rate of 8 lpm, and deviate slightly towards both the sides (i.e. lower and higher coolant flow rates)

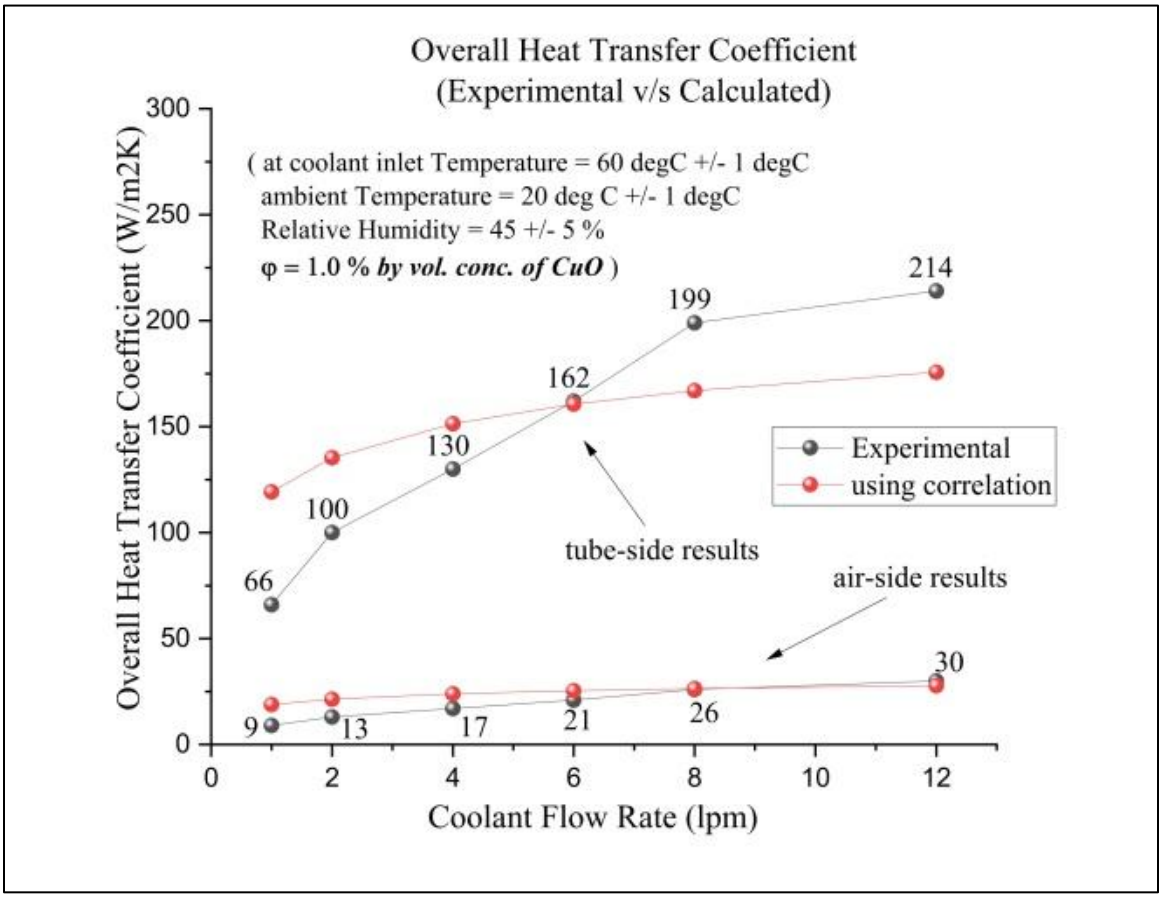

Figure 45: Comparison of experimental and calculated overall heat transfer coefficients for nanofluid (1.0 % *by vol*. conc. of CuO)

Taking the relative error of all the values of coolant flow rate, the deviation from calculated results is found to be 10.8 % and 12.3 % respectively for both the tube-side and air-side coefficients.

Figure 46 shows the comparison of experimental and calculated overall heat transfer coefficients for nanofluid having 1.5 % *by vol*. conc. of CuO. Deviation from theoretical results is observed for both the tube-side and air-side overall heat transfer coefficients. The experimental results for tube side coefficients are close to the theoretical results at coolant flow rate of 6 lpm, but deviate at both the sides (i.e. at lower and higher coolant flow rates). For air-side results, the experimental values exactly match with the theoretical ones at coolant flow rate of 8 lpm, and deviate slightly towards both the sides (i.e. lower and higher coolant flow rates)

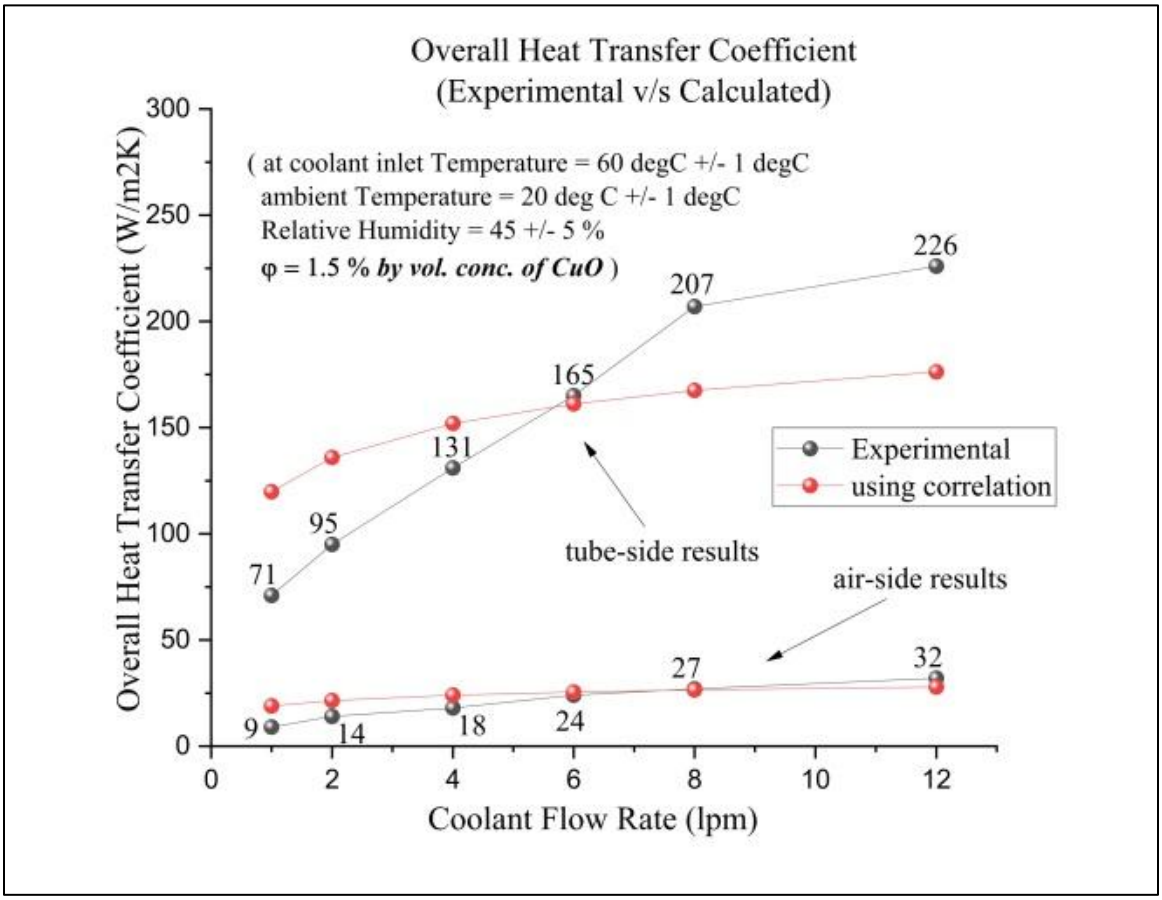

Figure 46: Comparison of experimental and calculated overall heat transfer coefficients for nanofluid (1.5 % *by vol*. conc. of CuO)

Taking the relative error of all the values of coolant flow rate, the deviation from calculated results is found to be 11.5 % and 10.7 % respectively for both the tube-side and air-side coefficients.

The values of tube side overall heat transfer coefficient are close to the calculated values at middle coolant flow rates (6 lpm, 8 lpm) but at lower (1 lpm, 2lpm, 4lpm) and at higher coolant flow rates (12 lpm), the results deviate significantly from the calculated data.

The values of air-side experimental overall heat transfer coefficients highly match those obtained using the correlations. At lower coolant flow rates, the experimental values deviate slightly from the calculated data, but at higher coolant flow rates, the experimental values tend to overlap with the calculated data.

The average deviation of experimental results from the calculated results has been calculated by using the relative error in the values across all coolant flow rates [48].

$$\theta(in\ \%) = \sqrt{\frac{1}{n}\sum_{i=1}^{n}\left(\frac{U_{cal,i} - U_{exp,i}}{U_{cal,i}}\right)^2}\ x100 \tag{43}$$

Where, θ is the average deviation, i represents coolant flow rate, n represents total number of coolant flow rates, and U is the overall heat transfer coefficient.

Concentration	Tube side average deviation	Air side average deviation
(a) 0.0% CuO	12.3%	16.8%
(b) 0.5% CuO	10.7%	14.2%
(c) 1.0% CuO	10.8%	12.3%
(d) 1.5% CuO	11.5%	10.7%

Table 14: Average deviation of experimental results from calculated results

5.4.8 Effect on Pumping Power

As stated earlier, pumping power is one of the key parameter to determine the efficiency of an automobile radiator. The effect of coolant flow rate on the pumping power was studied in section 5.1.3 (d). In this section, the effect of nanoparticle concentration on the pumping power has been studied for four different nanoparticle concentrations. The effect is more significant at lower coolant flow rates (1, 2, 4 lpm) but not much significant at higher coolant flow rates (6, 8, 12 lpm) as shown in Figure 47 and Figure 48 respectively.

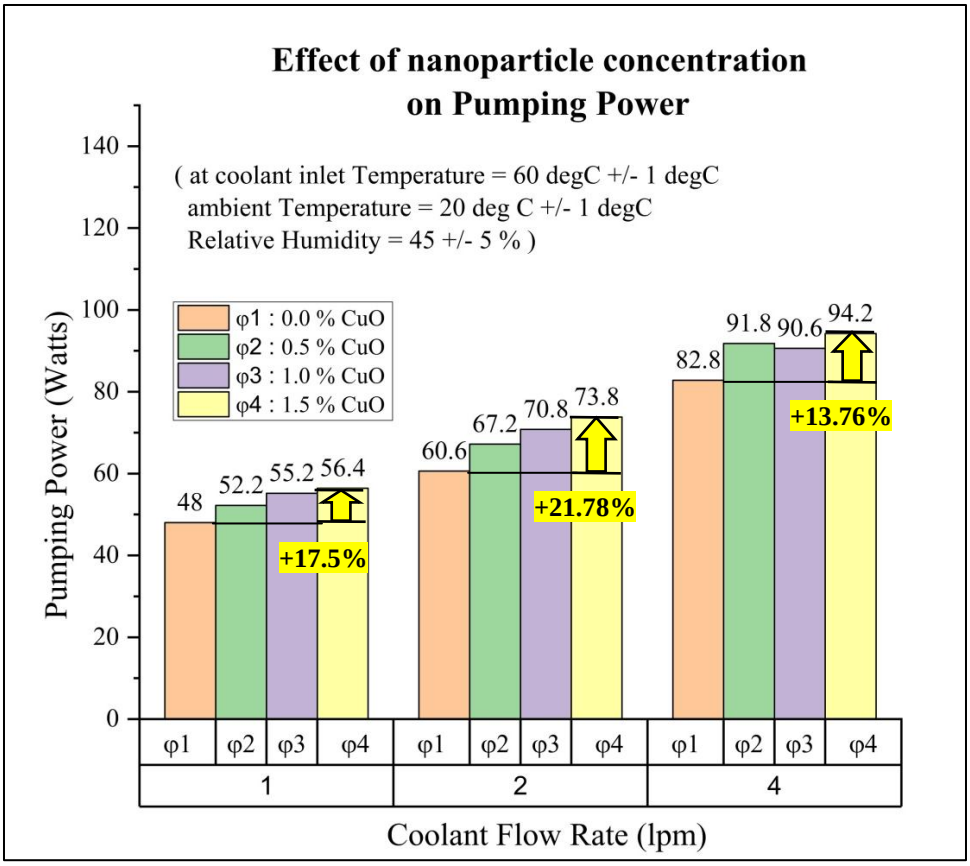

Figure 47: Effect of nanoparticle concentration on pumping power (at lower coolant flow rates)

Figure 47 shows the effect of nanoparticle concentration on the pumping power required at coolant flow rates of 1lpm, 2lpm, and 4lpm. At coolant flow rate of 1 lpm, pumping power required to pump coolant, increases by 17.5% when nanocoolant of 1.5% *by vol*. conc. of CuO is used. At the same coolant flow rate, the increase in pumping power for lower concentrations of 0.5% and 1.0% *by vol*. is 8.75% and 15.0% respectively.

Similarly at coolant flow rate of 2 lpm, the maximum increase of 21.78 % occurs at conc. of 1.5% *by vol*. and for lower concentrations of 0.5% and 1.0% it is 10.89% and 16.8% respectively.

At coolant flow rate of 4 lpm, the maximum increase of 13.76 % occurs at conc. of 1.5% *by vol*. and for lower concentrations of 0.5% and 1.0% it is 10.87% and 9.42 % respectively.

Thus, on the basis of above observations, it can be said that on increasing nanoparticle concentration, pumping power increases for lower coolant flow rates.

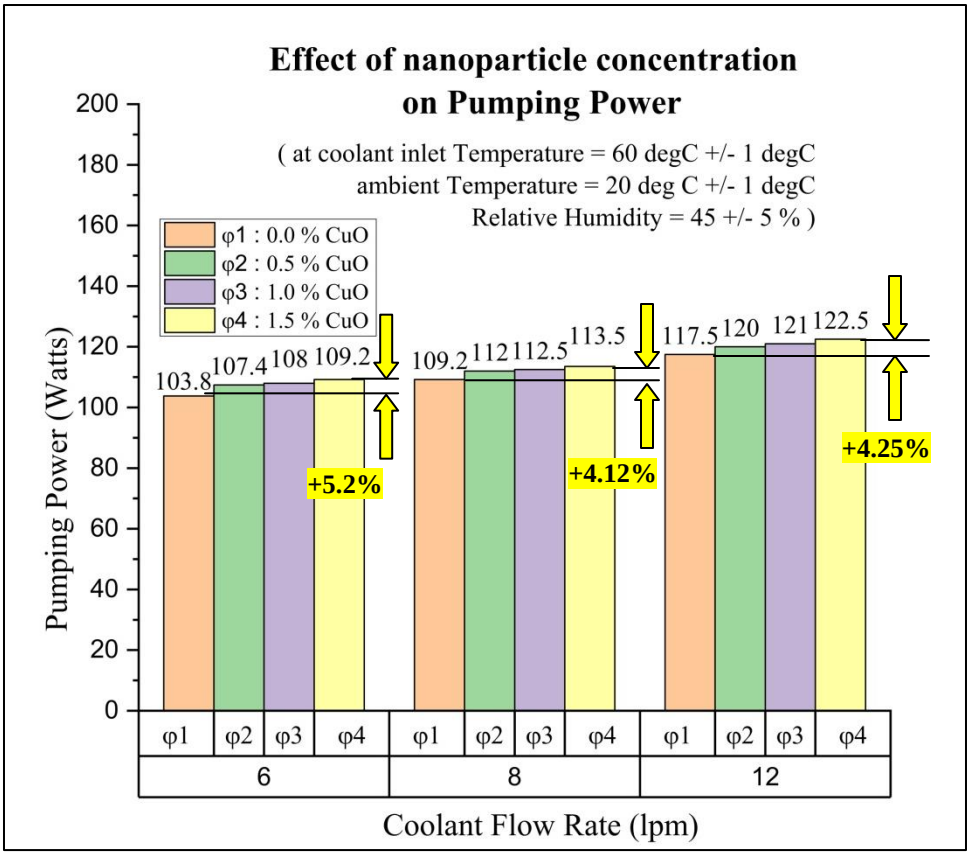

Figure 48: Effect of nanoparticle concentration on pumping power (at higher coolant flow rates)

Figure 48 shows the effect of nanoparticle concentration on the pumping power required at coolant flow rates of 6lpm, 8lpm, and 12lpm. At coolant flow rate of 6 lpm, pumping power required to pump coolant, increases by 5.2 % when nanocoolant of 1.5% *by vol*. conc. of CuO is used. At the same coolant flow rate, the increase in pumping power for lower concentrations of 0.5% and 1.0% *by vol*. is 3.46 % and 4.04 % respectively.

Similarly at coolant flow rate of 8 lpm, the maximum increase of 4.12 % occurs at conc. of 1.5% *by vol*. and for lower concentrations of 0.5% and 1.0% it is 2.56 % and 3.02 % respectively.

At coolant flow rate of 12 lpm, the maximum increase of 4.25 % occurs at conc. of 1.5% *by vol*. and for lower concentrations of 0.5% and 1.0% it is 2.12 % and 2.98 % respectively.

Thus, on the basis of above observations, it can be said that on increasing nanoparticle concentration, pumping power slightly increases at higher coolant flow rates.

[This page is intentionally left blank]

CHAPTER 6: CONCLUSION

As per the study undertaken, the experimental investigation of a radiator heat exchanger using CuO/glycerol-based nanofluid was successfully completed. Effects of various parameters such as: coolant flow rate, air flow rate, and ambient temperature on the thermal performance of an automobile radiator were studied. The effect of nanoparticles on the thermophysical properties of fluid was also determined. The effect of nanoparticle concentration on temperature drop, heat transfer rate, CHTC, and overall heat transfer coefficient was also studied and validated using the correlations available in the literature. The following conclusion can be made:

1. Temperature drop of coolant decreases with increase in coolant flow rate due to shorter contact time.
2. Heat transfer rate increases with increase in coolant flow rate and air flow rate.
3. Heat transfer rate increases with a decrease in ambient temperature
4. Thermal conductivity of nanofluid shows an enhancement of upto 4.48% for nanofluid with nanoparticle concentration of 1.5% *by vol*. w.r.t. the base fluid.
5. Effective dynamic viscosity increases by upto 13.6% on using CuO/glycerol nanofluid of conc. 1.5% *by vol*. w.r.t. the base fluid.
6. Specific heat capacity of nanofluid decreases by 6.97% on increasing nanoparticle concentration upto 1.5% *by vol*.
7. Heat transfer rate increases by upto 45.1% on using 1.5% *by vol*. conc. of CuO/glycerol nanofluid, compared with the base fluid.
8. Overall heat transfer coefficient increases on increasing nanoparticle concentration by upto 32.5% on using nanocoolant with 1.5 % *by vol*. conc. of CuO nanoparticles.

Future Scope:

- Experiments using different nanoparticles and different concentrations can be performed.
- Effect of glycerol strength on heat transfer performance of radiator can be studied.
- Effect of various parameters such as nanoparticle concentration, different surfactants, and ultrasonication time can be studied on stability of nanofluids.
- Effect of coolant inlet temperature on heat transfer performance can be studied.
- Effect on effectiveness of radiator can be studied.

Bibliography

[1] G. Prudhvi, G. Vinay, G.S. Babu, Cooling Systems in Automobiles & Cars, Int. J. Eng. Adv. Technol. 2 (2013) 688–695.

[2] İ. Durgun, A. Odabaşıoğlu, H. Ayartürk, Engine Cooling System Without Radiator, (2015) 144–152. https://doi.org/10.5151/engpro-simea2015-pap142.

[3] Radiator: definition, functions, parts, diagram, working - studentlesson, (n.d.). https://studentlesson.com/radiator-definition-functions-parts-diagram-working/ (accessed July 20, 2022).

[4] K.G. Sundari, L.G. Asirvatham, S. Joseph John Marshal, E. Ninolin, B. Surekha, Feasibility of glycerin/Al2O3 nanofluid for automotive cooling applications, J. Therm. Eng. 6 (2020) 619–632.

[5] A. Tarafdar, R. Sirohi, T. Negi, S. Singh, P.C. Badgujar, N. Chandra Shahi, S. Kumar, S. Jun Sim, A. Pandey, Nanofluid research advances: Preparation, characteristics and applications in food processing, Food Res. Int. 150 (2021) 110751.

[6] Stepehen U. S. CHoi, J.A. Eastman, Enhancing thermal conductivity of fluids with nanoparticles A metal-organic vapor phase epitaxy system for advanced in situ x-ray studies of III-nitride growth View project in situ oxide growth by radio frequency-magnetron sputtering View project, 1995.

[7] R.A. Bhogare, B.S. Kothawale, A review on applications and challenges of nanofluids as coolant in Automobile Radiator, Renew. Sustain. Energy Rev. 15 (2011) 1646–1668.

[8] A. Hajatzadeh Pordanjani, S. Aghakhani, M. Afrand, B. Mahmoudi, O. Mahian, S. Wongwises, An updated review on application of nanofluids in heat exchangers for saving energy, Energy Convers. Manag. 198 (2019) 111886.

[9] C. Selvam, D. Mohan Lal, S. Harish, Enhanced heat transfer performance of an automobile radiator with graphene based suspensions, Appl. Therm. Eng. 123 (2017) 50–60.

[10] Z.X. Li, F.L. Renault, A.O.C. Gómez, M.M. Sarafraz, H. Khan, M.R. Safaei, E.P.B. Filho, Nanofluids as secondary fluid in the refrigeration system: Experimental data, regression, ANFIS, and NN modeling, Int. J. Heat Mass Transf. 144 (2019).

[11] S.A. Ahmed, M. Ozkaymak, A. Sözen, T. Menlik, A. Fahed, Improving car radiator performance by using TiO2-water nanofluid, Eng. Sci. Technol. an Int. J. 21 (2018) 996–1005.

[12] M. Allen Zennifer, S. Manikandan, K.S. Suganthi, V. Leela Vinodhan, K.S. Rajan, Development of CuO-ethylene glycol nanofluids for efficient energy management: Assessment of potential for energy recovery, Energy Convers. Manag. 105 (2015) 685–696.

[13] R.J. Sengwa, M. Saraswat, P. Dhatarwal, Comprehensive characterization of glycerol/ZnO green nanofluids for advances in multifunctional soft material technologies, J. Mol. Liq. 355 (2022) 118925.

[14] M. Eltaweel, A.A. Abdel-Rehim, A.A.A. Attia, A comparison between flat-plate and evacuated tube solar collectors in terms of energy and exergy analysis by using nanofluid, Appl. Therm. Eng. 186 (2021) 116516.

[15] Z. Said, A.A. Hachicha, S. Aberoumand, B.A.A. Yousef, E.T. Sayed, E. Bellos, Recent advances on nanofluids for low to medium temperature solar collectors: energy, exergy, economic analysis and environmental impact, Prog. Energy Combust. Sci. 84 (2021).

[16] H.B. Ma, C. Wilson, Q. Yu, K. Park, U.S. Choi, M. Tirumala, An Experimental Investigation of Heat Transport Capability in a Nanofluid Oscillating Heat Pipe, J. Heat Transfer. 128 (2006) 1213–1216.
[17] H. Reza Seyf, S. Kim, Y. Zhang, Thermal Performance of an Al2O3–Water Nanofluid Pulsating Heat Pipe, J. Electron. Packag. 135 (2013).
[18] G. V Pradeep, K. Rama Narasimha, Experimental Investigations on the Thermal Performance of a Single Closed Loop Pulsating Heat Pipe Using TiO2 Nanofluid, J. Heat Transfer. 141 (2019).
[19] S. Azarfar, R. Soleymani, Investigation and optimization of effective factors on the thermal conductivity and stability of water-based CuO nanofluid Shahriar, in: SRPioneers, 2015.
[20] H. Zhu, D. Han, Z. Meng, D. Wu, C. Zhang, Preparation and thermal conductivity of cuo nanofluid via a wet chemical method, Nanoscale Res. Lett. 6 (2011) 2–7.
[21] M. Kole, T.K. Dey, Effect of prolonged ultrasonication on the thermal conductivity of ZnO-ethylene glycol nanofluids, Thermochim. Acta. 535 (2012) 58–65.
[22] G. Xia, H. Jiang, R. Liu, Y. Zhai, Effects of surfactant on the stability and thermal conductivity of Al 2O3/de-ionized water nanofluids, Int. J. Therm. Sci. 84 (2014) 118–124.
[23] M.H. Ahmadi, A. Mirlohi, M. Alhuyi Nazari, R. Ghasempour, A review of thermal conductivity of various nanofluids, J. Mol. Liq. 265 (2018) 181–188.
[24] M. Sahooli, S. Sabbaghi, M. Shariaty Niassar, Preparation of CuO/Water Nanofluids Using Polyvinylpyrolidone and a Survey on Its Stability and Thermal Conductivity, Int . J . Nanosci . Nanotechnol. 8 (2012) 27–34.
[25] L.S. Sundar, M.H. Farooky, S.N. Sarada, M.K. Singh, Experimental thermal conductivity of ethylene glycol and water mixture based low volume concentration of Al2O3 and CuO nanofluids, Int. Commun. Heat Mass Transf. 41 (2013) 41–46.
[26] S.M. Peyghambarzadeh, S.H. Hashemabadi, M. Naraki, Y. Vermahmoudi, Experimental study of overall heat transfer coefficient in the application of dilute nanofluids in the car radiator, Appl. Therm. Eng. 52 (2013) 8–16.
[27] A. Ijam, A. Moradi Golsheikh, R. Saidur, P. Ganesan, A glycerol-water-based nanofluid containing graphene oxide nanosheets, J. Mater. Sci. 49 (2014) 5934–5944.
[28] S.A. Adio, M. Sharifpur, J.P. Meyer, Influence of ultrasonication energy on the dispersion consistency of Al2O3–glycerol nanofluid based on viscosity data, and model development for the required ultrasonication energy density, J. Exp. Nanosci. 11 (2016) 630–649.
[29] J. Shah, M. Ranjan, K.P. Sooraj, Y. Sonvane, S.K. Gupta, Surfactant prevented growth and enhanced thermophysical properties of CuO nanofluid, J. Mol. Liq. 283 (2019) 550–557.
[30] K.G. Sundari, L.G. Asirvatham, S.J.J. Marshal, S. Manova, M. Sahu, M.J. Aaron, Heat transfer studies using glycerin based nanocoolant for car radiator cooling applications, Mater. Today Proc. (2021).
[31] Pramod Warrier, A. Teja*, Effect of particle size on effective thermal conductivity of nanofluids, Asian J. Sci. Res. 6 (2013) 339–345.
[32] T. Hayat, S. Nadeem, Heat transfer enhancement with Ag–CuO/water hybrid nanofluid, Results Phys. 7 (2017) 2317–2324.
[33] S. Suresh, K.P. Venkitaraj, P. Selvakumar, M. Chandrasekar, Effect of Al 2O 3-Cu/water hybrid nanofluid in heat transfer, Exp. Therm. Fluid Sci. 38 (2012) 54–60.

[34] R. Rekha Sahoo, Effect of various shape and nanoparticle concentration based ternary hybrid nanofluid coolant on the thermal performance for automotive radiator, Heat Mass Transf. Und Stoffuebertragung. 57 (2021) 873–887.
[35] M.B. Maisuria, D.M. Sonar, M.K. Rathod, Nanofluid selection used for coolant in heat exchanger by multiple attribute decision-making method, J. Mech. Sci. Technol. 35 (2021) 689–695.
[36] M.H.U. Bhuiyan, R. Saidur, M.A. Amalina, R.M. Mostafizur, A.K.M.S. Islam, Effect of nanoparticles concentration and their sizes on surface tension of nanofluids, in: Procedia Eng., Elsevier Ltd, 2015: pp. 431–437.
[37] B.R. Ponangi, V. Krishna, K.N. Seetharamu, Effect of Ultralow Concentrated Reduced Graphene Oxide Nanofluid on Radiator Performance, J. Heat Transfer. 143 (2021).
[38] P.C. Mishra, S. Mukherjee, S.K. Nayak, A. Panda, A brief review on viscosity of nanofluids, Int. Nano Lett. 4 (2014) 109–120. https://doi.org/10.1007/s40089-014-0126-3.
[39] A.O. Al, Measurement and Validation of Thermophysical Properties of Al_2O3 Nanofluids, Mater. Soc. Annu. Meet. 3 (2009) 2–5.
[40] H.U. Kang, S.H. Kim, J.M. Oh, Estimation of Thermal Conductivity of Nanofluid Using Experimental Effective Particle Volume Nanofluid using Experimental Effective, 6152 (2006).
[41] V. Bianco, O. Manca, S. Nardini, K. Vafai, Heat Transfer Enhancement with Nanofluids, 2015.
[42] E.N. Sieder, G.E. Tate, Heat Transfer and Pressure Drop of Liquids in Tubes, Ind. Eng. Chem. 28 (1936) 1429–1435.
[43] D.G. Subhedar, B.M. Ramani, A. Gupta, Experimental investigation of heat transfer potential of Al2O3/Water-Mono Ethylene Glycol nanofluids as a car radiator coolant, Case Stud. Therm. Eng. 11 (2018) 26–34.
[44] S. El Bécaye Maïga, S.J. Palm, C.T. Nguyen, G. Roy, N. Galanis, Heat transfer enhancement by using nanofluids in forced convection flows, Int. J. Heat Fluid Flow. 26 (2005) 530–546.
[45] M. Dehghandokht, M.G. Khan, A. Fartaj, S. Sanaye, Numerical study of fluid flow and heat transfer in a multi-port serpentine meso-channel heat exchanger, Appl. Therm. Eng. 31 (2011) 1588–1599.
[46] G.A. Oliveira, E.M. Cardenas Contreras, E.P. Bandarra Filho, Experimental study on the heat transfer of MWCNT/water nanofluid flowing in a car radiator, Appl. Therm. Eng. 111 (2017) 1450–1456.
[47] J. Segur, Physical properties of glycerol and its solutions, Aciscience.Org. 1999 (1953) 1–27.
[48] Z. Liu, W. Xu, Z. Li, L. Zhang, J. Li, A. Li, A. Feng, Research on heating performance of heating radiator at low temperature, J. Build. Eng. 36 (2021).

R_Thesis

ORIGINALITY REPORT

15%	10%	10%	4%
SIMILARITY INDEX	INTERNET SOURCES	PUBLICATIONS	STUDENT PAPERS

PRIMARY SOURCES

1	link.springer.com Internet Source	1%
2	www.ijraset.com Internet Source	1%
3	Farrukh Abbas, Hafiz Muhammad Ali, Muhammad Shaban, Muhammad Mansoor Janjua et al. "Towards convective heat transfer optimization in aluminum tube automotive radiators: Potential assessment of novel Fe2O3-TiO2/water hybrid nanofluid", Journal of the Taiwan Institute of Chemical Engineers, 2021 Publication	1%
4	archive.org Internet Source	1%
5	ijeat.org Internet Source	<1%
6	coek.info Internet Source	<1%
	Iwaponline.Com	

7	Internet Source	<1%
8	www.degruyter.com Internet Source	<1%
9	Submitted to Charotar University of Science And Technology Student Paper	<1%
10	www.hindawi.com Internet Source	<1%
11	slideplayer.com Internet Source	<1%
12	Peyghambarzadeh, S.M., S.H. Hashemabadi, M. Naraki, and Y. Vermahmoudi. "Experimental study of overall heat transfer coefficient in the application of dilute nanofluids in the car radiator", Applied Thermal Engineering, 2013. Publication	<1%
13	Rashmi Rekha Sahoo. "Thermo-hydraulic characteristics of radiator with various shape nanoparticle-based ternary hybrid nanofluid", Powder Technology, 2020 Publication	<1%
14	Submitted to De Montfort University Student Paper	<1%
15	tudr.thapar.edu:8080	